

**RAT BONE MARROW DERIVED MESENCHYMAL
STEM CELLS AND THEIR HEPATOGENIC
DIFFERENTIATION**

Danna Ye

**A Thesis Submitted in Partial Fulfillment of the Requirements for the
Degree of Doctor of Philosophy in Biotechnology
Suranaree University of Technology
Academic Year 2011**

เซลล์ต้นกำเนิดชนิดมีเซนไคม์จากไขกระดูกหนูแรทและ
การเปลี่ยนแปลงไปเป็นเซลล์ตับ

นางสาวดানা เย

วิทยานิพนธ์นี้เป็นส่วนหนึ่งของการศึกษาตามหลักสูตรปริญญาวิทยาศาสตรดุษฎีบัณฑิต
สาขาวิชาเทคโนโลยีชีวภาพ
มหาวิทยาลัยเทคโนโลยีสุรนารี
ปีการศึกษา 2554

RAT BONE MARROW DERIVED MESENCHYMAL STEM CELLS AND THEIR HEPATOGENIC DIFFERENTIATION

Suranaree University of Technology has approved this thesis submitted in partial fulfillment of the requirements for the Degree of Doctor of Philosophy.

Thesis Examining Committee

(Assoc. Prof. Dr. Montarop Yamabhai)

Chairperson

(Asst. Prof. Dr. Rangsun Parnpai)

Member (Thesis Advisor)

(Assoc. Prof. Dr. Supat Sinawat)

Member

(Dr. Waraporn Tanthanuch)

Member

(Asst. Prof. Dr. Jaruwan Siritapetawee)

Member

(Dr. Parinya Noisa)

Member

(Prof. Dr. Sukit Limpijumnong)

Vice Rector for Academic Affairs

(Asst. Prof. Dr. Suwayd Ningsanond)

Dean of Institute of Agricultural Technology

दानนำ เย : เซลล์ต้นกำเนิดชนิดมีเซนไคม์จากไขกระดูกหนูแรทและการเปลี่ยนแปลงไป
เป็นเซลล์ตับ (RAT BONE MARROW DERIVED MESENCHYMAL STEM CELLS
AND THEIR HEPATOGENIC DIFFERENTIATION) อาจารย์ที่ปรึกษา : ผู้ช่วย
ศาสตราจารย์ ดร.รังสรรค์ พาลพ่าย, 176 หน้า

โรคตับเป็นโรคร้ายแรงถึงชีวิตที่สำคัญ โรคหนึ่งหากมีความรุนแรงมากจนกระทั่งตับไม่สามารถเพิ่มจำนวนเซลล์เพื่อทดแทนเซลล์ที่เสียหายได้ การใช้เซลล์ต้นกำเนิดเพื่อการรักษาโรคตับระยะสุดท้ายจึงได้รับความสนใจในด้านการรักษาทางเลือก โดยเซลล์ต้นกำเนิดชนิดมีเซนไคม์จากไขกระดูก (Bone marrow derived mesenchymal stem cells : BM-MSCs) ถือว่าเป็นตัวเลือกหนึ่งที่มีความเหมาะสม วัตถุประสงค์ของการทดลองครั้งนี้เพื่อศึกษาถึงวิธีที่เหมาะสมในการเพาะเลี้ยง BM-MSCs โดยใช้หนูแรทเป็นตัวอย่างในการศึกษา (rBM-MSCs) รวมไปถึงการเหนี่ยวนำเซลล์ดังกล่าวให้เปลี่ยนแปลงไปเป็นเซลล์ตับอย่างมีประสิทธิภาพสูงสุดทั้งในห้องปฏิบัติการและการศึกษาในสัตว์ทดลอง ผลจากการศึกษาพบว่าสามารถแยก rBM-MSCs จากไขกระดูกหนูแรทและทำการเพาะเลี้ยงโดยเซลล์มีคุณสมบัติในการเกาะกับผิวจานเลี้ยงเซลล์ อีกทั้งพบว่าปริมาณตั้งต้นที่เหมาะสมในการเพาะเลี้ยงคือ 100 เซลล์/ตารางเซนติเมตร จากการศึกษาด้วยวิธี Flow cytometry พบว่าเซลล์ดังกล่าวให้ผลบวกต่อมาร์คเกอร์ที่จำเพาะต่อเซลล์ต้นกำเนิดชนิดมีเซนไคม์ (CD29, CD37 และ CD105) รวมถึงมีศักยภาพในการเปลี่ยนแปลงไปเป็นเซลล์กระดูก เซลล์กระดูกอ่อน และเซลล์ไขมันได้เมื่อได้รับการเหนี่ยวนำ อีกทั้งยังพบว่า rBM-MSCs สามารถคงคุณสมบัติของเซลล์ต้นกำเนิดชนิดมีเซนไคม์ได้ไม่น้อยกว่า 10 พาสเสจ จากการทำการศึกษาการเปลี่ยนแปลงทางชีวเคมีในระดับโมเลกุลของ rBM-MSCs ระหว่างที่เหนี่ยวนำให้มีการเปลี่ยนแปลงไปเป็นเซลล์ตับในห้องปฏิบัติการโดยใช้ Fourier transform infrared (FTIR) microspectroscopy พบว่ามีองค์ประกอบของไขมันภายในเซลล์เพิ่มสูงขึ้นเรื่อยๆ ในระหว่างการเหนี่ยวนำไปเป็นเซลล์ตับ ซึ่งสามารถใช้บ่งชี้ถึงการเปลี่ยนแปลงไปเป็นเซลล์ตับได้ ในการศึกษาที่ยังทำการทดลองเพิ่มเติมว่าการใช้ 5-Aza-2'-deoxycytidine (5-Aza-dC) และ Trichostatin A (TSA) สามารถเพิ่มศักยภาพการเปลี่ยนแปลงไปเป็นเซลล์ตับของ rBM-MSCs ได้หรือไม่โดยพบว่าเมื่อใช้ TSA ขนาด 1 μM จะ

ช่วยเพิ่มศักยภาพในการเปลี่ยนแปลงไปเป็นเซลล์ตับใน rBM-MSCs อย่างไรก็ตามการใช้ 5-Aza-dC ในขนาด 20 μ M เพียงอย่างเดียว หรือใช้ร่วมกับกับ TSA ไม่มีผลต่อการศักยภาพในการเปลี่ยนแปลงไปเป็นเซลล์ตับ โดยใช้ผลจาก FTIR microspectroscopy ช่วยยืนยันถึงความเปลี่ยนแปลงในระดับโมเลกุลที่เกิดขึ้นระหว่างการใส่สารเคมีดังกล่าว ในส่วนสุดท้ายได้ ทำการศึกษาถึงผลของการปลูกถ่าย rBM-MSCs ให้แก่หนูแรทที่ถูกเหนี่ยวนำให้เกิดพยาธิสภาพขึ้น ที่ตับด้วยสาร dimethylnitrosamine (DMN) และศึกษาความเปลี่ยนแปลงที่เกิดขึ้นโดยการใช้ FTIR microspectroscopy ที่มีต้นกำเนิดจากแสงซินโครตรอน (SR-FTIR) ผลจากการศึกษาพบว่าเซลล์ตับที่เปลี่ยนแปลงมาจาก rBM-MSCs สามารถบรรเทาพยาธิสภาพในตับของหนูแรทได้ และความเปลี่ยนแปลงดังกล่าวสามารถยืนยันได้ด้วยผลจาก SR-FTIR microspectroscopy

สาขาวิชาเทคโนโลยีชีวภาพ

ปีการศึกษา 2554

ลายมือชื่อนักศึกษา _____

ลายมือชื่ออาจารย์ที่ปรึกษา _____

ลายมือชื่ออาจารย์ที่ปรึกษาร่วม _____

ลายมือชื่ออาจารย์ที่ปรึกษาร่วม _____

DANNA YE : RAT BONE MARROW DERIVED MESENCHYMAL
STEM CELLS AND THEIR HEPATOGENIC DIFFERENTIATION.

THESIS ADVISOR : ASST. PROF. RANGSUN PARNPAI, Ph.D., 176 PP.

MESENCHYMAL STEM CELLS/HEPATOGENIC DIFFERENTIATION/FTIR
MICROSPECTROSCOPY/LIVER DISEASE/TRANSPLANTATION

Liver diseases are leading cause of the inability of hepatocyte to regenerate. The use of stem cells as a therapeutic option for patients with end-stage liver diseases is attractive. Bone marrow derived mesenchymal stem cells (BM-MSCs) are presently considered to be the most promising cell source for the cell therapy of liver diseases. The aims of this study are to optimize the rat BM-MSCs (rBM-MSCs) culture system and to investigate the hepatic differentiation *in vitro* and *in vivo*. First, the suitable culture system for rBM-MSCs was studied. The results indicated that rBM-MSCs could be isolated by selective plastic surface attachment method and the optimal rBM-MSCs growth was found at a seeding density of 100 cells/cm². Flow cytometry indicated that the rBM-MSCs maintained expression of mesenchymal markers (CD29, CD37 and CD105). Differentiation tests showed that they maintained mesenchymal (osteoblastic, chondrocytic, and adipocytic) differentiation potential for at least over 10 passages. The later experiment employed Fourier transform infrared (FTIR) microspectroscopy as an explorative method to investigate the biochemical

and molecular composition changes during rBM-MSCs differentiation to hepatocyte *in vitro*. The results suggested that the rBM-MSCs derived hepatocytes can be characterized by the high lipid content which facilitates a means of identifying hepatocytes from their derived stem cells. The FTIR microspectroscopy provides biochemical information which is complimentary to what obtained from conventional techniques. Based on this study, we further investigated whether the 5-Aza-2'-deoxycytidine (5-Aza-dC) and Trichostatin A (TSA) could promote the hepatic differentiation potential of rBM-MSCs. FTIR microspectroscopy was used to monitor the biochemical and molecular composition changes upon 5-Aza-dC and/or TSA exposure during hepatic differentiation. The results demonstrated that exposure of rBM-MSCs to 1 μ M TSA in both differentiation and maturation steps considerably improved the hepatic differentiation. Meanwhile, the treatment of rBM-MSCs with 20 μ M 5-Aza-dC only or in combination with TSA ineffectively improved the hepatic differentiation. The effect of 5-Aza-dC and/or TSA on the biochemical composition of the cells confirmed that FTIR microspectroscopy is an explorative method in monitoring how the chromatin remodeling agents function on the cells. We further performed *in vivo* analysis using dimethylnitrosamine (DMN) treated rats model for rBM-MSCs transplantation and assessed biochemical molecular alteration of the liver tissue by synchrotron radiation FTIR (SR-FTIR) microspectroscopy. The studies revealed that transplantation of rBM-MSCs derived hepatocytes could

effectively cured liver diseases in rats. This finding was confirmed by SR-FTIR microspectroscopy.

School of Biotechnology

Academic Year 2011

Student's Signature _____

Advisor's Signature _____

Co-advisor's Signature _____

Co-advisor's Signature _____

ACKNOWLEDGEMENTS

I would like to express my deepest appreciation and thanks for everyone who has supported me during this long endeavor.

First and foremost, I wish to express my sincere gratitude to my advisor, Asst. Prof. Dr. Rangsun Parnpai, for all of his guidance and support in my research project over the past four years. He enthusiastic support, breadth of knowledge, and unyielding scientific aspirations has showed me the significance of being patient, dedicated, and hard working.

I would like to express my deeply thank to my co-advisor, Dr. Waraporn Tanthanuch, at Synchrotron Light Research Institute, who guidance me to the FTIR microspectroscopy world and help me in experiment and data analysis. Her scientific advices contribute significantly for the completion of this dissertation work. I am also profoundly indebted to my co-advisor, Assoc. Prof. Dr. Supat Sinawat, for his guidance.

I also want to extend my appreciation to my committee, Assoc. Prof. Dr. Montarop Yamabhai, Asst. Prof. Dr. Jaruwan Siritapetawee and Dr. Parinya Noisa for serving on my committee and their insightful advice and invaluable comments on my doctorate research. Their guidance was instrumental in my graduate career.

Many thanks to my former adviser, Prof. Kehuan Lu, at Animal Reproduction Institute, GuangXi University, China, for his integral role in guiding

my scientific development.

I wish to acknowledge Dr. Philip Heraud at Center for Biospectroscopy and the Monash Immunology and Stem Cell Laboratories, Monash University, for his advice and revise paper for me. I also thanks to Dr. Mark J. Tobin at Australian Synchrotron, for his help in bean line (2BM1B) use.

I would like to express my gratitude to all former and current members in the Embryo Technology and Stem Cell Research Center, Suranaree University of Technology. Besides lending me support, they have made my workdays more enjoyable through interesting discussions.

My acknowledgments would not be complete had I not mentioned my best friends, Vivian, Aiko, Shanshan and Haijie in China, who go with the proverb “A friend in need is a friend indeed”. They have always been with me during the ups and downs.

I am dedicating this thesis to my mother and father. I know I never would have completed this effort were it not for my incredible family – above all, my parents, whom I strive to emulate in their embodiment of love, and my younger sister, who is my best friend.

And finally, I would like to express my definitely appreciation to Mr. Tong Li for all his care and love. He always knows the right thing to say to motivate me whenever I feel frustrated.

CONTENTS

	Page
ABSTRACT IN THAI.....	I
ABSTRACT IN ENGLISH.....	III
ACKNOWLEDGEMENTS.....	VI
CONTENTS.....	VIII
LIST OF TABLES.....	XV
LIST OF FIGURES.....	XVI
LIST OF ABBREVIATIONS.....	XX
CHAPTER	
I INTRODUCTION.....	1
1.1 Introduction.....	1
1.2 References.....	3
II LITERATURE REVIEW.....	8
2.1 Liver disease.....	8
2.2 Regenerative medicine and stem cell therapy.....	9
2.3 Mesenchymal stem cells.....	11
2.3.1 Sources of primary MSCs.....	12
2.3.2 Isolation of primary MSCs.....	13
2.3.3 <i>In vitro</i> characteristics of MSCs.....	14
2.3.4 Self-renewing potential of MSCs.....	15
2.3.5 Differentiation potential of MSCs.....	16

CONTENTS (Continued)

	Page
3.3.3 Characterization of rBM-MSCs.....	54
3.3.3.1 <i>In vitro</i> differentiation potential.....	54
3.3.3.2 Phenotype determination by flow cytometry.....	56
3.3.3.3 Immunocytochemistry.....	57
3.3.4 Statistical analysis.....	57
3.4 Results.....	58
3.4.1 Generation of primary cultures from adherent bone marrow cells.....	58
3.4.2 Effect of seeding density on expansion of rBM-MSCs.....	58
3.4.3 Charaterization of rBM-MSCs from efficiency expansion Culture.....	59
3.4.3.1 Expression of mesenchymal markers in rBM-MSCs.....	59
3.4.3.2 Immunophenotype.....	60
3.4.3.3 Differentiation potential.....	60
3.5 Discussion.....	61
3.6 Conclusion.....	64
3.7 References.....	72
IV DISCRIMINATION OF FUNCTIONAL MESENCHYMAL STEM CELLS DERIVED HEPATOCYTE USING FTIR MICROSPECTROSCOPY.....	79

CONTENTS (Continued)

	Page
4.1 Abstract.....	79
4.2 Introduction.....	80
4.3 Material and methods.....	82
4.3.1 Isolation, culture and characterization of rBM-MSCs.....	82
4.3.2 Hepatic differentiation.....	82
4.3.3 Immunocytochemistry for hepatocyte specific marker.....	83
4.3.4 Indocyanine green (ICG) uptake study.....	84
4.3.5 Periodic Acid-Shiff (PAS) histochemical staining.....	84
4.3.6 Albumin ELISA.....	84
4.3.7 Urea production.....	84
4.3.8 Reverse transcription-polymerase chain reaction (RT-PCR) analysis.....	85
4.3.9 Sample preparation for FTIR microspectroscopy.....	86
4.3.10 FTIR microspectroscopy and data analysis.....	87
4.3.11 Statistical analysis.....	88
4.4 Results.....	88
4.4.1 Characterization of rBM-MSCs derived hepatocyte.....	88
4.4.2 FTIR microspectroscopy.....	90
4.4.3 Multivariate analysis.....	93
4.5 Discussions.....	95
4.6 Conclusions.....	98
4.7 References.....	106

CONTENTS (Continued)

		Page
V	CHROMATIN REMODELING AGENTS IN HEPATIC DIFFERENTIATION OF BONE MARROW MESENCHYMAL STEM CELLS AND ANALYSIS BY FTIR MICROSPECTROSCOPY	113
	5.1 Abstract.....	113
	5.2 Introduction.....	114
	5.3 Materials and methods.....	117
	5.3.1 Isolation and culture of rBM-MSCs.....	117
	5.3.2 Hepatic differentiation.....	117
	5.3.3 Characterization of hepatocyte-like cells.....	118
	5.3.4 FTIR microspectroscopy and data acquisition.....	118
	5.3.5 Statistical analysis.....	119
	5.4 Results.....	120
	5.4.1 The effect of 5-Aza-dC and TSA on the hepatogenic process.....	120
	5.4.1.1 Morphological features.....	120
	5.4.1.2 Liver-specific protein expression.....	121
	5.4.1.3 Liver-specific gene expression.....	122
	5.4.1.4 Hepatic functionality.....	123
	5.4.2 Macromolecular changes identified by FTIR microspectroscopy.....	123

CONTENTS (Continued)

	Page
6.3.7 Data analysis.....	156
6.4 Results.....	156
6.4.1 The liver-damaged rat model.....	156
6.4.2 Tracing of transplanted cells in the DNM-injured liver.....	157
6.4.3 Recovery of albumin production by stem cells transplantation.....	157
6.4.4 Suppression of liver inflammation by stem cells transplantation.....	158
6.4.5 Synchrotron Radiation Fourier Transform Infrared (SR-FTIR) microspectroscopy investigation of liver tissue.....	158
6.5 Discussion.....	160
6.6 Conclusion.....	162
6.7 References.....	168
VII OVERALL CONCLUSION.....	172
APPENDIX.....	173
BIOGRAPHY.....	176

LIST OF TABLES

Table	Page
4.1 Primers used for RT-PCR characterization.....	86
4.2 FTIR frequencies and tentative band assignments.....	102
5.1 Chromatin remodeling agent inducing hepatic differentiation protocols.....	118

LIST OF FIGURES

Figure	Page
2.1 Hierarchy of stem cells	11
2.2 Heamatopoietic and stromal cell differentiation.....	12
2.3 Mesenchymal stem cells multilineage differentiation potential.....	18
2.4 Schematic presentation of fetal liver development.....	19
3.1 Morphology of primary cultures of rBM-MSCs.....	66
3.2 The growth kinetics of rBM-MSCs plated at difference density across multiple passages.....	67
3.3 The growth patterns of rBM-MSCs plated at difference initial plating density.....	68
3.4 FACS analyses of the selected surface antigens expression by the rBM-MSCs during expansion in culture.....	69
3.5 Immunocytochemistry analyses of rBM-MSCs at passage.....	70
3.6 Differentiation potential of rBM-MSCs.....	71
4.1 Changes in cell morphology during hepatic differentiation of rBM-MSCs.....	100

LIST OF FIGURES (Continued)

Figure	Page
4.2 RT-PCR analyses of the temporal expression pattern of selected Hepatocyte specific gene during hepatic differentiation of rBM-MSCs.....	100
4.3 The expression of HNF 3 β , AFP, CK18, HNF 1 α , ALB and C/EBP α at the maturation stage of differentiation by immunocytochemistry	101
4.4 The induced rBM-MSCs showed liver function.....	101
4.5 Average second derivative FTIR spectra of rBM-MSCs differentiation into hepatocyte-like cells.....	103
4.6 PCA score plots and loading plot of rBM-MSCs differentiation into hepatocytes.....	104
4.7 Cluster analysis of different stage of rBM-MSCs differentiation to hepatocytes.....	105
5.1 Changes in cell morphology during hepatic differentiation of rBM-MSCs.....	135
5.2 The expression of HNF 3 β , AFP, CK18, HNF 1 α , ALB and C/EBP α at the last day of hepatic differentiation of each experimental group by immunocytochemistry.....	136

LIST OF FIGURES (Continued)

Figure	Page
5.3 Comparative of hepatocyte specific proteins expression upon chromatin remodeling agent exposure.....	137
5.4 RT-PCR analyses of the temporal expression pattern of selected hepatocyte specific gene during hepatic differentiation of rBM-MSCs.....	138
5.5 Comparative analysis of hepatocyte like functionality at the last day of hepatic differentiation.....	139
5.6 Average second derivative FTIR spectra of rBM-MSCs differentiation into hepatocyte-like cell upon exposure of chromatin remodeling agent at different stage.....	140
5.7 PCA scores plots (a, c and e) and loading plot (b, d and f) of rBM-MSCs differentiation into hepatocytes upon exposure of chromatin remodeling agent at different stage.....	143
6.1 Representative liver tissues stained with hematoxylin and eosin.....	164
6.2 Engraftment of PKH-stained rBM-MSCs and hepatocyte in DMN-injured rat liver.....	165
6.3 Biochemical analysis.....	166
6.4 Hematoxylin and Eosin staining of liver sections from DNM-injured rats that received cell transplant.....	166
6.5 Average second derivative FTIR spectra from 1800 to 950 cm^{-1}	167

LIST OF FIGURES (Continued)

Figure	Page
6.6 PCA scores plots and loading plot.....	167

LIST OF ABBREVIATIONS

ml	=	milliliter
IU	=	international unit
µg	=	microgram
µl	=	microlitre
IgG	=	gamma immunoglobulin
mM	=	millimolar
kg	=	kilogram
°C	=	degree celsius
mg	=	milligram
mm	=	millimeter
M	=	molar
SEM	=	standard error means
ng	=	nanogram

CHAPTER I

INTRODUCTION

1.1 Introduction

The previous reports about adult stem cell multipotency have generated tremendous interest regarding their potential therapeutic value, while bypassing ethical concerns surrounding the use of human embryonic stem cells (Reiser et al., 2005). Among the different adult stem cells, the bone marrow derived mesenchymal stem cells (BM-MSCs) may represent the best hope for cell replacement therapy, in addition to their multipotency and accessibility, BM-MSCs may also be used in autologous transplantation to minimize immune rejection (Scolding et al., 2008). Along with human BM-MSCs, the better characterized cultures are those of rat (Santa Maria et al. 2004) and mouse (Baddoo et al., 2003) origin, although therapeutic potential in large animal models had been investigated with BM-MSCs from horse (Ringe et al., 2003), cow (Bosnakovski et al., 2005), pig (Moscoso et al., 2005), dog (Silva et al., 2005), sheep (Rhodes et al., 2004) and baboon (Devine et al., 2001). For BM-MSCs' clinical applications, an adequate number of cells are necessary, and considering the low number of BM-MSCs, an extensive *in vitro* expansion is required in order to maintain BM-MSCs' morphology, biological and functional property (Wexler et al., 2003; Caplan, 2007; Neuhuber et al., 2008; Pal et al., 2009). The harvesting and expansion methods used by different laboratories are relatively standard, BM-MSCs culturing protocols vary widely. Initial densities, level of

confluence at passage and harvest, and time in culture are factors with unclear impact on therapeutic efficacy (Neuhuber et al., 2008).

Liver transplantation is the primary treatment for various end-stage hepatic diseases but is hindered by the lack of donor organs and by complications associated with rejection and immunosuppression. The establishment of stem cell therapy for the liver is of great significance. There is increasing evidence to suggest the bone marrow derived MSC is a transplantable source of hepatocyte *in vivo* and *in vitro* (Schwartz et al., 2002; Anjos-Afonso et al. 2004; Lee et al. 2004; Wang et al. 2004; Sato et al. 2005; Aurich et al. 2007; Kuo et al., 2008). Until now, several models for *in vitro* hepatocyte differentiation are available. These models include addition of soluble medium factors (Growth Factors/Cytokines/Corticosteroids/Hormones), reconstruction of *in vivo* cell-matrix and cell-cell interactions, determination of cell fate via genetic modification (Snykers et al., 2009). However, the degree of differentiation obtained in these models is incomplete, and they still demand additional characterization and optimization. Recently, the point of interest is the role of epigenetic modifiers in mediating hepatic-conditioned postnatal progenitor cells toward fully functional hepatocytes. This process is still young, critical factors of this process are needed to be studied. Both *in vivo* and *in vitro* of hepatic differentiation need to be carefully studied in greater depth.

Fourier transform infrared (FTIR) microspectroscopy has been introduced into various biological fields and found to be a very useful tool, particularly for the identification of cellular phenotype. Many research works in medical sciences have shown the successful use of this technique to characterize various types of cells and tissues. For example, cervical cancer (Wood et al., 2004), oral cancer (Schultz et al., 1998) as well as stem cell differentiation state (Ami et al., 2008; Krafft et al., 2007;

Heraud et al., 2010; Tanthanuch et al., 2010) are amenable to characterization by FTIR microspectroscopy as it offers the possibility to overcome all problems regarding the detection of macromolecular content of whole cell. The current information about using FTIR microspectroscopy to study stem cell is still limited and to use FTIR microspectroscopy to monitor the differentiation of stem cell *in vitro* and *in vivo* will give us promising information on stem cell therapy.

In an attempt to clarify these issues, the aim of this study is to optimize rBM- MSCs culture system and investigate their hepatic differentiation *in vitro* and *in vivo*, which will be determined based on conventional characterization method and FTIR microspectroscopy.

1.2 References

- Ami, D., Neri, T., Natalello, A., Mereghetti, P., Doglia, S. M., Zanoni, M., Zuccotti, M., Garagna, S. and Redi, C. A. (2008). Embryonic stem cell differentiation studied by FT-IR spectroscopy. **Biochim. Biophys. Acta.** 1783: 98-106.
- Anjos-Afonso, F., Siapati, E. K. and Bonnet, D. (2004). *In vivo* contribution of murine mesenchymal stem cells into multiple cell-types under minimal damage conditions. **J. Cell Sci.** 117: 5655-5664.
- Aurich, I., Mueller, L. P., Aurich, H., Luetzkendorf, J., Tisljar, K., Dollinger, M., Schormann, W., Walldorf, J., Hengstler, J., Fleig, W. E. and Christ, B. (2007). Functional integration of hepatocytes derived from human mesenchymal stem cells into mouse livers. **Gut.** 56: 405-415.
- Baddoo, M., Hill, K., Wikinson, R., Gaupp, D., Hughes, C., Kopen, G. C. and Phinney D. G. (2003). Characterization of mesenchymal stem cells isolated from

- murine bone marrow by negative selection. **J. Cell Biochem.** 89: 1235-1249.
- Bosnakovski, D., Mizuno, M., Kim, G., Takagi, S., Okumura, M. and Fujinaga, T. (2005). Isolation and multi-lineage differentiation of bovine bone marrow mesenchymal stem cells. **Cell Tissue Res.** 319: 243-253.
- Caplan, A. I. (2007). Adult mesenchymal stem cells for tissue engineering versus regenerative medicine. **J. Cell Physiol.** 213: 341-347.
- Devine, S. M., Bartholomew, A. M., Mahmud, N., Nelson, M., Patil, S., Hardy, W., Sturgeon, C., Hewett, T., Chung, T., Stock, W., Sher, D., Weissman, S., Ferrer, K., Mosca, J., Deans, R., Moseley, A. and Hoffman, R. (2001). Mesenchymal stem cells are capable of homing to the bone marrow of non-human primates following systemic infusion. **Exp. Hematol.** 29: 255-255.
- Heraud, P., Ng, E. S., Caine, S., Yu, Q. C., Hirst, C., Mayberry, R., Bruce, A., Wood, B. R., McNaughton, D., Stanley, E. G. and Elefanty, A. G. (2010). Fourier transform infrared microspectroscopy identifies early lineage commitment in differentiating human embryonic stem cells. **Stem Cell Res.** 4: 140-147.
- Krafft, C., Salzer, R., Seitz, S., Ern, C. and Schieker, M. (2007). Differentiation of individual human mesenchymal stem cells probed by FTIR microscopic imaging. **Analyst** 132: 647-653.
- Kuo, T. K., Hung, S. P., Chuang, C. H., Chen, C. T., Shih, Y. R., Fang, S. C., Yang, W. V. and Lee, O. K. (2008). Stem cell therapy for liver disease: parameters governing the success of using bone marrow mesenchymal stem cells. **Gastroenterology** 134: 2111-2121.
- Lee, K. D., Kuo, T. K., Whang-Peng, J., Chung, Y. F., Lin, C. T., Chou, S. H., Chen, J. R., Chen, Y. P. and Lee, O. K. (2004). *In vitro* hepatic differentiation of

- human mesenchymal stem cells. **Hepatology** 40: 1275-1284.
- Moscoso, I., Centeno, A., Lopez, E., Rodriguez-Barbosa, J. I., Santamarina, I., Filgueira, P., Sanchez, M. J., Domingues-Perles, R., Penuelas-Rivas, G. and Domenech, N. (2005). Differentiation “*in vitro*” of primary and immortalized porcine mesenchymal stem cells into cardiomyocytes for cell transplantation. **Transplant Proc.** 37: 481-482.
- Neuhuber, B., Swanger, S. A., Howard, L., Mackay, A. and Fischer, I. (2008). Effects of plating density and culture time on bone marrow stromal cell characteristics. **Exp. Hematol.** 36: 1176-1185.
- Pal, R., Hanwate, M., Jan, M. and Totey, S. (2009). Phenotypic and functional comparison of optimum culture conditions for upscaling of bone marrow-derived mesenchymal stem cells. **J. Tissue Eng. Regen. Med.** 3: 163-174.
- Reiser, J., Zhang, X. Y., Hemenway, C. S., Mondal, D., Pradhan, L. and Russa, V. F. L. (2005). Potential of mesenchymal stem cells in gene therapy approaches for inherited and acquired diseases. **Expert. Opin. Biol. Ther.** 5: 1571-1584.
- Rhodes, N. P., Srivastava, J. K., Smith, R. F. and Longinotti, C. (2004). Heterogeneity in proliferative potential of ovine mesenchymal stem cell colonies. **J. Mater Sci. Mater Med.** 15: 397-402.
- Ringe, J., Haupl, T. and Sitterling, M. (2003). Characterization of mesenchymal stem cells isolated from murine bone marrow. **Med. Klin.** 98: 35-40.
- Santa Maria, L., Rojas, C. V. and Minguell, J. J. (2004). Signal from damaged but not undamaged skeletal muscle induce myogenic differentiation of rat bone marrow derived mesenchymal stem cells. **Exp. Cell Res.** 300: 418-426.
- Sato, Y., Araki, H., Kato, J., Nakamura, K., Kawano, Y., Kobune, M., Sato, T.,

- Miyanishi, K., Takayama, T., Takahashi, M., Takimoto, R., Iyama, S., Matsunaga, T., Ohtani, S., Matsuura, A., Hamada, H. and Niitsu, Y. (2005). Human mesenchymal stem cells xenografted directly to rat liver differentiated into human hepatocytes without fusion. **Blood** 106: 756-776.
- Schultz, C. P., Liu, K. Z., Kerr, P. D. and Mantsch, H. H. (1998). In situ infrared histopathology of keratinization in human oral/oropharyngeal squamous cell carcinoma. **Oncol. Res.** 10: 277-286.
- Schwartz, R. E., Reyes, M., Koodie, L., Jiang, Y., Blackstad, M., Lund, T., Lenvik, T., Johnson, S., Hu, W. S. and Verfaillie, C. M. (2002). Multipotent adult progenitor cells from bone marrow differentiate into functional hepatocyte-like cells. **J. Clin. Invest.** 109: 1291-1302.
- Scolding, N., Marks, D. and Rice, C. (2008). Autologous mesenchymal bone marrow stem cells: Practical considerations. **J. Neurological Sciences** 265: 111-115.
- Silva, G. V., Litovsky, S., Assad, J. A., Sousa, A. L., Vela, D., Coulter, S. C., Lin, J., Ober, J., Vaughn, W. K., Branco, R. V. C. and Oliveira, E. M. (2005). Mesenchymal stem cells differentiate into an endothelial phenotype, enhance vascular density and improve heart function in a canine chronic ischemia model. **Circulation** 111: 150-156.
- Snykers, S., De Kock, J., Rogiers, V. and Vanhaecke, T. (2009). *In vitro* differentiation of embryonic and adult stem cells into hepatocytes: state of the art. **Stem Cells** 27: 577-605.
- Tanthanuch, W., Thumanu, K., Lorthongpanich, C., Parnpai, R. and Heraud, P. (2010). Neural differentiation of mouse embryonic stem cells studied by FTIR spectroscopy. **J. Mol. Structure** 967: 189-195.

- Wang, P. P., Wang, J. H., Yan, Z. P., Hu, M. Y., Lau, G. K., Fan, S. T. and Luk, J. M. (2004). Expression of hepatocyte-like phenotypes in bone marrow stromal cells after HGF induction. **Biochem. Biophys. Res. Commun.** 320: 712-716.
- Wexler, S. A., Donaldson, C., Denning-Kendall, P., Rice, C., Bradley, B. and Hows, J. M. (2003). Adult bone marrow is a rich source of human mesenchymal stem cells but umbilical cord and mobilized adult blood are not. **Br. J. Haematol.** 121: 368-374.
- Wood, B. R., Chiriboga, L., Yee, H., Quinn, M. A., McNaughton, D. and Diem, M. (2004). Fourier transform infrared (FTIR) spectral mapping of the cervical transformation zone, and dysplastic squamous epithelium. **Gynecol. Oncol.** 93: 59-68.

CHAPTER II

REVIEW OF LITERATURES

2.1 Liver disease

Liver disease (also called hepatic disease) is a broad term describing any single number of diseases affecting the liver. They are caused by infectious agents (Soemohardjo, 2003), autoimmune attack (Strassburg et al., 2003), malignant transformation (Zhu, 2003), inborn genetic deficiencies (Ballas et al., 2002), or secondary defects (Gill and sterling, 2001). Most liver diseases lead to hepatocyte dysfunction with the possibility of eventual organ failure. Liver transplantation is currently the major therapeutic option for patients with acute and chronic end-stage liver disease. However, a shortage of suitable donor organs and a requirement for immunosuppressive therapy restrict its usage, highlighting the importance of finding suitable alternatives. Furthermore, liver transplantation comes with considerable long term side effects, such as chronic renal failure, post-transplantation lympho proliferative disorder and cardiovascular complications (Chung et al., 2007; Francoz et al., 2007; Patel et al. 2007; Tamsel et al., 2007). The emerging field of stem cell therapy has raised great hope for improving the treatment of liver diseases, as it has the potential to promote liver repair and regeneration with fewer complications.

2.2 Regenerative medicine and stem cell therapy

Regenerative medicine is the process of creating living, functional tissues to repair or replace tissue or organ function lost due to damage, or congenital defects (Mason and Dunnill, 2008). It includes both the regeneration of tissues in vitro for subsequent in vivo implantation, as well as regeneration directly in vivo by engineering the basic building blocks of the human body. It has been proposed that regenerative medicine is an amalgamation of a multitude of disciplines including cell biology, tissue engineering, biomaterials science, endocrinology and transplantation science. If realized, it offers the prospect of extending healthy life span and improving the quality of life by supporting and activating the body's own natural healing. Recent interest in stem cell biology and novel biomaterial have raised hopes that manipulation and delivery of patient compatible cells and tissues could recapitulate the regenerative process and lead to more functional responses to injury (Gurtner et al., 2007).

Stem cell refers to a diverse group of unprogrammed cells which are capable of self-renewal and retain the plasticity to differentiate into various tissues. Their potency largely varies, ranging from pluripotency, the capacity to differentiate to cells from any of the three germ layers, to unipotency, the ability to produce only one cell type (Fig. 2.1). Stem cells can be divided into two major classes: one is embryonic stem cells (ES cells) which derived from the inner cell mass of a blastocyst or morula stage embryos and exhibit pluripotency, the other is adult stem cells (AS cells) which

are found in most tissues of the adult body, but possess a limited capacity to differentiate into various cell types. It is hoped that stem cell-based therapies will help people who have and are suffering from devastating disease. The use of stem cells has been featured in several untreatable conditions, such as spinal cord injury, heart disease and liver disease (Patel and Genovese, 2007; Barnabe-Heider and Frisen, 2008; Ucceli, 2008; Gordon et al., 2006; Mohamadnejad et al., 2007a). Apart from safety and ethical concerns, one of the most particular aspects of ES cell therapy for liver disease is the question of whether the cells are really differentiated as desired, so, there have been many clinical trials for stem cell therapy of liver diseases by using adult stem cell especially bone marrow derived stem cells (Terai et al., 2006; Gaia et al., 2006; Gupta et al., 2007; Mohamednejad et al., 2007a; Mohamadnejad et al., 2007b; Lyra et al., 2007). Recently, the emergencies of induced pluripotent stem cells (iPS), which are derived from adult somatic cells (e.g., skin fibroblasts) by their infection with retroviruses carrying factors that are important in maintaining the “stemness” of ES cell, giving the promising tool for stem cells therapy (Takahashi et al., 2007; Park et al., 2008). However, this type of cell is at an early stage which means that more research is needed to be done. Although adult stem cells may be proven to be useful to improve liver functionality and extend the length and quality of life, the difficulty in evaluating mechanisms in human studies poses some questions in identifying the best method for various cases in the future.

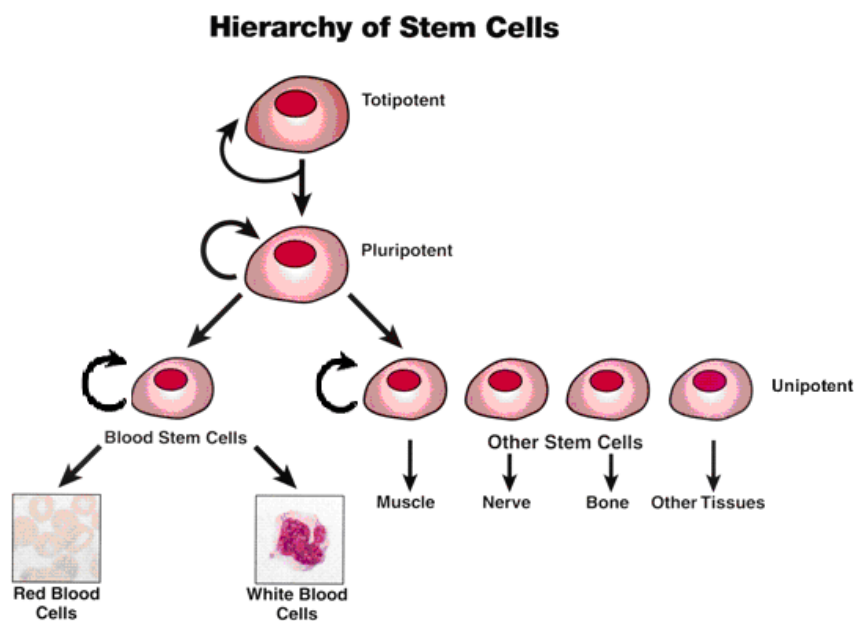


Figure 2.1 Hierarchy of stem cells. Stem cells can be totipotent (they are produced by the fusion of an egg and sperm), pluripotent (they are totipotent cells' descendants) and unipotent (can make only one cell type).

(www.patentbaristas.com/archives/2008/03/03/ding-warf-wins-round-2-as-stem-cell-patent-upheld)

2.3 Mesenchymal stem cells (MSCs)

The concept of MSCs arose from the work of Friedenstein and colleagues four decades ago (Friedenstein et al., 1976), which are commonly isolated by adherence to plastic and consecutive passages in tissue culture after acquiring a homogeneous fibroblast-like appearance. MSCs are the non-haematopoietic cell component of the bone marrow stroma which is capable of generating the cells of mesenchymal lineages, including bone, cartilage, adipose, tendon and muscle tissue (Fig 2.2). The *in vivo* existence of MSCs is supported by the fact that the tissue remodeling process during development and throughout postnatal growth, repair and

regeneration requires a continuous supply of new cells suggesting the subsistence of these cells (Caplan and Bruder, 2001; Baksh et al. 2004).

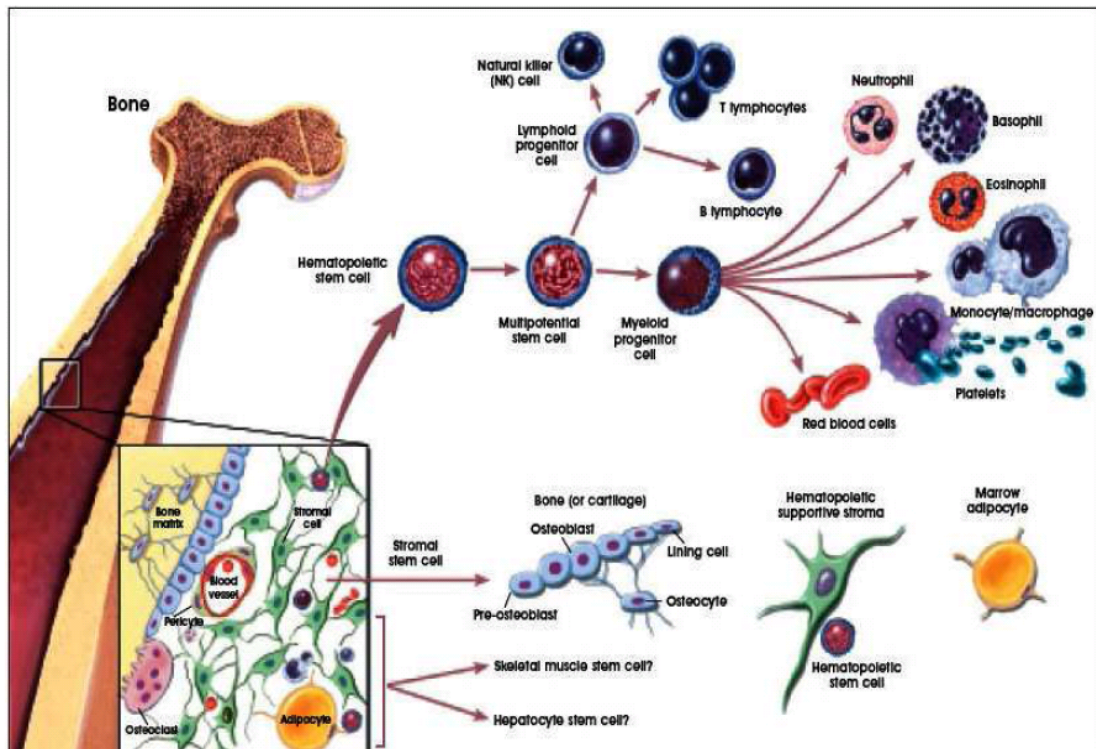


Figure 2.2 Hematopoietic and stromal cell differentiation. It shows that bone marrow as a reservoir for two distinct developmental systems: the hematopoietic system and the marrow stromal network. The hematopoietic system gives rise to blood cell phenotype and the stromal cell network comprises a mixed cell population that generates bone, cartilage, fat, fibrous connective tissue and the reticular network that supports blood cell formation.

(www.chroma.med.mimi.edu/micro/faculty-jurecic.html)

2.3.1 Sources of Primary MSCs

MSCs are typically isolated from the stromal fraction of adult bone marrow

and are rare in bone marrow, representing only 0.01-0.0001% of nucleated cells (Dazzi et al., 2006; Sakaguchi et al., 2005). Normally, murine MSCs are obtained from the femurs and tibias of mice by flushing the marrow out of the bones with culture medium and transferring the resultant cell suspension in culture (Friedenstein et al., 1976). Human MSCs can be similarly obtained from healthy volunteers by taking aspirates of bone marrow from the iliac crest and expanding on tissue-culture plastic (Risbud et al., 2006). At present, MSCs can be isolated from bone marrow (BM; Jiang et al., 2002), adipose tissue (Zuk et al., 2001), dental pulp (Gronthos et al., 2002), placenta (Yen et al., 2005), umbilical cord blood (UCB; Lee et al., 2004b), and from a variety of fetal tissues, such as spleen, lung, pancreas, kidney and amniotic fluid during mid-gestation (De Coppi et al., 2007). Amniotic fluid has also been cited as a source of MSCs, with potential far-reaching implications for such areas as prenatal diagnosis and gene therapy (Pieternella et al., 2003).

2.3.2 Isolation of primary MSCs

Mesenchymal stem cells have been isolated from human and a number of other species, such as rat (Santa Maria et al., 2004), mouse (Baddoo et al., 2003), horse (Ringe et al., 2003), cow (Bosnakovski et al., 2005), pig (Moscoso et al., 2005), dog (Silva et al., 2005), sheep (Rhodes et al., 2004) and baboon (Devine et al., 2001). Three main approaches have been described for the isolation of MSCs and can either be used independently or combined together to obtain a more homogeneous culture. The traditional isolation method relies on the fact that MSCs selectively adhere to

plastic surfaces, whereas hematopoietic cells do not and can therefore be removed through medium changes (Luria et al., 1971). While this eliminates most contaminating cells, the remaining heterogeneity of the culture progressively decreases by serial passaging and after a number of passages the culture is enriched in the self-renewing fraction, the stem cells. Another published isolation protocol involves centrifugation over a Percoll gradient, which separates cell populations based on their density and allows the enrichment of nucleated cells (Dazzi et al., 2006). However, both methods are quite nonspecific and an approach that is now increasingly being used, resorts to sorting of bone marrow populations by flow cytometry (FACS), based on MSC reactivity to a number of antibodies. This can either be achieved by positively selecting for expressed antigens or by a process of immunodepletion of cells expressing hematopoietic and/or other lineage antigens. For instance, antibodies against CD34, a surface marker found on hematopoietic cells, are frequently used to identify and remove nonmesenchymal cells from a marrow culture (Pittenger et al., 1999). Since there is no single specific marker available to unequivocally identify the MSC, different groups have opted for a variety of marker combinations. MSCs appear relatively stable as primary cultures (Mareschi et al., 2006; Bernardo et al., 2007), although spontaneous transformation events have been observed in long-term cultures (De la Fuente et al., 2010).

2.3.3 *In vitro* characteristics of MSCs

The identification of MSCs remains elusive (Dominici et al., 2006) and

relies upon the ability of the cells to differentiate *in vitro* into multiple lineages and the expression of CD13, CD29, CD31, CD44, CD54, CD63, CD73, CD 90, CD105, CD106, CD140b, CD166, Stro1 as well as the absence of hematopoietic markers (Pittenger et al., 1999; Colter et al., 2000). Comparisons of the various combinations used by different investigators show that the majority of subsets include either CD29, CD105 or both. Although these markers have been used by various groups, there is still no general consensus on the optimal marker combination for MSCs. In the absence of a specific cell marker, MSCs may well incorporate a number of different cell populations all potentially variable in their phenotypic and growth characteristics, with mesenchymal differentiation as a common denominator.

2.3.4 Self-renewing potential of MSCs

One of the defining characteristics of stem cells is their self-renewal potential, the ability to generate identical copies of themselves through mitotic division over extended periods (Gronthos et al., 2003). It has been proposed that stem cells are in an *in vivo* resting state and only divide when a stimulus is provided by neighboring cells in the microenvironments (Wilson and Trumpp, 2006; Moore and Lemischka, 2006). Depending on the stimulus, cells are known to undergo either symmetric or asymmetric division, thus the stem cell pool is kept constant but may expand in case of an injury or damage (Satija et al., 2007).

As a population, bone marrow derived MSCs have been demonstrated to have a significant but highly variable self-renewal potential during *in vitro* serial

propagation (Colter et al., 2000). Their entry into the cell cycle and subsequent development into colonies depend on serum growth factors, such as basic fibroblast growth factor-2 (FGF-2) which have been demonstrated to maintain human bone marrow stromal cells in an immature state during *in vitro* expansion (Martin et al., 1997; Bianchi et al., 2003). Cell seeding density also plays a role in the expansion capacity of MSCs. Colter et al. demonstrated that higher expansion profiles of MSCs can be attained when plated at low density (1.5-3 cells/cm²) resulting in the remarkable increase in the fold expansion of total cells (Colter et al., 2000). Similar results were obtained by other researchers suggesting that MSC clones are highly heterogeneous with respect to their self-renewal capacity (Bianco et al., 2001; Basksh et al., 2004). In addition, coordinated activities of a number of signaling pathways, such as Wnt, Notch and BMP, have been reported to influence the process of self-renewal in a context dependent manner (Satija et al., 2007). In order to harness the clinical potential of MSCs, new protocols must be established which allows the generation of large numbers of MSCs without affecting their differentiation potential so as to meet the needs of tissue engineering.

2.5.5 Differentiation potential of MSCs

Considerable research has been done in assessing the ability of MSCs derived from a variety of different species to develop into terminally differentiated mesenchymal phenotypes both *in vitro* and *in vivo*. The commitment and differentiation of MSCs to specific matured cell types was influenced by the activities

of various transcription factors, cytokines, growth factors and extracellular matrix molecules. An optimal culturing strategy would involve mimicking the *in vivo* environment of MSCs. Under defined inductive conditions, MSCs are able to acquire characteristics of cells derived from embryonic mesoderm such as osteoblasts, chondrocytes, adipocytes, tendon cells, as well as cells possessing ectodermal and neuronal properties (Baksh et al., 2004) (Fig. 2.3). However, the molecular mechanisms that govern MSCs differentiation are incompletely understood. As lack of standard characterization method for other source of MSCs, bone marrow is still a traditional source of MSCs. Recently, MSCs from bone marrow have been shown to develop into various terminally differentiated cells and tissues including bone, cartilage, fat, muscle, tendon, pancreatic, neural tissue and liver (Johnstone et al., 1998; Wakitani et al., 2002; Ryden et al., 2003; Woodbury et al., 2000; Sanchez-Ramos et al., 2000; Deng et al., 2001; Lee et al., 2004a; Shu et al., 2004). Since bone marrow derived MSCs hold promising for cell therapy, further research on characterizing their phenotype, understanding their mechanisms of action, optimizing their *in vitro* expansion, investigating their differentiation mechanism, and tracing their *in vivo* migration are necessary before clinical use.

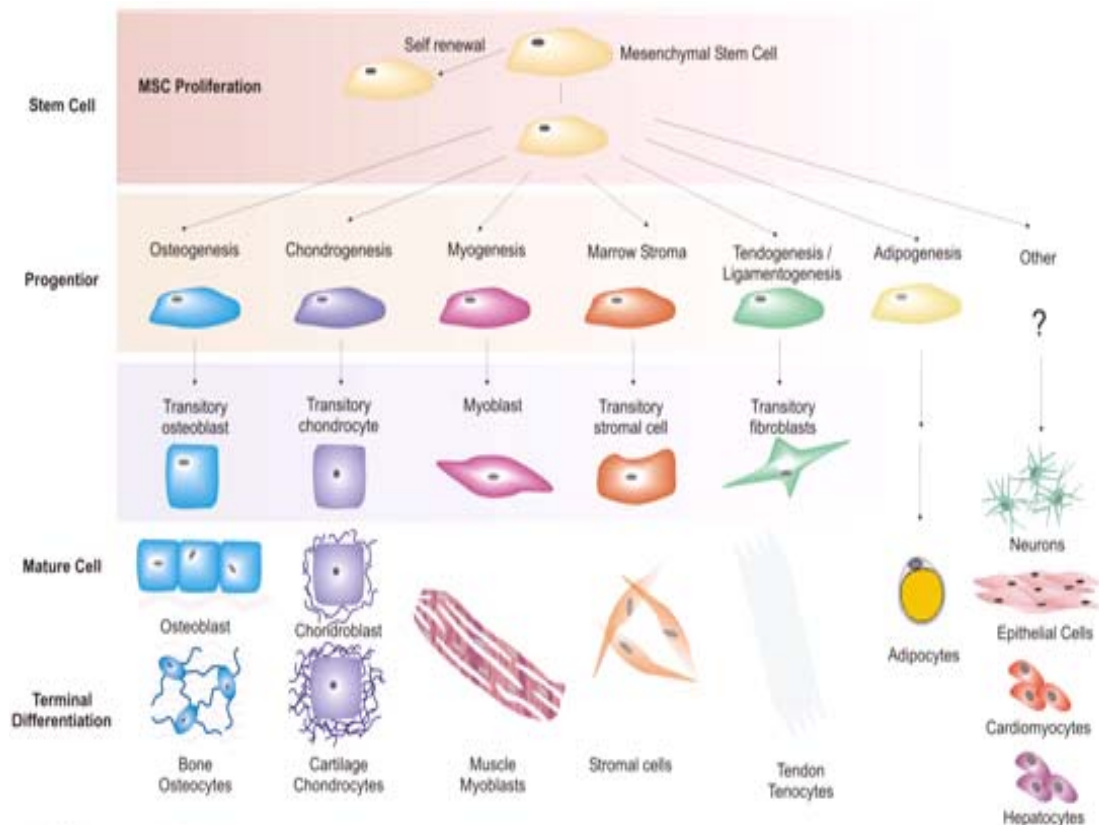


Figure 2.3 Mesenchymal stem cells multilineage differentiation potential. The stepwise cellular transitions from the putative mesenchymal stem cell to highly differentiated phenotypes are depicted schematically (Caplan and Bruder, 2001).

2.4 Hepatogenic differentiation of mesenchymal stem cell

2.4.1 Early liver development

The process of liver development can be divided into several distinct stages based on molecular and functional properties (Fig. 2.4). Each stage of cell growth and differentiation is tightly regulated by extra- and intra-cellular communications, as well as cell autonomous mechanisms. The most essential extracellular signals include

fibroblast growth factors (FGFs), bone morphogenic proteins (BMP), Nodal (activin), hepatocyte growth factor (HGF), and oncostatin M (OSM) (Kinoshita and Miyajima, 2002; Lemaigre and Zaret, 2004; Zhao and Duncan, 2005; Clotman and Lemaigre, 2006; Shafritz et al., 2006). At the intracellular level, the liver-enriched transcription factors hepatocyte nuclear factor (HNF) 3 α , β , HNF4 α , HNF1 α , β , HNF6, and CCAAT enhancer binding protein (C/EBP) α , β act consecutively, in essence, in a cross-regulatory manner, at specific developmental stages to regulate liver-specific gene expression (Duncan, 2000; Kinoshita and Miyajima, 2002; Lemaigre and Zaret, 2004; Zhao and Duncan, 2005; Kyrmizi et al., 2006).

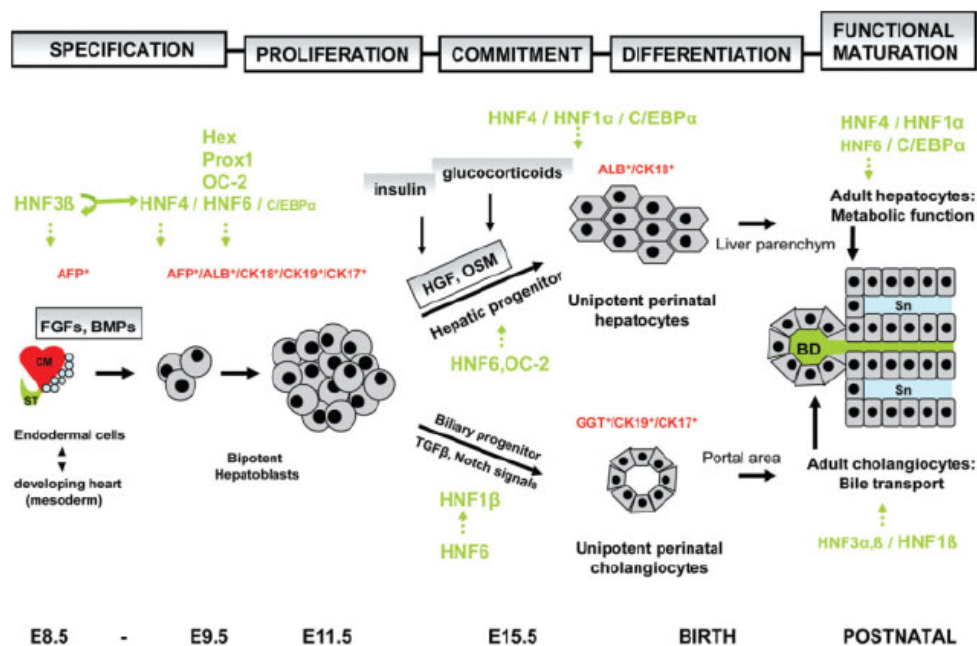


Figure 2.4 Schematic presentation of fetal liver development. (Snykers et al., 2008).

The initial event in the development is the commitment of the foregut endoderm stem cells to the hepatic epithelial lineages, which was regulated by FGFs (FGF1 and basic bFGF) from the cardiogenic mesoderm cells and BMPs (BMP2,

BMP4 and BMP5) from the septum transversum mesenchyme (Duncan, 2000; Kinoshita and Miyajima, 2002; Lemaigre and Zaret, 2004). At approximately rodent E9.0-9.5, cells start to massively proliferate and bud into the stromal environment of the septum transversum mesenchyme. The cells defined as bipotent hepatoblasts at this stage. Then (at rodent around E11-12), the liver primarily becomes a primarily hematopoietic organ. Hematopoietic stem cells (HSCs) which form the extrahepatic organ colonize the liver bud and secrete a growth signal for the liver, thereby, hepatoblasts continue to proliferate (Kinoshita and Miyajima, 2002; Lemaigre and Zaret, 2004). At commitment stage, three cells population which include bipotential hepatoblast, cholangiocyte-committed progenitor cells and hepatocyte-committed cells exist. Notch signaling pathways regulates the differentiation along the cholangiocytic lineage (Duncan, 2000; Lemaigre and Zaret, 2004; Shafritz et al., 2006). Mesenchymal cells or nonparenchymal liver cells excrete HGF, which support the growth and differentiation of the fetal hepatocytes and hormone insulin, synergistically promotes this effect (Shafritz et al., 2006; Kinoshita and Miyajima, 2002; Kamiya et al., 2001). Subsequently, cooperative action of OSM, mostly produced by HSCs, together with glucocorticoids induces partial hepatic maturation and suppression of embryonic hematopoiesis (Shafritz et al., 2006; Zhao and Duncan, 2005; Kinoshita and Miyajima, 2002; Kamiya et al., 2001). Kinoshita and Miyajima demonstrated that OSM alone fails to induce differentiated liver phenotypes, implying the essence of glucocorticoids as triggers for hepatic maturation (Kinoshita and

Miyajima, 2002). Meanwhile, the number of bipotential hepatoblast is markedly reduced. Although cells continue to proliferate, most of them are unipotent and irreversibly committed to either the hepatocytic or cholangiocytic lineage (Shafritz et al., 2006; Zhao and Duncan, 2005; Lemaigre and Zaret, 2004). Complete functional hepatic maturation ultimately takes place after birth upon coassistance of HGF, produced by the surrounding nonparenchymal liver cells like sinusoidal, stellate, and endothelial cells (Kamiya et al., 2001).

2.4.2 Hepatocyte differentiation of mesenchymal stem cells

Mesenchymal stem cell differentiation to hepatocyte is driven by complex processes that are only beginning to be understood. The natural developmental process provides a great deal of information. Several growth factors and hormones are used to mimic these processes. Yet, the complexity of interactions between various cell types and their temporal changes make it difficult to replicate this process. On the other hand, non-natural or semi-toxic chemical drugs are often used to reset the cell's preprogrammed status with some success.

2.4.2.1 Growth factors/Cytokines/Corticosteroids/Hormones

The pioneer study of hepatic differentiation of mesenchymal stem cells was discovered by Verfaillie and coworkers, who demonstrated that multipotent adult progenitor cells (MAPCs) found within adult bone marrow exposure to FGF + HGF + insulin-transferrin-sodium selenite (ITS) + dexamethasone gained the ability to undergo hepatic differentiation. MAPCs transformed into cells with morphological,

phenotypic, and functional characteristics of hepatocytes (Schwartz et al., 2002). However, the resultant population was far from homogeneous. Significantly optimized differentiation was obtained via exposure of bone marrow stem cells to the same hepatogenic factors, but in a time-specific sequential manner, reflecting their secretion pattern during the hepatogenesis *in vivo*. More than 85% of the thus sequentially cultured cells featured a highly differentiated hepatic phenotype and functionality, including inducible cytochrome P450 (CYP)-dependent activity (Snykers et al., 2006). The following studies showed that added either as a mixture (FGF + HGF; FGF + HGF + OSM) or separately (HGF; HGF/OSM; FGF/HGF/OSM) stimulation of MSCs which result in expression of distinct hepatocyte markers and functions, that is, albumin and urea secretion, glycogen storage, and low-density lipoprotein uptake (Kang et al., 2005; Shi et al., 2005; Li et al., 2006; Hong et al., 2005; Lee et al., 2004a). The same result obtained by combinations thereof FGF + HGF followed by OSM (Ong et al., 2006; Talens-Visconti et al., 2006). In contrast, others emphasized the necessity of supplementary differentiation-inducing factors to enforce functional hepatic conversion of MSCs (Lange et al., 2005). Basically, soluble medium factors such as dexamethasone, ITS, and nicotinamide synergistically affect the hepatic driving pathways (Seo et al., 2005). In sharp contrast to the critical role of serum in MSC expansion, serum-free conditions have been successfully applied on a routine basis for hepatic differentiation of MSCs (Lee et al., 2004a; Talens-Visconti et al., 2006; Lange et al., 2005; Seo et al., 2005).

2.4.2.2 Reconstruction of *in vivo* cell-matrix and cell-cell interactions

Cocultures of stromal bone marrow cells with primary hepatocytes were at first designated to develop long-term functional hepatic *in vitro* models (Mizuguchi et al., 2001). Jagged1 protein was considered responsible for the benign effects on hepatocyte differentiation by mediating differentiation events via the Notch signaling pathway (Mizuguchi et al., 2001; Okumoto et al., 2003). Later, Jagged1 and Notch were considered essential in drive bone marrow progenitors toward hepatocyte-lineage cells (Okumoto et al., 2003). In a recent study by Lange et al., coculture with liver cells was claimed to be the sole trigger able to shift MSC into cells with a hepatobiliary phenotype (Lange et al., 2005). The impaired differentiation capability of the chosen clonal MSCs or the high purity of high passaged MSCs (thus not contaminated with hematopoietic stem cells) was held responsible for failing growth factor-stimulated hepatic differentiation. Another critical factor affecting cellular differentiation status is the spatial distribution between cells (Aurich et al., 2007; Luk et al., 2005). Differentiation is usually initiated upon 60%–100% confluence. Significantly promoted hepatic differentiation in areas of highest cellular density (maximal cell-cell contact) versus that in lower cellular density emphasized the relevance of intercellular communication during differentiation processes (Schwartz et al., 2002; Snykers et al., 2006; Hong et al., 2005; Ong et al., 2006; Aurich et al., 2007; Snykers et al., 2007). Minor roles are ascribed to the type of coatings used. The natural scaffold collagen turns out to be most effective (Snykers et

al., 2006; Snykers et al., 2007).

2.4.2.3 Liver-enriched transcription factors (LETFS) overexpression

By far, only one study has investigated the putative inductive effect of liver enriched transcription factors (LETFS) on hepatic differentiation of MSCs. More specifically, Talens-Visconti et al. confirmed the contribution of C/EBP β in inducing adipose tissue-derived stem cells (ADSCs) and bone marrow-derived MSCs towards hepatocyte, however, C/EBP α failed to driving hepatic differentiation (Talens-Visconti et al., 2006).

2.4.2.4 Epigenetic modification

Epigenetic modification may contribute to overcome cell fate. Snykers et al. found previously that addition of 1 μ M trichostatin A (TSA) to cultured human (h) MSCs, triggers their “transdifferentiation” into cells with phenotypic and functional characteristics similar to those of primary hepatocytes (Snykers et al., 2007). In line with other reports that enhance hepatic differentiation upon addition of 0.1% dimethylsulfoxide (DMSO) to hADSCs, prestimulated for 10 days with a mixture of hepatogenic cytokines (Seo et al., 2005). Recently, DNA methyl transferase inhibitors (DNMTis), either alone or combined with HDACis, also were introduced to alter cell fate (Milhem et al., 2004; Schmittwolf et al., 2005; Sgodda et al., 2007; Yoshida et al., 2007). Basically, DNMTis function as preconditioning agents before hepatic differentiation (Sgodda et al., 2007; Yoshida et al., 2007; Stock et al., 2008), whereas HDACis act as stimulants during or after differentiation (Snykers et

al., 2006; Seo et al., 2005; Yamazaki et al., 2003; De Kock et al., 2008). In general, chromatin remodeling seems to be a potential innovative strategy to overcome cell fate determinism and favor lineage-specific differentiation.

2.4.3 Characterization of hepatocyte-like cells

Stem cell-derived hepatocyte-like cells may be characterized *in vitro* by their morphological, RNA expression, protein expression, and functional activity. Most studies that employed the use of endodermal markers include LETFs (HNF1 α , β , HNF3 β , HNF4 α , and C/EBP α , β), plasma proteins (α -fetoprotein, albumin, transthyretin), and cytoskeletal proteins (CK18, CK8). A minority of studies have examined the expression of CYPs and other “late” enzymes such as tryptophan 2, 3-dioxygenase (TO) and tyrosine amino transferase (TAT).

The differentiation of stem cells toward the hepatocyte lineage often involves uncontrolled processes, resulting in a heterogeneous cell population. Some genes such as AFP and TTR are both expressed in liver tissue and in the extra embryonic yolk sac (Dziadek and Adamson, 1978; Gulbis et al., 1998). Hence, exclusive analysis of one of the latter markers cannot count as proof for a genuine hepatic phenotype. The need thus arises to identify genes that are predominantly expressed in the liver and not in other tissues, enabling an accurate follow-up of the differentiation process and precise characterization of the end populations. So the functional analyses need to be accounted. The ultimate proof of functional hepatic behavior is no doubt *in vivo* transplantation of *ex vivo* generated stem cells-based

hepatic cells in animal models with liver injury (Imamura et al., 2004; Tang et al., 2006; Seo et al., 2005; Aurich et al., 2007; Luk et al., 2005; Sgodda et al., 2007; Brulport et al., 2007). Animal liver disease model like carbon tetrachloride-injured or dimethylnitrosamine-injured murine provides a suitable condition for transplant of *ex vivo* generated stem cells-based hepatic cells. Positive homing, engraftment, repopulation, and functional maturation are basically explored by means of molecular imaging techniques, immunohistochemistry, in situ hybridization, and serology, which give the evidence that stem/progenitor cells could contribute to liver reconstitution. Confirmation of the *in vitro* obtained results via rigorous *in vivo* tools might shed light on the therapeutic potential of stem/progenitor cells in various acute and chronic liver disorders.

2.5 Fourier transforms infrared (FTIR) microspectroscopy

FTIR microspectroscopy is a form of absorption spectroscopy that detects the vibrational characteristics of chemical functions within a sample by interrogating the absorption spectra of the sample using the mid-infrared region of light. Changes in the dipole moment of the sample molecule when infrared light is incident on it produces an absorption spectrum in a very specific wave number range characteristic for the chemical functional groups within that molecule. Both qualitative and quantitative information about chemical composition, functional group, and conformation may be determined. Thus, by analyzing the absorption spectrum, the biochemical nature of

the sample can be elucidated. FTIR microspectroscopy has been widely used in biophysical research, proven to provide sensitive and precise measurement of biochemical changes in biological cells and tissue (Lasch and Boese, 2002).

This method has been recognized as an analytical tool in medical diagnostics. The differences in the absorbance spectra in the mid-IR region between normal and abnormal tissue have been shown to be a possible criterion for detection and characterization of various tissue sample, such as breast (Fabian et al., 1995), colon (Lasch et al., 1998), cervix (Chiriboga et al., 1998; skin (McIntosh et al., 1999), oral mucosa (Fukuyama et al., 1999), heart (Liu et al., 1999), liver (Chiriboga et al., 2000), lung (Yano et al., 2000) and brain (Kneipp et al., 2002). It also have been employed to study human (Bentley et al., 2007; Hoshino et al., 2007; Krafft et al., 2007; Heraud et al., 2010) and murine stem cells (Ami et al., 2008; Tanthanuch et al., 2010) characterization and differentiation by detecting and defining biochemical changes occurring during the differentiation process in the cells. These studies demonstrated that different cell types possessed distinct IR spectral phenotypes, which can be used to distinguish between stem cells and their derivatives. This approach has an ability to characterize different cell types by sensitive IR spectroscopic fingerprints and give the information changes in macromolecular cellular components such as lipids, proteins nucleic acids and carbohydrates (Miler et al., 2003) which seen as an easy, rapid, sensitive, nondestructive, noninvasive, label-free method which can be applied to monitoring or sorting large populations of cells (Downes et al., 2010).

Recently, synchrotron infrared microspectroscopy has been used for the early detection of liver fibrosis (Liu et al., 2006). FTIR imaging analysis could become a valuable analytic method in brain tumor research and possibly in the diagnosis of human brain tumours (Bamberg et al., 2006). Wang et al. used FTIR microspectroscopy to study the compositional changes in inflammatory cardiomyopathy and the results demonstrate chemical difference between the inflammatory responses in mouse model, providing insight into why the disease can be self-limiting in some cases while fatal in others (Wang et al., 2005).

2.6 References

- Ami, D., Neri, T., Natalello, A., Mereghetti, P., Doglia, S. M., Zanoni, M., Zuccotti, M., Garagna, S. and Redi, C. A. (2008). Embryonic stem cell differentiation studied by FT-IR spectroscopy. **Biochim. Biophys. Acta.** 1783: 98-106.
- Aurich, I., Mueller, L. P., Aurich, H., Luetzkendorf, J., Tisljar, K., Dollinger, M. M., Schormann, W., Walldorf, J., Hengstler, J. G., Fleig, W. E. and Christ, B. (2007). Functional integration of human mesenchymal stem cell-derived hepatocytes into mouse livers. **Gut.** 56: 405-415.
- Baddoo, M., Hill, K., Wilkinson, R., Gaupp, D., Hughes, C., Kopen, G. C. and Phinney, D. G. (2003). Characterization of mesenchymal stem cells isolated from murine bone marrow by negative selection. **J. Cell Biochem.** 89: 1235-1249.

- Baksh, D., Song, L. and Tuan, R. S. (2004). Adult mesenchymal stem cells: characterization, differentiation, and application in cell and gene therapy. **J. Cell Mol. Med.** 8: 301-316.
- Ballas, C. B., Zielske, S. P. and Gerson, S. L. (2002). Adult bone marrow stem cells for cell and gene therapies: implications for greater use. **J. Cell. Biochem. Suppl.** 38: 20-28.
- Bamberg, K. R., Schultke, E., Wood, B. R., MacDonald, S. T. R., Ataelmannan, K., Griebel, R. W., Juurlink, B. H. J. and McNaughton, D. (2006). A fourier transform infrared microspectroscopic imaging investigation into an animal model exhibiting glioblastoma multiforme. **Bioch. Biophys. Acta.** 1758: 900-907.
- Barnabe-Heider, F. and Frisen, J. (2008). Stem cells for spinal cord repair. **Cell Stem Cell** 3: 16-24.
- Bentley, A. J., Nakamura, T., Hammiche, A., Pollock, H. M., Martin, F. L., Kinoshita, S. and Fullwood, N. J. (2007). Characterization of human corneal stem cells by synchrotron infrared micro-spectroscopy. **Mol. Vis.** 13: 237-242.
- Bernardo, M. E., Avanzini, M. A., Perotti, C., Cometa, A. M., Moretta, A., Lenta, E., Del Fante, C., Novara, F., de Silvestri, A., Amendola, G., Zuffardi, O., Maccario, R. and Locatelli, F. (2007). Optimization of *in vitro* expansion of human multipotent mesenchymal stromal cells for cell-therapy approaches: further insights in the search for a fetal calf serum substitute. **J. Cell Physiol.**

211: 121-130.

Bianchi, G., Banfi, A., Mastrogiacomo, M., Notaro, R., Luzzatto, L. and Cancedda, R. and Quarto, R. (2003). *Ex vivo* enrichment of mesenchymal cell progenitors by fibroblast growth factor 2. **Exp. Cell Res.** 287: 98-105.

Bianco, P., Riminucci, M., Gronthos, S. and Robey, P. G. (2001). Bone marrow stromal stem cells: nature, biology, and potential applications. **Stem Cells** 19: 180-192.

Bosnakovski, D., Mizuno, M., Kim, G., Takagi, S., Okumura, M. and Fujinaga, T. (2005). Isolation and multilineage differentiation of bovine bone marrow mesenchymal stem cells. **Cell Tissue Res.** 319: 243-253.

Brulport, M., Schormann, W., Bauer, A., Hermes, M., Elsner, C., Hammersen, F. J., Beerheide, W., Spitkovsky, D., Härtig, W., Nussler, A., Horn, L. C., Edelmann, J., Pelz-Ackermann, O., Petersen, J., Kamprad, M., von Mach, M., Lupp, A., Zulewski, H. and Hengstler, J. G. (2007). Fate of extrahepatic human stem and precursor cells after transplantation into mouse livers. **Hepatology** 46: 861-870.

Caplan, A. I. and Bruder, S. P. (2001). Mesenchymal stem cells: building blocks for molecular medicine in the 21st century. **Trends Mol. Med.** 7: 259-264.

Chiriboga, L., Xie, P., Yee, H., Vigorita, V., Zarou, D., Zakim, D. and Diem, M. (1998). Infrared spectroscopy of human tissue. I. Differentiation and maturation of epithelial cells in the human cervix. **Biospectroscopy** 4: 47-53.

- Chiriboga, L., Yee, H. and Diem, M. (2000). Infrared Spectroscopy of Human Cells and Tissue. Part VI: A Comparative Study of Histopathology and Infrared Microspectroscopy of Normal, Cirrhotic, and Cancerous Liver Tissue. **Applied Spectroscopy** 54: 1-8.
- Chung, H., Kim, K. H., Kim, J. G., Lee, S. Y. and Yoon, Y. H. (2007). Retinal complications in patients with solid organ or bone marrow transplantations. **Transplantation** 83: 694-699.
- Clotman, F. and Lemaigre, F. P. (2006). Control of hepatic differentiation by activin/TGF β signaling. **Cell Cycle** 5: 168-171.
- Colter, D. C., Class, R., DiGirolamo, C. M. and Prockop, D. J. (2000). Rapid expansion of recycling stem cells in cultures of plastic-adherent cells from human bone marrow. **Proc. Natl. Acad. Sci. U S A** 97: 3213-3218.
- Dazzi, F., Ramasamy, R., Glennie, S., Jones, S. P. and Roberts, I. (2006). The role of mesenchymal stem cells in haemopoiesis. **Blood Rev.** 20: 161-171.
- De Coppi, P. D., Bartsch, G., Siddiqui, M. M., Xu, T., Santos, C. C., Perin, L., Mostoslavsky, G., Serre, A. C., Snyder, E. Y., Yoo, J. J., Furth, M. E., Soker, S. and Atala, A. (2007). Isolation of amniotic stem cell lines with potential for therapy. **Nat. Biotechnol.** 25: 100-106.
- De Kock, J., Vanhaecke, T., Rogiers, V. and Snykers, S. (2008). Chromatin remodelling, a novel strategy to expedite the hepatic differentiation of adult bone marrow stem cells *in vitro*. **Aatex** 14: 605-611.

- De la Fuente, R., Bernad, A., Garcia-Castro, J., Martin, M. C. and Cigudosa, J. C. (2010). Retraction: Spontaneous human adult stem cell transformation. **Cancer Res.** 70: 6682.
- Deng, W., Obrocka, M., Fischer, I. and Prockop, D. J. (2001). *In vitro* differentiation of human marrow stromal cells into early progenitors of neural cells by conditions that increase intracellular cyclic AMP. **Biochem. Biophys. Res. Commun.** 282: 148-152.
- Devine, S. M., Bartholomew, A. M., Mahmud, N., Nelson, M., Patil, S., Hardy, W., Sturgeon, C., Hewett, T., Chung, T., Stock, W., Sher, D., Weissman, S., Ferrer, K., Mosca, J., Deans, R., Moseley, A. and Hoffman, R. (2001). Mesenchymal stem cells are capable of homing to the bone marrow of non-human primates following systemic infusion. **Exp. Hematol.** 29: 244-255.
- Dominici, M., Blanc, K., Mueller, I., Slaper-Cortenbach, I., Marini, F., Krause, D., Deans, R., Keating, A., Prockop, D.J. and Horwitz, E. (2006). Minimal criteria for defining multipotent mesenchymal stromal cells. The International Society for Cellular Therapy position statement. **Cytherapy** 8: 315-317.
- Downes, A., Mouras, R. and Elfick, A. (2010). Optical spectroscopy for noninvasive monitoring of stem cell differentiation. **J. Biomed. Biotechnol.** 101864.
- Duncan, S. A. (2000). Transcriptional regulation of liver development. **Dev. Dyn.** 219: 131-142.

- Dziadek, M. and Adamson, E. (1978). Localization and synthesis of α -foetoprotein in post-implantation mouse embryos. **J. Embryol. Exp. Morphol.** 43: 289-313.
- Fabian, H., Jackson, M., Murphy, L., Watson, P. H., Fichtner, I. and Mantsch, H. H. (1995). A comparative IR study of human breast tumors and breast tumor xenografts. **Biospectroscopy** 1: 37-45.
- Francoz, C., Belghiti, J. and Durand, F. (2007). Indications of liver transplantation in patients with complications of cirrhosis. **Best Pract. Res. Clin. Gastroenterol.** 21: 175-190.
- Friedenstein, A. J., Gorskaja, J. F. and Kulagina, N. N. (1976). Fibroblast precursors in normal and irradiated mouse hematopoietic organs. **Exp. Hematol.** 4: 267-274.
- Fukuyama, Y., Yoshida, S., Yanagisawa, S. and Shimizu, M. (1999). A study on the differences between oral squamous cell carcinomas and normal oral mucosas measured by Fourier transform infrared spectroscopy. **Biospectroscopy** 5: 117-126.
- Gaia, S., Smedile, A., Omede, P., Olivero, A., Sanavio, F., Balzola, F., Ottobrelli, A., Abate, M. L., Marzano, A., Rizzetto, M. and Tarella, C. (2006). Feasibility and safety of G-CSF administration to induce bone marrow-derived cells mobilization in patients with end stage liver disease. **J. Hepatol.** 45: 13-19.
- Gill, R. Q. and Sterling, R. K. (2001). Acute liver failure. **J. Clin. Gastroenterol.** 33: 191-198.

- Gordon, M. Y., Levicar, N., Pai, M., Bachellier, P., Dimarakis, I., Al-Allaf, F., M'Hamdi, H., Thalji, T., Welsh, J. P., Marley, S. B. Davies, J, Dazzi F, Marelli-Berg, F., Tait, P., Playford, R., Jiao, L., Jensen, S., Nicholls, J. P., Ayav, A., Nohandani, M., Farzaneh, F., Gaken, J., Dodge, R., Alison, M., Apperley, J. F., Lechler, R. and Habib, N. A. (2006). Characterization and clinical application of human CD34⁺ stem/progenitor cell populations mobilized into the blood by granulocyte colony-stimulating factor. **Stem Cells** 24: 1822-1830.
- Gronthos, S., Brahim, J., Li W., Fisher, L. W., Cherman, N., Boyde, A., DenBesten, P., Gehron Robey, P. and Shi, S. (2002). Stem cell properties of human dental pulp stem cells. **J. Dent. Res.** 81: 531-535.
- Gronthos, S., Zannettino, A. C., Hay, S. J., Shi, S., Graves, S. E., Kortessidis, A. and Simmons, P. J. (2003). Molecular and cellular characterization of highly purified stromal stem cells derived from human bone marrow. **J. Cell Sci.** 116: 1827-1835.
- Gulbis, B., Jauniaux, E., Cotton, F. and Stordeur, P. (1998). Protein and enzyme patterns in the fluid cavities of the first trimester gestational sac: relevance to the absorptive role of secondary yolk sac. **Mol. Hum. Reprod.** 4: 857-862.
- Gupta, D. K., Sharma, S., Venugopal, P., Kumar, L., Mohanty, S. and Dattagupta, S. (2007). Stem cells as a therapeutic modality in pediatric malformations. **Transplant Proc.** 39: 700-702.

- Gurtner, G. C., Callaghan, M. J. and Longaker, M. T. (2007). Progress and potential for regenerative medicine. **Annu. Rev. Med.** 58: 299-312.
- Heraud, P., Ng, E. S., Caine, S., Yu, Q. C., Hirst, C., Mayberry, R., Bruce, A., Wood, B. R., McNaughton, D., Stanley, E. G. and Elefanty, A. G. (2010). Fourier transform infrared microspectroscopy identifies early lineage commitment in differentiating human embryonic stem cells. **Stem Cell Res.** 4: 140-147.
- Hong, S. H., Gang, E. J., Jeong, J. A., Ahn, C., Hwang, S. H., Yang, I. H., Park, H. K., Han, H. and Kim, H. (2005). *In vitro* differentiation of human umbilical cord blood-derived mesenchymal stem cells into hepatocyte-like cells. **Biochem. Biophys. Res. Commun.** 330: 1153-1161.
- Hoshino, K., Ly, H. Q., Frangioni, J. V. and Hajjar, R. J. (2007). *In vivo* tracking in cardiac stem cell-based therapy. **Prog. Cardiovasc. Dis.** 49: 414-420.
- Imamura, T., Cui, L., Teng, R., Johkura, K., Okouchi, Y., Asanuma, K., Ogiwara, N. and Sasaki, K. (2004). Embryonic stem cell-derived embryoid bodies in three-dimensional culture system form hepatocyte-like cells *in vitro* and *in vivo*. **Tissue Eng.** 10: 1716-1724.
- Jiang, Y., Jahagirdar, B. N., Reinhardt, R. L., Schwartz, R. E., Keene, C. D., Ortiz-Gonzalez, X. R., Reyes, M., Lenvik, T., Lund, T., Blackstad, M., Du, J., Aldrich, S., Lisberg, A., Low, W., Largaespada, D. A. and Verfaillie, C. M. (2002). Pluripotency of mesenchymal stem cells derived from adult marrow. **Nature** 418: 41-49.

- Johnstone, B., Hering, T. M., Caplan, A. I., Goldberg, V. M. and Yoo, J. U. (1998). *In vitro* chondrogenesis of bone marrow-derived mesenchymal progenitor cells. **Exp. Cell Res.** 238: 265-272.
- Kamiya, A., Kinoshita, T. and Miyajima, A. (2001). Oncostatin M and hepatocyte growth factor induce hepatic maturation via distinct signaling pathways. **FEBS Lett.** 492: 90-94.
- Kang, X. Q., Zang, W. J., Bao, L. J., Li, D. L., Song, T. S., Xu, X. L. and Yu, X. J. (2005). Fibroblast growth factor-4 and hepatocyte growth factor induce differentiation of human umbilical cord blood-derived mesenchymal stem cells into hepatocytes. **World J. Gastroenterol.** 11: 7461-7465.
- Kinoshita, T. and Miyajima, A. (2002). Cytokine regulation of liver development. **Biochim. Biophys. Acta.** 1592: 303-312.
- Kneipp, J., Beekes, M., Lasch, P. and Naumann, D. (2002). Molecular changes of preclinical scrapie can be detected by infrared spectroscopy. **J. Neurosci.** 22: 2989-2997.
- Krafft, C., Salzer, R., Seitz, S., Ern, C. and Schieker, M. (2007). Differentiation of individual human mesenchymal stem cells probed by FTIR microscopic imaging. **Analyst** 132: 647-653.
- Kyrmizi, I., Hatzis, P., Katrakili, N., Tronche, F., Gonzalez, F. J. and Talianidis, I. (2006). Plasticity and expanding complexity of the hepatic transcription factor network during liver development. **Genes. Dev.** 20: 2293-2305.

- Lange, C., Bassler, P., Lioznov, M. V., Bruns, H., Kluth, D., Zander, A. R. and Fiegel, H. C. (2005). Hepatocytic gene expression in cultured rat mesenchymal stem cells. **Transplant Proc.** 37: 276-279.
- Lasch, P. and Boese, M. (2002). FT-IR spectroscopic investigations of single cells on the subcellular level. **Vibrational Spectroscopy** 28: 147-157.
- Lasch, P., Wasche, W., McCarthy, W.J., Muller G. and Naumann, D. (1998). Imaging of human colon carcinoma thin sections by FT-IR microspectrometry Proc. **SPIE** 3257: 187.
- Lee, K. D., Kuo, T. K., Whang-Peng, J., Chung, Y. F., Lin, C. T., Chou, S. H., Chen, J. R., Chen, Y. P. and Lee, O. K. (2004a). *In vitro* hepatic differentiation of human mesenchymal stem cells. **Hepatolog.** 40: 1275-1284.
- Lee, O. K., Kuo, T. K., Chen, W. M., Lee, K. D., Hsieh, S. L. and Chen, T. H. (2004b). Isolation of multipotent mesenchymal stem cells from umbilical cord blood. **Blood** 103: 1669-1675.
- Lemaigre, F. and Zaret, K. S. (2004). Liver development update: new embryo models, cell lineage control, and morphogenesis. **Curr. Opin. Genet. Dev.** 14: 582-590.
- Li, W., Liu, S. N., Luo, D. D., Zhao, L., Zeng, L. L., Zhang, S. L. and Li, S. L. (2006). Differentiation of hepatocytoid cell induced from whole-bone-marrow method isolated rat myeloid mesenchymal stem cells. **World J. Gastroenterol.** 12: 4866-4869.

- Liu, K. Z., Dixon, I. M. and Mantsch, H. H. (1999). Distribution of collagen deposition in cardiomyopathic hamster hearts determined by infrared microscopy. **Cardiovasc. Pathol.** 8: 41-47.
- Liu, K. Z., Man, A., Shaw, R. A., Liang, B., Xu, Z. L. and Gong, Y. W. (2006). Molecular determination of liver fibrosis by synchrotron infrared microspectroscopy. **Bioch. Biophys. Acta.** 1758: 960-967.
- Luk, J. M., Wang, P. P., Lee, C. K., Wang, J. H. and Fan, S. T. (2005). Hepatic potential of bone marrow stromal cells: development of *in vitro* co-culture and intra-portal transplantation models. **J. Immunol. Methods** 305: 39-47.
- Luria, E. A., Panasyuk, A. F. and Friedenstein, A. Y. (1971). Fibroblast colony formation from monolayer cultures of blood cells. **Transfusion** 11: 345-349.
- Lyra, A. C., Soares, M. B., da Silva, L. F., Fortes, M. F., Silva, A. G., Mota, A. C., Oliveira, S. A., Braga, E. L., de Carvalho, W. A., Genser, B. Dos Santos, R. R. and Lyra, L. G. (2007). Feasibility and safety of autologous bone marrow mononuclear cell transplantation in patients with advanced chronic liver disease. **World J. Gastroenterol.** 13: 1067-1073.
- Mareschi, K., Ferrero, I., Rustichelli, D., Aschero, S., Gammaitoni, L., Aglietta, M., Madon, E. and Fagioli, F. (2006). Expansion of mesenchymal stem cells isolated from pediatric and adult donor bone marrow. **J. Cell Biochem.** 97: 744-754.
- Martin, I., Muraglia, A., Campanile, G., Cancedda, R. and Quarto, R. (1997).

- Fibroblast growth factor-2 supports *ex vivo* expansion and maintenance of osteogenic precursors from human bone marrow. **Endocrinology** 138: 4456-4462.
- Mason, C. and Dunnill, P. (2008). A brief definition of regenerative medicine. **Regen. Med.** 3: 1-5.
- McIntosh, L. M., Jackson, M., Mantsch, H. H., Stranc, M. F., Pilavdzic, D. and Crowson, A. N. (1999). Infrared spectra of basal cell carcinomas are distinct from non-tumor-bearing skin components. **J. Invest. Dermatol.** 112: 951-956.
- Miler, L. M., Smith, G. D. and Carr, G. L. (2003). Synchrotron-based biological microspectroscopy: From the mid- to the far-infrared regimes. **J. Biol. Phys.** 29: 219-239.
- Milhem, M., Mahmud, N., Lavelle, D., Araki, H., DeSimone, J., Sauntharajah, Y. and Hoffman, R. (2004). Modification of hematopoietic stem cell fate by 5-aza 2'-deoxycytidine and trichostatin A. **Blood** 103: 4102-4110.
- Mizuguchi, T., Hui, T., Palm, K., Sugiyama, N., Mitaka, T., Demetriou, A. A. and Rozga, J. (2001). Enhanced proliferation and differentiation of rat hepatocytes cultured with bone marrow stromal cells. **J. Cell Physiol.** 189: 106-119.
- Mohamadnejad, M., Alimoghaddam, K., Mohyeddin-Bonab, M., Bagheri, M., Bashtar, M., Ghanaati, H., Baharvand, H., Ghavamzadeh, A. and Malekzadeh, R.

- (2007a). Phase 1 trial of autologous bone marrow mesenchymal stem cell transplantation in patients with decompensated liver cirrhosis. **Arch. Iran Med.** 10: 459-466.
- Mohamadnejad, M., Namiri, M., Bagheri, M., Hashemi, S. M., Ghanaati, H., Zare Mehrjardi, N., Kazemi Ashtiani, S., Malekzadeh, R. and Baharvand, H. (2007b). Phase 1 human trial of autologous bone marrow-hematopoietic stem cell transplantation in patients with decompensated cirrhosis. **World J. Gastroenterol.** 13: 3359-3363.
- Moore, K. A. and Lemischka, I. R. (2006). Stem cells and their niches. **Science** 311: 1880-1885.
- Moscoso, I., Centeno, A., Lopez, E., Rodriguez-Barbosa, J. I., Santamarina, I., Filgueira, P., Sanchez, M. J, Dominguez-Perles, R., Peñuelas-Rivas, G. and Domenech, N. (2005). Differentiation "*in vitro*" of primary and immortalized porcine mesenchymal stem cells into cardiomyocytes for cell transplantation. **Transplant Proc.** 37: 481-482.
- Okumoto, K., Saito, T., Hattori, E., Ito, J. I., Adachi, T., Takeda, T., Sugahara, K., Watanabe, H., Saito, K., Togashi, H. and Kawata, S. (2003). Differentiation of bone marrow cells into cells that express liver-specific genes *in vitro*: implication of the Notch signals in differentiation. **Biochem. Biophys. Res. Commun.** 304: 691-695.
- Ong, S. Y., Dai, H. and Leong, K. W. (2006). Hepatic differentiation potential of

commercially available human mesenchymal stem cells. **Tissue Eng.** 12: 3477-3485.

Park, I. H., Zhao, R., West, J. A., Yabuuchi, A., Huo, H., Ince, T. A., Lerou, P. H., Lensch, M. W. and Daley, G. Q. (2008). Reprogramming of human somatic cells to pluripotency with defined factors. **Nature** 451: 141-146.

Patel, A. N. and Genovese, J. A. (2007). Stem cell therapy for the treatment of heart failure. **Curr. Opin. Cardiol.** 22: 464-470.

Patel, H., Vogl, D. T., Aqui, N., Shaked, A., Olthoff, K., Markmann, J., Reddy, R., Stadtmauer, E. A., Schuster, S. and Tsai, D. E. (2007). Posttransplant lymphoproliferative disorder in adult liver transplant recipients: a report of seventeen cases. **Leuk. Lymphoma.** 48: 885-891.

Pieterella, S., Scherjon, S. A., Kleijburg-van der Keur, C., Noort, W. A., Claas, F. H., Willemze, R., Fibbe, W. E. and Kanhai, H. H. (2003). Amniotic fluid as a novel source of mesenchymal stem cells for therapeutic transplantation. **Blood** 102: 1548-1549.

Pittenger, M. F., Mackay, A. M., Beck, S. C., Jaiswal, R. K., Douglas, R., Mosca, J. D., Moorman, M. A., Simonetti, D. W., Craig, S. and Marshak, D. R. (1999). Multilineage potential of adult human mesenchymal stem cells. **Science** 284: 143-147.

Rhodes, N. P., Srivastava, J. K., Smith, R. F. and Longinotti, C. (2004). Heterogeneity in proliferative potential of ovine mesenchymal stem cell colonies. **J. Mater**

Sci. Mater Med. 154: 397-402.

Ringe, J., Haupl, T. and Sitterling, M. (2003). Mesenchymal stem cells for tissue engineering of bone and cartilage. **Med. Klin. (Munich)** 98: 35-40.

Risbud, M. V., Shapiro, I. M., Guttapalli, A., Di Martino, A., Danielson, K. G., Beiner, J. M., Hillibrand, A., Albert, T. J., Anderson, D. G. and Vaccaro, A. R. (2006). Osteogenic potential of adult human stem cells of the lumbar vertebral body and the iliac crest. **Spine** 31: 83-89.

Ryden, M., Dicker, A., Gotherstrom, C., Astrom, G., Tammik, C., Arner, P. and LeBlance, K. (2003). Functional characterization of human mesenchymal stem cell-derived adipocytes. **Biochem. Biophys. Res. Commun.** 311: 391-397.

Sakaguchi, Y., Sekiya, I., Yagishita, K. and Muneta, T. (2005). Comparison of human stem cells derived from various mesenchymal tissues: Superiority of synovium as a cell source. **Arthritis Rheum.** 52: 2521-2529.

Sanchez-Ramos, J., Song, S., Cardozo-Pelaez, F., Hazzi, C., Stedeford, T., Willing, A., Freeman, T. B., Saporta, S., Janssen, W., Patel, N., Cooper, D. R. and Sanberg, P. R. (2000). Adult bone marrow stromal cells differentiate into neural cells *in vitro*. **Exp. Neurol.** 164: 247-256.

Santa Maria, L., Rojas, C. V. and Minguell, J. J. (2004). Signals from damaged but not undamaged skeletal muscle induce myogenic differentiation of rat bone marrow derived mesenchymal stem cells. **Exp. Cell Res.** 300: 418-426.

- Satija, N. K., Gurudutta, G. U., Sharma, S., Afrin, F., Gupta, P., Verma, Y. K., Singh, V. K. and Tripathi, R. P. (2007). Mesenchymal stem cells: molecular targets for tissue engineering. **Stem Cells Dev.** 16: 7-23.
- Schmittwolf, C., Kirchhof, N., Jauch, A., Dürr, M., Harder, F., Zenke, M. and Muller, A. M. (2005). *In vivo* haematopoietic activity is induced in neurosphere cells by chromatin-modifying agents. **EMBO J.** 24: 554-566.
- Schwartz, R. E., Reyes, M., Koodie, L., Jiang, Y., Blackstad, M., Lund, T., Lenvik, T., Johnson, S., Hu, W. S. and Verfaillie, C. M. (2002). Multipotent adult progenitor cells from bone marrow differentiate into functional hepatocyte-like cells. **J. Clin. Invest.** 109: 1291-1302.
- Seo, M. J., Suh, S. Y., Bae, Y. C. and Jung, J. S. (2005). Differentiation of human adipose stromal cells into hepatic lineage *in vitro* and *in vivo*. **Biochem. Biophys. Res. Commun.** 328: 258-264.
- Sgodda, M., Aurich, H., Kleist, S., Aurich, I., König, S., Dollinger, M. M., Fleig, W. E. and Christ, B. (2007). Hepatocyte differentiation of mesenchymal stem cells from rat peritoneal adipose tissue *in vitro* and *in vivo*. **Exp. Cell Res.** 313: 2875-2886.
- Shafritz, D. A., Oertel, M., Menthen, A., Nierhoff, D. and Dabeva, M. D. (2006). Liver stem cells and prospects for liver reconstitution by transplanted cells. **Hepatology** 43: S89-S98.
- Shi, X. L., Qiu, Y. D., Wu, X. Y., Xie, T., Zhu, Z. H., Chen, L. L., Li, L. and Ding, Y.

- T. (2005). *In vitro* differentiation of mouse bone marrow mononuclear cells into hepatocyte-like cells. **Hepatol. Res.** 31: 223-231.
- Shu, S. N., Wei, L., Wang, J. H., Zhan, Y. T., Chen, H. S. and Wang, Y. (2004). Hepatic differentiation capability of rat bone marrow-derived mesenchymal stem cells and hematopoietic stem cells. **World J. Gastroenterol.** 10: 2818-2822.
- Silva, G. V., Litovsky, S., Assad, J. A., Sousa, A. L., Martin, B. J., Vela, D., Coulter, S. C., Lin, J., Ober, J., Vaughn, W. K., Branco, R. V., Oliveira, E. M., He, R., Geng, Y. J., Willerson, J. T. and Perin, E. C. (2005). Mesenchymal stem cells differentiate into an endothelial phenotype, enhance vascular density, and improve heart function in a canine chronic ischemia model. **Circulation** 111: 150-156.
- Snykers, S, De Kock, J, Rogiers, V, Vanhaecke, T. (2009). *In vitro* differentiation of embryonic and adult stem cells into hepatocytes: state of the art. **Stem Cells** 27: 577-605.
- Snykers, S., Vanhaecke, T., De Becker, A., Papeleu, P., Vinken, M., Van Riet, I. and Rogiers, V. (2007). Chromatin remodeling agent trichostatin A: a key-factor in the hepatic differentiation of human mesenchymal stem cells derived of adult bone marrow. **BMC Dev. Biol.** 7: 24-38.
- Snykers, S., Vanhaecke, T., Papeleu, P., Luttun, A., Jiang, Y., Vander Heyden, Y., Verfaillie, C. and Rogiers, V. (2006). Sequential exposure to cytokines

reflecting embryogenesis: the key for *in vitro* differentiation of adult bone marrow stem cells into functional hepatocyte-like cells. **Toxicol. Sci.** 94: 330-341.

Soemohardjo, S. (2003). New options in the treatment of chronic hepatitis. **Adv. Exp. Med. Biol.** 531: 191-198.

Stock, P., Staeger, M. S., Muller, L.P., Sgodda, M., Völker, A., Volkmer, I., Lutzkendorf, J. and Christ, B. (2008). Hepatocytes derived from adult stem cells. **Transplant Proc.** 40: 620-623.

Strassburg, C. P., Vogel, A. and Manns, M. P. (2003). Autoimmunity and hepatitis C. **Autoimmun. Rev.** 2: 322-331.

Takahashi, K., Tanabe, K., Ohnuki, M., Narita, M., Ichisaka, T., Tomoda, K. and Yamanaka, S. (2007). Induction of pluripotent stem cells from adult human fibroblasts by defined factors. **Cell** 131: 861-872.

Talens-Visconti, R., Bonora, A., Jover, R., Mirabet, V., Carbonell, F., Castell, J. V. and Gomez-Lechon, M. J. (2006). Hepatogenic differentiation of human mesenchymal stem cells from adipose tissue in comparison with bone marrow mesenchymal stem cells. **World J. Gastroenterol.** 12: 5834-5845.

Tamsel, S., Demirpolat, G., Killi, R., Aydin, U., Kilic, M., Zeytunlu, M., Parildar, M., Oran, I. and Ucar, H. (2007). Vascular complications after liver transplantation: evaluation with Doppler US. **Abdom. Imaging** 32: 339-347.

Tang, H., Liao, C. X., Zhou, J., Jin, H. S., Tan, Y. F., Su, J., Zhang, C. X. and Zhang, S.

- H. (2006). Differentiation of transplanted mouse c-Kit⁺lin⁻ bone marrow cells into hepatocytes *in vitro*. **Nan Fang Yi Ke Da Xue Xue Bao** 26: 567-569.
- Terai, S., Ishikawa, T., Omori, K., Aoyama, K., Marumoto, Y., Urata, Y., Yokoyama, Y., Uchida, K., Yamasaki, T., Fujii, Y. Okita, K. and Sakaida, I. (2006). Improved liver function in patients with liver cirrhosis after autologous bone marrow cell infusion therapy. **Stem Cells** 24: 2292-2298.
- Thumanu, K., Tanthanuch, W., Lorthongpanich, C., Heraud, P. and Parnpai, R. (2010). Neural differentiation of mouse embryonic stem cells studied by FTIR spectroscopy. **J. Mol. Structure** 967: 189-195.
- Ucceli, A. (2008). Adult stem cells for spinal cord injury: what types and how do they work? **Cytherapy** 10: 541-542.
- Wakitani, S., Imoto, K., Yamamoto, T., Saito, M., Murata, N. and Yoneda, M. (2002). Human autologous culture expanded bone marrow mesenchymal cell transplantation for repair of cartilage defects in osteoarthritic knees. **Osteoarthritis Cartilage** 10: 199-206.
- Wang, Q., Sanad, W., Miller, L. M., Viogt, A., Klingel, K., Kandolf, R., Strangl, K. and Baumann, G. (2005). Infrared imaging of compositional changes in inflammatory cardiomyopathy. **Vibra. Spectroscopy** 38: 217-222.
- Wilson, A. and Trumpp, A. (2006). Bone-marrow haematopoietic-stem-cell niches. **Nat. Rev. Immunol.** 6: 93-106.
- Woodbury, D., Schwarz, E. J., Prockop, D. J. and Black, I. B. (2000). Adult rat and

- human bone marrow stromal cells differentiate into neurons. **J. Neurosci. Res.** 61: 364-370.
- Yano, K., Ohoshima, S., Gotou, Y., Kumaido, K., Moriguchi, T. and Katayama, H. (2000). Direct measurement of human lung cancerous and noncancerous tissues by fourier transform infrared microscopy: can an infrared microscope be used as a clinical tool? **Anal. Biochem.** 287: 218-225.
- Yen, B. L., Huang, H. I., Chien, C. C., Jui, H. Y., Ko, B. S., Yao, M., Shun, C. T., Yen, M. L., Lee, M. C. and Chen, Y. C. (2005). Isolation of multipotent cells from human term placenta. **Stem Cells** 23: 3-9.
- Yoshida, A., Shimomura, T., Sakabe, T., Ishii, K., Gonda, K., Matsuoka, S., Watanabe, Y., Takubo, K., Tsuchiya, H., Hoshikawa, Y., Kurimasa, A., Hisatome, I., Uyama, T., Terai, M., Umezawa, A. and Shiota, G. (2007). A role of Wnt/b-catenin signals in hepatic fate specification of human umbilical cord blood derived mesenchymal stem cells. **Am. J. Physiol. Gastrointest Liver Physiol.** 293: 1089-1098.
- Zhao, R. and Duncan, S. A. (2005). Embryonic development of the liver. **Hepatology** 41: 956-967.
- Zhu, A. X. (2003). Hepatocellular carcinoma: are we making progress? **Cancer Invest.** 21: 418-428.
- Zuk, P. A., Zhu, M., Mizuno, H., Huang, J., Futrell, J. W., Katz, A. J., Benhaim, P., Lorenz, H. P. and Hedrick, M. H. (2001). Multilineage cells from human

adipose tissue: implication for cell-based therapies. **Tissue Eng.** 7: 221-228

CHAPTER III

CHARACTERIZATION OF BONE MARROW DERIVED MESENCHYMAL STEM CELLS EXPANDED IN CULTURE

3.1 Abstract

Bone marrow mesenchymal stem cells (BM-MSCs) are multipotent adult stem cells that have emerged as promising candidates for cell therapy. The low frequency of this subpopulation of stem cells in bone marrow necessitates their *in vitro* expansion prior to clinical use. We evaluated the effect of initial seeding density and long term culture on cells' proliferation, differentiation potential and phenotype. In this experiment, rat BM-MSCs (rBM-MSCs) could be isolated by using the selective plastic surface attached method. The growing fibroblastic cell population primarily consisted of spindle shaped and polygonal cells with significant renewal capacity as they were cultured at the density of 100 cells/cm². The cell clones proliferated extensively with at least 33.4 population doublings with ten passages. Moreover, the cells expressed CD29, CD37 and CD105 but not CD34 and CD45 and they maintained mesenchymal (osteoblastic, chondrocytic, and adipocytic) differentiation potential in all passages analyzed. Our finding supports the concept that low initial seeding densities result in higher yields and faster expansion of

rBM-MSCs, and this expansion culture fully retained the multipotent character of rBM-MSCs, which could maintain mesenchymal lineage differentiation potential and MSCs' phenotype up to the 10th passage. This experiment provides the method which could be used to isolate, culture and expand relatively homogenous population of MSCs from adult rat bone marrow.

3.2 Introduction

Adult MSCs have generated immense research interest in cell base therapies owing to their multipotentiality and capacity for self-renewal. Bone marrow stromal tissue has been regarded as the most likely source to obtain MSCs. Several preclinical and clinical studies have confirmed the great therapeutic potential of MSCs (Brooke et al., 2007; Caplan, 2007; Yu and Silva, 2008; Abdallah and Kassem, 2009). For MSCs' preclinical applications, an adequate number of cells are necessary, and considering the low number of MSCs (Wexler et al., 2003; Caplan, 2007), an extensive *ex vivo* expansion is required. The MSCs culture conditions are crucial in order to maintain MSCs' morphology and biological and functional properties intact for prolonged passages (Shahdadfar et al., 2005; Meuleman et al., 2006; Neuhuber et al., 2008; Pal et al., 2009).

Isolation of MSCs relied on their ability to adhere to plastic surfaces and MSCs have been successfully isolated from human (Pittenger et al., 1999), feline (Martin et al., 2002), canine (Kadiyala et al., 1997), rabbit (Johnstone et al., 1998), rat

(Wakitani et al., 1995), baboon (Devine et al., 2001), goat (Mosca et al., 2000), sheep (Jessop et al., 1994), chicken (Berry et al., 1992), and pig (Ringe et al., 2002) bone marrow by selecting the clonally growing adherent cells plastic surface in cultures. The purity of MSCs in marrow adherent cells differs among species. Human and canine marrow adherent cells are relatively homogeneous and contain a high percentage of MSCs. In many respects, the rat is an ideal model to study the cell biology and biochemical characteristics of MSCs. However, there is no standardized method for culturing MSCs; specifically, there are no standards for seeding densities, levels of confluence, and duration of cell expansion. Some studies suggested that seeding MSCs at low density results in the most rapid proliferation as well as the highest percentage of multipotent cells (Colter et al., 2000; Javason et al., 2001; Sekiya et al., 2002; Neuhuber et al., 2008). Others have suggested that strict maintenance of very-low cell densities throughout expansion is necessary to select for homogeneous cultures of a subpopulation of cells with high proliferation and differentiation potential (Jiang et al., 2002; Reyes and Verfaillie, 2001). In fact, the heterogeneity cell populations exist in MSCs cultures among different species (Phinney et al., 1999a; Peister et al., 2004) even in MSCs donations obtained from the same human donor (Phinney et al., 1999b). What is well-recognized is the variability found in MSCs culture. It is obvious that these cultures are composed of different cell types with distinct morphologies. These cells type have been classified as spindle-shape type I and flattened type II cells (Mets and Verdonk, 1981) or rapidly

self-renewing cells and mature MSC (Colter et al., 2000; Colter et al., 2001; Sekiya et al., 2002) by shape, marker expression and growth kinetics. How should these subpopulation be culture-expanded become the principal issue for preclinical study? It is necessary to use standardized culture protocols that preferentially expand undesired cells population.

Long term expansion culture has proven that environmental conditions significantly increase and decrease the culture life span of MSCs. The telomere length of MSCs have been shown to shorten in culture expansion, leading to a gradual senescence, which is normally recorded in population doubling (PD) (Stenderup et al., 2003; Baxter et al., 2004; Parach et al., 2004;). In the high passages, MSCs showed a reduced sensitivity to undergo adipogenic differentiation (Muraglia et al., 2000; Goodwin et al., 2001; Campagnoli et al., 2001; Bieback et al., 2004; Bonab et al., 2006). With this in mind, it is necessary to evaluate the effect of long term in vitro culture on the proliferation, differentiation and phenotype of MSCs. In the context, it is important to choose optimal culture condition to expansion of MSCs and maintain MSCs' morphology and biological and functional property intact for prolong passages. We aimed to evaluate the effects of initial seeding density in culture on proliferation and cell morphology of rBM-MSC cultures and determine the phenotype and mesenchymal differentiation potential for long time culture.

3.3 Materials and Methods

All chemicals used in this study were purchased from Sigma (Sigma Chemical Company, St. Louis, MO, USA).

3.3.1 Isolation and culture of rBM-MSCs

The rBM-MSCs were isolated from 8-week-old Wistar rats. The tibias and femurs were excised aseptically. The epiphyses were then removed, the marrow were flushed out with a stream of standard complete culture medium (CCM), which consisted of alpha-modified minimum essential medium (α -MEM) supplemented with 10% fetal bovine serum (FBS; Gibco BRL, Grand Island, NY, USA) and antibiotics (streptomycin-penicillin) through a 20-gauge needle attached to a 5 ml syringe. The pooled cell suspension was centrifuged at $600 \times g$ for 5 minutes. The pellet was resuspended in CCM. The rBM-MSCs culture were performed by plating the cell suspension in a 75 cm^2 tissue culture flask (Nunc, Roskilde, Denmark) containing 20 ml of CCM at 37°C in a humidified atmosphere of 5% CO_2 . No culture medium changes were made in the initial two days; from the third day onwards, culture medium was changed every three days until the culture flask was confluent. Upon confluence the cells were detached with 0.25% trypsin and 1 mM ethylenediamine tetraacetic acid (EDTA) and the cells were seeding at 10, 100 or 1000 cells/ cm^2 . The rBM-MSCs were passaged upon reaching 90% confluence. The rBM-MSCs were frozen and stored at each passage with culture medium supplement with 30% FBS and 7% dimethyl sulfoxide (DMSO) in liquid nitrogen for future experiment.

3.3.2 Proliferation Kinetics

The rBM-MSCs were passaged and counted once they reached a sub-confluence of 90%. The PD rate was determined using the following formula: $X = \log_{10} (N_H) - \log_{10} (N_1) / \log_{10} (2)$. N_H is the harvested cell number and N_1 is the seeded cell number. The PD for each passage was calculated and added to the PD of the previous passages to generate data for cumulative population doublings levels (PDL).

3.3.3 Characterization of rBM-MSCs

3.3.3.1 *In vitro* differentiation potential

For osteogenic differentiation, rBM-MSCs were seeded in 6-well plates (Nunc) at a density of 5000 cells/cm² and cultured in CCM for reaching 90% confluence. Thereafter, the CCM was removed and cells were incubated in osteogenic induction medium (OIM) for an additional 21 days with media changes every other day. OIM consisted of CCM supplemented with 50 μM ascorbic acid, 100 nM dexamethasone and 5 mM KH₂PO₄. After 21 days, the cell monolayer was washed twice with PBS without calcium and magnesium [without calcium and magnesium [PBS (-)], fixed in 4% paraformaldehyde (PFA) for 10 minutes, and then stained with 2% Alizarin Red solution (pH 4.1) for 15 minutes at room temperature. Following this the removal Alizarin Red solution was performed the cells were rinsed with PBS (-) 1-2 times, recorded staining results with microphotography. Experiments were performed in triplicate.

To induce chondrogenic differentiation, rBM-MSC were plated in a 6-well plate at 5000 cells/cm² and cultured in CCM for reaching confluence. After confluence, cells were trypsinized and transferred to a 15 ml polypropylene conical tube (Nunc), centrifuged at 3000 rpm to create a pellet, and cultured 21 days in chondrogenic induction medium, including 15% FBS, 50 mg/ml ascorbate 2-phosphate, 40 µg/ml proline, 1 mM pyruvate, 6.25 µg/ml ITS, 100 nM dexamethasone (Dex) and 10 ng/ml transforming growth factor-β (TGF-β) in α-MEM by feeding twice a week. Subsequently, the cell pellet was embedded in optimal temperature cutting (OCT; Richard-Allan Scientific, Kalamazoo, MI, USA) compound, sectioned at 5 µm in a cryostat at -18°C and mounted on slide. Then the cryosections were fixed with 4% PFA. Matrix deposition of glycosaminoglycan was detected by staining the cells with 1% Alcian blue in 3% acetic acid for 15 minutes and then the excess stain was rinsed with distilled water, air dried and observed under a light microscope and captured the image.

The rBM-MSCs were plated in a 6-well plate at 5000 cells/cm² and culture in CCM for reaching 90% confluence. To induce adipogenic differentiation, the cells were cultured in CCM supplement with 0.5 mM methylisobutylxanthine (IMBT), 1 µM Dex, 10 µg/ml insulin, 100 µM indomethacin and 4.5 g/ml glucose for up to 21 days. The medium was replaced twice weekly. Then the cells monolayer was washed with PBS (-), fixed with 4% PFA and stained with Oil red-O. The Oil red-O solution was prepared by vigorously mixing 3 parts solution (0.5% in isopropanol)

with 2 parts water for 5 minutes and filtered through a 0.4 μm filter. The cells were stained for 15 minutes to detect the lipid droplets within the differentiated cells. Excess stain was removed by rinsing with 60% isopropanol and water. Clusters of lipid droplets were detected by observing under a light microscope and captured the image.

3.3.3.2 Phenotype determination by flow cytometry

Clonal surface marker expression was characterized by flow cytometry. Confluent culture was harvested by treating with 0.25% trypsin/EDTA for 3 minutes and pelleted at 600 $\times g$ for 5 minutes. About 1×10^6 cells were re-suspended in PBS (-), after being washed three times, followed by being incubated with primary unconjugated antibodies mouse anti-CD29 (1:150; BD Pharmingen, San Diego, CA, USA), mouse anti-CD34 (1:150; BD Pharmingen), rabbit anti-Endoglin (CD 105; 1:100; Santa Cruz Biotechnology, CA, USA), rabbit anti-CD45 (1:100; Santa Cruz Biotechnology) and rabbit anti-CD73 (1:100; Santa Cruz Biotechnology) for 1 hour at room temperature. The cells were then washed and incubated with secondary antibody conjugated with either Alexa 488 donkey anti-mouse IgG (1:1000; Molecular probes, Eugene, OR, USA) or Rhodamine RedTM-goat anti-rabbit IgG (1:1000; Molecular probes) for 15 minutes. The cells stained with Alexa 488 donkey anti-mouse IgG or Rhodamine RedTM-goat anti-rabbit IgG were used as negative control. The cells were then washed and analysed by flow cytometry on a BD fluorescence activated cell sorter (FACSCaliburTM) flow cytometer using CellQuestTM software with 20,000

events recorded for each sample. For each marker, three independent samples were run.

3.3.3.3 Immunocytochemistry

The cells were fixed with 4% PFA solution for 30 minutes at room temperature, then washed three times with PBS (-), followed by incubation in blocking solution for 2 hours. The cells were subsequently incubated with the following primary antibody, mouse anti-CD29 (1:200, BD Pharmingen), mouse anti-CD34 (1:200, BD Pharmingen), rabbit anti-Endoglin (CD 105, 1:200, Santa Cruz Biotechnology), rabbit anti-CD45 (1:200, Santa Cruz Biotechnology) and rabbit anti-CD73 (1:200, Santa Cruz Biotechnology) at 4°C overnight. Afterward, the excess primary antibodies were washed out, the cells were treated with second antibody Alexa 488 donkey anti-mouse IgG (1:1000, Molecular probes) or Rhodamine RedTM-goat anti-rabbit IgG (1:1000, Molecular probes) for 1 hour. The cells were co-stained with 4'6'-diamidino-2-phenylindole (DAPI) for 5 minutes and then examined under fluorescence microscopy. For negative controls, replacing the primary antibodies with normal rabbit serum or staining without secondary antibody was investigated in each experiment, and in either case, no specific positive staining was detected.

3.3.4 Statistical analysis

All data are represented as arithmetic mean \pm SD. The data collected in ten passages was compared by Repeated Measurement analysis of variance test. *P*. values

only less than 0.05 ($P < 0.05$) were considered significant.

3.4 Results

3.4.1 Generation of primary cultures from adherent bone marrow cells

After plating the bone marrow cells, only a few cells attached to the surface of plastic culture flasks and formed adherent cells within one week. The onset of colony formation could be observed at first after 4 to 7 days. Cells confluence was reached after approximately 12 days of culture. These rBM-MSCs grown from the bone marrow suspension by selective attached to plastic tissue culture flask exhibit two major subpopulations: 1) cells with an elongated, spindly shape with two processes that extend in opposite directions from the cell body (Figurer 3.1 a-c); and 2) polygonal cells with or without short processes or large flattened cells (Figurer 3.1 d-e). During initial growth, they formed colonies, that is, the colony-forming-unit fibroblasts (CFU-F) (Figurer 3.1 f and g) and dislodged readily on trypsinization in 3 minutes.

3.4.2 Effect of seeding density on expansion of rBM-MSCs

The rBM-MSCs were plated at densities of 10, 100, 1000 cells/cm², and expanded from passage 1 to passage 5 (10 cells/cm²) or passage 10 (100 and 1000 cells/cm²) up to 61 days, with replicate cultures counted each day (Fig 3.2). When rBM-MSCs plated at low density of 10 cells/cm², the cells expanded up to 33.4 population doublings over about 61 days in culture (passage 5) with a the population

doubling time of 87.6 hours. When the rBM-MSCs plated at 100 cells/cm², the cells had completed 54.1 populations doubling in 64 days culture (passage 10) and with a population doubling time of 28.3 hours. When the rBM-MSC plated at high density of 1000 cells/cm², displayed a population doubling time of 36.2 hours over 21.2 population doublings (10 passage; 32 days in culture). When the rBM-MSC plated at density of 100 cells/cm², the cells exhibited three phases of growth kinetics: lag phase, a log phase of rapid growth and a stationary phase.

The rBM-MSC growth patterns were found to have a difference in initial plating density. MSCs plated at 10 cells/cm² grew into few large, very dense colonies. The more numerous colonies formed by cell plated at cells/cm² were smaller and less dense. MSCs plated at 1000 cells/cm² grew evenly on the plastic (Fig 3.3).

3.4.3 Characterization of rBM-MSCs from efficiency expansion culture

3.4.3.1 Expression of mesenchymal markers in rBM-MSCs

The mean percent of CD expression of the five antigens was compared using Repeated Measurement Analysis of Variance at passage 1, 5 and 10 (Figure 3.4). Results demonstrated that the number of positive of CD29 (73±2.3, 80±0.5, 89.4±1.2, respectively), CD73 (69.5±1.8, 72.8±0.4, 76.3±0.8, respectively) and CD105 (72.5±1.2, 79.4±0.2, 82.1±0.9, respectively) increased, meanwhile CD34 (22.5±2.6, 12.8±0.9, 8.1±2.1, respectively) and CD45 (24.5±0.5, 17.6±0.7, 9.2±0.3, respectively) decreased for extent expansion, indicating that the changes in marker-positive population associated with reduction in marker-negative population.

The expression of CD29, CD105, CD34 and CD45 were significantly different between passage 1 and passage 10, and no different in the CD73 expression. The results showed that rBM-MSCs at higher passages displayed elevated expression of mesenchymal markers with more uniform distributions.

3.4.3.2 Immunophenotype

Typical CD29, CD34, CD45, CD73, CD90 and CD105 surface marker expressions were detected in rBM-MSCs culture at passage 5 (Figure 3.3). The results demonstrated that the cells were negative for CD34 and CD45, cell surface markers associated with lymphohematopoietic cells. Therefore, there was no evidence of hematopoietic precursors in the cultures. In contrast, the rBM-MSCs expressed CD29, CD73 and CD105, consistent with their undifferentiated state. Basically, identical results were obtained by FACS examination.

3.4.3.3 Differentiation potential

The differentiation capacity was quantitatively assessed at passage 1, 5 and 10. Adipogenic differentiation was apparent after 1 week of incubation with adipogenic supplementation. By the end of the third week, all passages examined contained numerous oil Red-O positive lipid droplets (Fig 3.6 a, d and g). As showed in Fig 3.6 b, e and h, there were osteoblasts like morphological changed in the rBM-MSCs, and many mineral depositions were observed on the surface in all passage analyzed. In chondrogenic differentiation assay, rBM-MSCs of all passages analyzed consolidated within 1 day, forming aggregates that dislodged to float freely

in the suspension culture. After 21 days differentiation, cryosections of the aggregates stained with Alcian blue showed a condensed structure with chondrocyte like lacunae (Fig 3.6 e, f and i). These suggested that rBM-MSCs maintain mesenchymal differentiation potential for extended expansion.

3.5 Discussion

In our experiment, we found that two major subpopulations of rBM-MSCs existed in the culture, one is a spindle shape and the other is a polygonal shape cell and these cells maintained these phenotypes in every passage. The rBM-MSCs attained in our laboratory were similar to previous reports in morphological characteristics and the trait of growth (Aizi et al., 1998; Colter et al., 2000; Colter et al., 2001; Javazon et al., 2001; Sekiya et al., 2002). Colter et al. (2000) used FACS for analysis and demonstrated that stationary cultures contained a major population of large and moderately granular cells and a minor population of small and a granular cell which is referred to as recycling stem cells or RS-1 cells. During the lag phase, the RS-1 cells gave rise to a new population of small and densely granular cells (RS-2 cells). During the late log phase, the RS-2 cells decreased in number and regenerated the pool of RS-1 cells found in stationary cultures. In other previous studies (Sekiya et al., 2002; Colter et al., 2001), spindle-shaped cells have been classified as “immature,” while polygonal cells have been characterized as “mature”. Because the correlation between cell shape and stem-cell characteristics has yet to be definitively

determined, Neuhuber et al. (2008) described the two subpopulations simply as “spindle-shaped” and “flat”. They found that time is a critical factor for increased proportions of flat cells and they cultured spindle-shaped and flat cells superlatively, and found that the cells maintained these phenotypes even in between subsequent passages. Most clones could be cultured with at least ten passages and approximately 20 population doublings, showing neither changed morphology nor reduced proliferation. Some protocols strived to select for these cells in culture (Smith et al., 2004; Neuhuber et al., 2008), however, there is no clear evidence that this specific population is more efficacious in animal models of diseases and injury. This relatively subpopulation may not be the determining factor as the beneficial effect of MSCs, but may rely on secretion of therapeutic factors and regulation of extracellular matrix molecules, in addition, the identity of the desirable subpopulation may depend on specifics of the disease and therapy.

Previous studies have suggested that low initial seeding densities resulted in higher yields and faster expansion of MSCs (Colter et al., 2000; Sekiya et al., 2002). Cells seeded at low densities yielded more doublings per passage, as growth at higher densities becomes constrained by density-dependent growth inhibition. In our hands, rBM-MSCs seeded at 100 cells/cm² had the fastest doubling times. A possible reason may be that cell-to-cell contact or factors that the cells secrete into the medium will affect the growth rate (Colter et al., 2000; Javazon et al., 2001; Neuhuber et al., 2008). Our results showed that the growth patterns of rBM-MSCs cultures also depended on

the initial seeding densities. At low seeding density, rBM-MSCs grew as very dense colonies (Fig 3.3 a-c), whereas at high seeding density, rBM-MSCs spread evenly across the plate (Fig 3.3 d-f). In addition, at intermediate density, the growth pattern was a mix of colonies, neither as densely clustered as the ones observed at low plating density, nor as single cells dispersed across the plate observed at high seeding density (Fig 3.3 g-f). This indicated that the difference in growth patterns can certainly affect growth kinetics. In the dense colonies observed at low seeding density, cell growth is likely to be inhibited at the colony center because of contact inhibition. Conversely, the sparse single cell distribution observed at high seeding density may not have provided sufficient stimulus for growth and loss of cell-cell contact. Gregory et al. (2005) suggested that MSCs differentiation is affected by the microenvironment presented both at the center of dense colonies and in the sparse colony periphery, so the similar mechanisms may also regulate cell proliferation. Seeding cells sparsely without a program of early re-seeding to avoid overcrowding at the colony center may affect proliferation directly or indirectly through the induction of early differentiation of rBM-MSCs. In order to avoid this problem, seeding cells at intermediate densities is necessary.

We found optimal rBM-MSCs growth at a seeding density of 100 cells/cm², and further characterization of rBM-MSCs yielded at this seeding density. MSCs expression of cell surface antigens and differentiation into other lineages has been used as markers for the multipotent nature of these cells (Pittenger et al., 1999). The

results showed that the rBM-MSCs maintained the phenotype and mesenchymal differentiation potential even at high passages (Passage 10). The rBM-MSCs at higher passages displayed elevated expression of mesenchymal markers with more uniform distributions indicated the homologous populations were yielded. The previous reports showed that MSCs lost adipogenic potential and osteogenic potential drop at high passages (Digirolamo et al., 1999; Conget and Minguell, 1999; Sekiya et al., 2002), in our hands, we found that rBM-MSCs maintenance high differentiation potential up to the passage that we analyzed (passage 10). The possible reason maybe attributed to the initial density of the rBM-MSCs, which have been shown to still have a high proliferation potential at high passages, as seen in the population doubling levels (Fig 3.2). The rBM-MSCs at this suitable seeding density seem possible that paracrine or autocrine factors secreted into the medium are responsible for the transition.

3.6 Conclusion

MSCs from adult rat bone marrow were successfully isolated, cultured and expanded by using the selective plastic surface attached method. A relatively homogenous population was attained. The results confirmed that low initial seeding density affects the growth of kinetics and morphology of rBM-MSCs and the initial seeding density is critical for the long-term culture of rBM-MSCs. The homologous population of rBM-MSCs yield at less passage 10. This study provides an optimal

culture condition for later experiment.

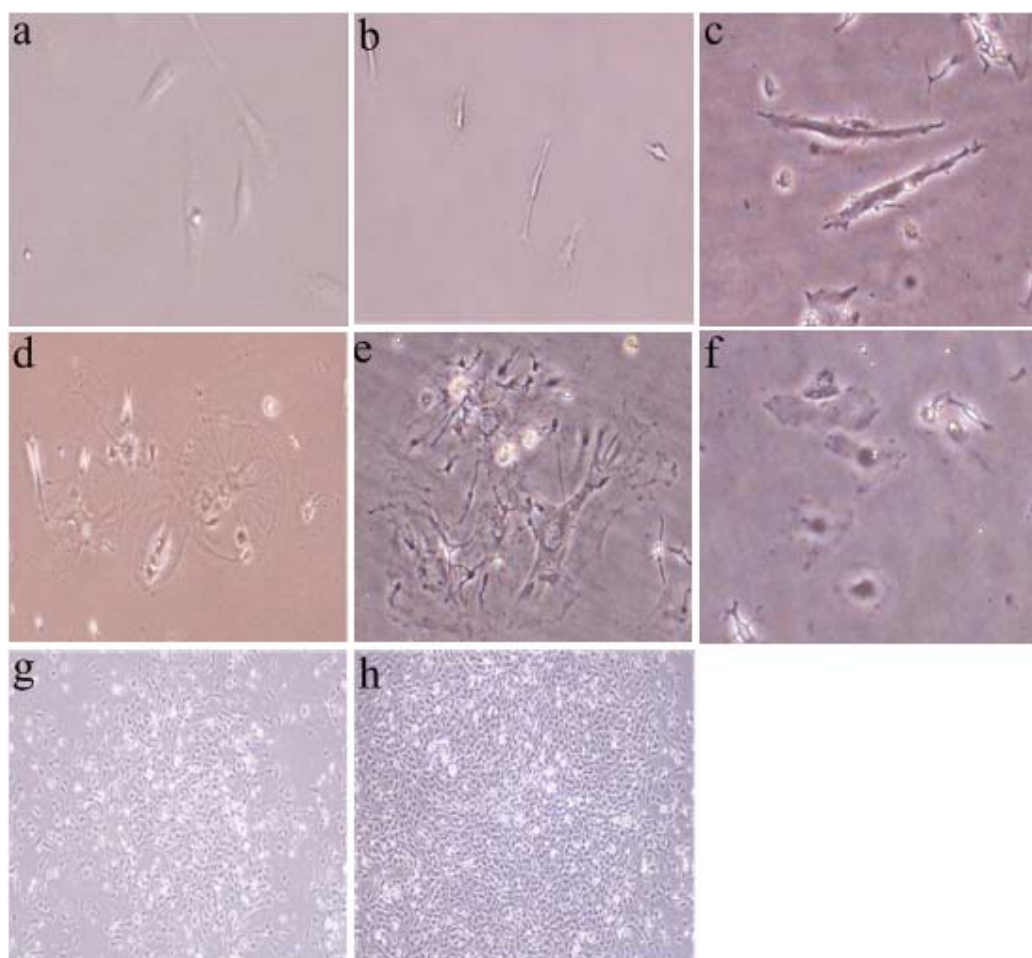


Figure 3.1 Morphology of primary cultures of rBM-MSCs. A subpopulation of rBM-MSCs exhibit elongated, spindle shaped cells (a-c). A second subpopulation of rBM-MSCs exhibit flattened polygonal morphology with short or no processes (d-f). Colony-forming-unit fibroblasts (CFU-F) of rBM-MSCs after 7 days (g) and 12 days (h) cultivated. Original magnification, (a-f) 200 \times ; (g, h) 40 \times .

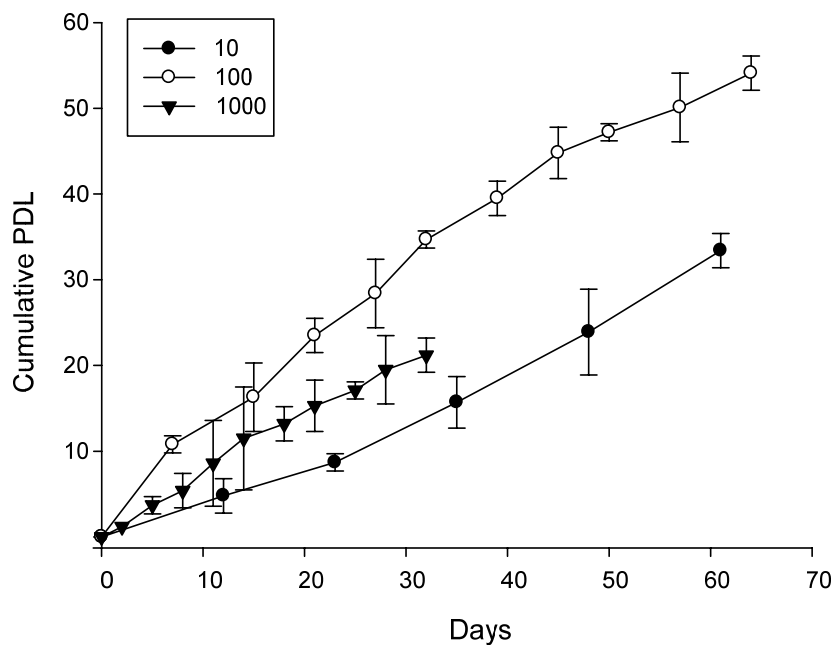


Figure 3.2 The growth kinetics of rBM-MSCs plated at different densities across multiple passages. rBM-MSCs were plated at 10 cells/cm², 100 cells/cm² and 1000 cells/cm² and cumulative population doubling level (PDL) and doubling times were calculated.

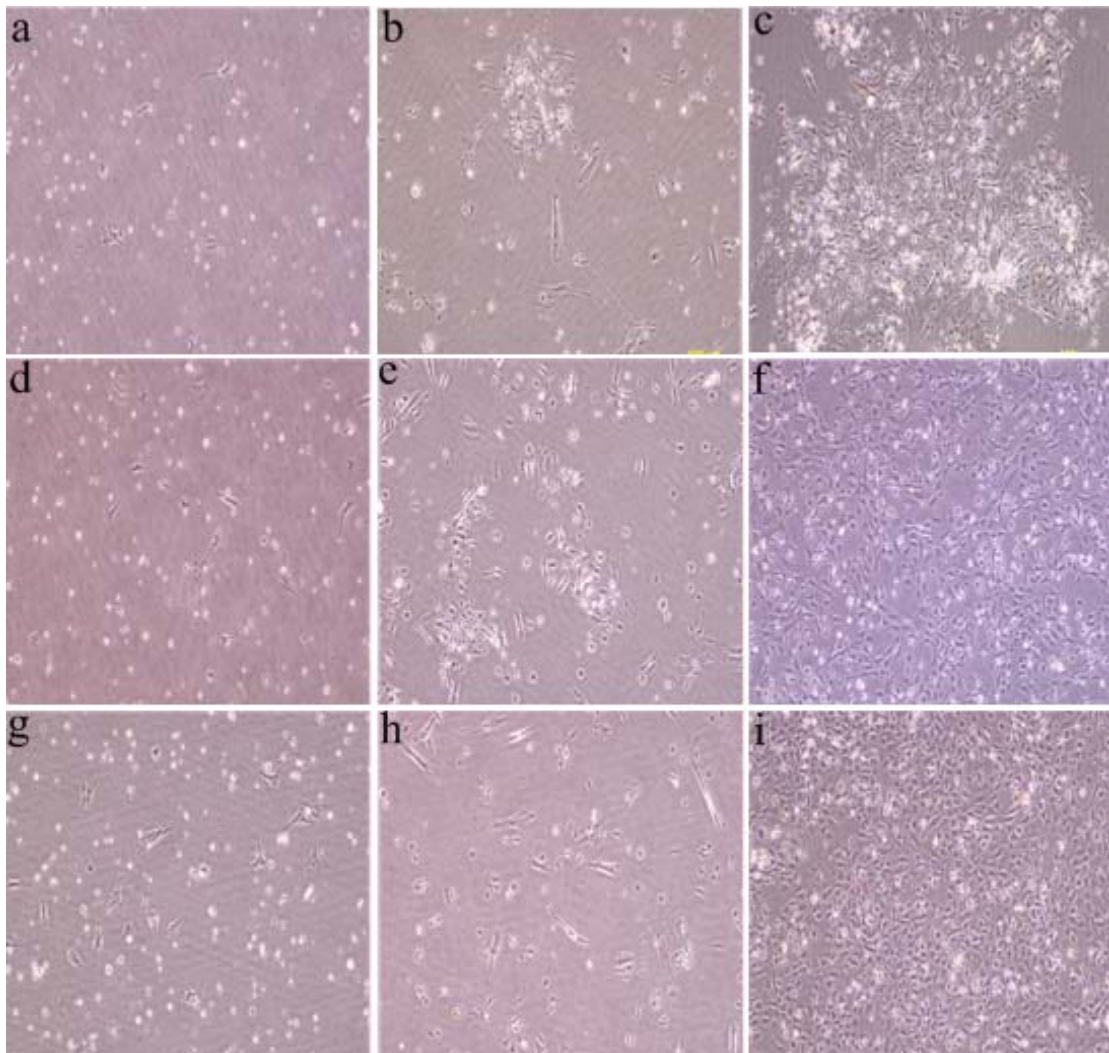


Figure 3.3 The growth patterns of rBM-MSCs plated at different initial plating densities. Micrographs depict growth patterns of rBM-MSC plated at 10 cells/cm² (a-c), 100 cells/cm² (d-f) and 1000 cells/cm² (g-i). Pictures are representative of cultures one day after seeding (a, d and g), mid-way through the culture (b, e and h) and on the day of passaging (c, f and i). Original magnification, 40 \times .

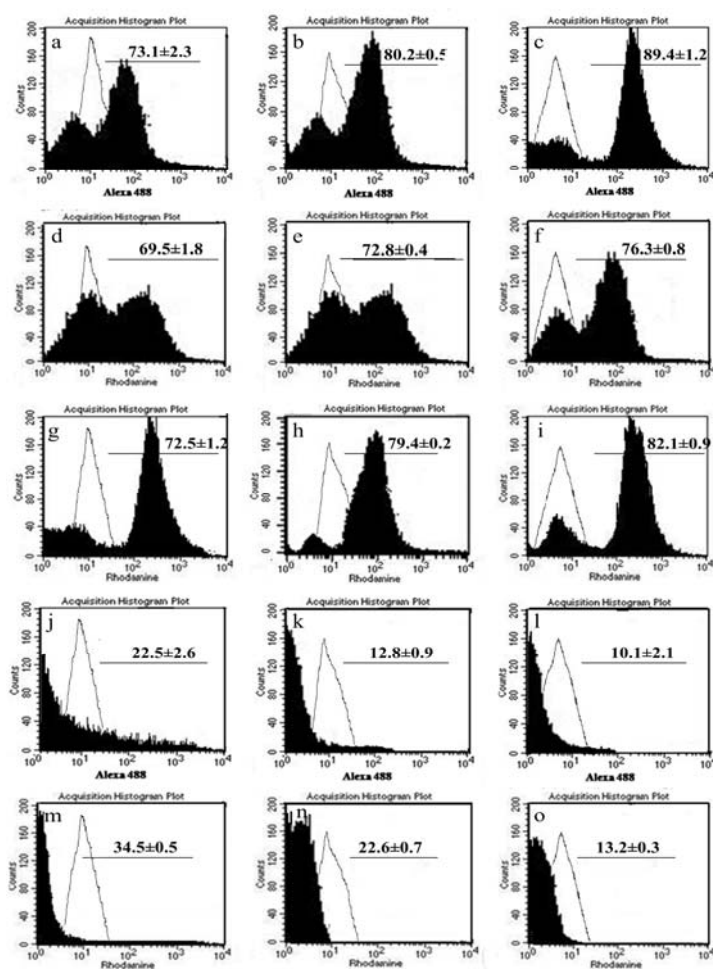


Figure 3.4 FACS analyses of the selected surface antigens expression by the rBM-MSCs during expansion in culture. rBM-MSCs at passage 1 (a, d, g, j and m), passage 5 (b, e, h, k and n) and passage 10 (c, f, i, l and o) were incubated with CD29 (a-c), CD73 (d-f), CD105 (g-i), CD34 (j-l) and CD45 (m-o) and analyzed by FACS Callibur cytometer and cell Quest. Black lines represent control patterns obtained without primary antibody, whereas black areas represent antibody against the indicated mesenchymal markers. Numbers in panels represent mean fluorescent intensity of the cells expressing each marker.

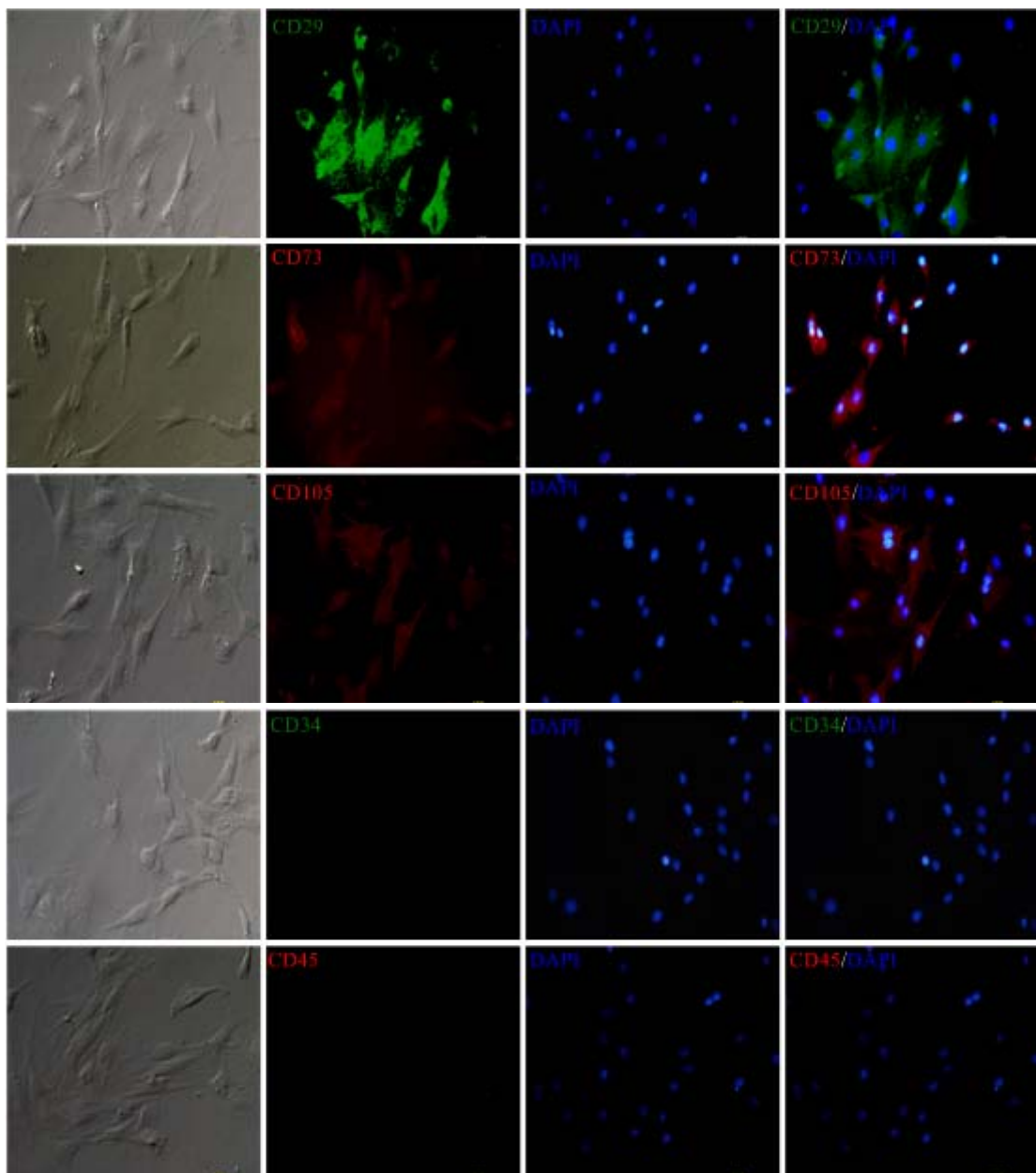


Figure 3.5 Immunocytochemistry analyses of rBM-MSCs at passage 5. rBM-MSCs at passage 5 was stained with CD29 (Green), CD73 (Red), CD105 (Red), CD34 (Green), CD45 (Red) and DAPI (Blue). Original magnification, 200 \times .

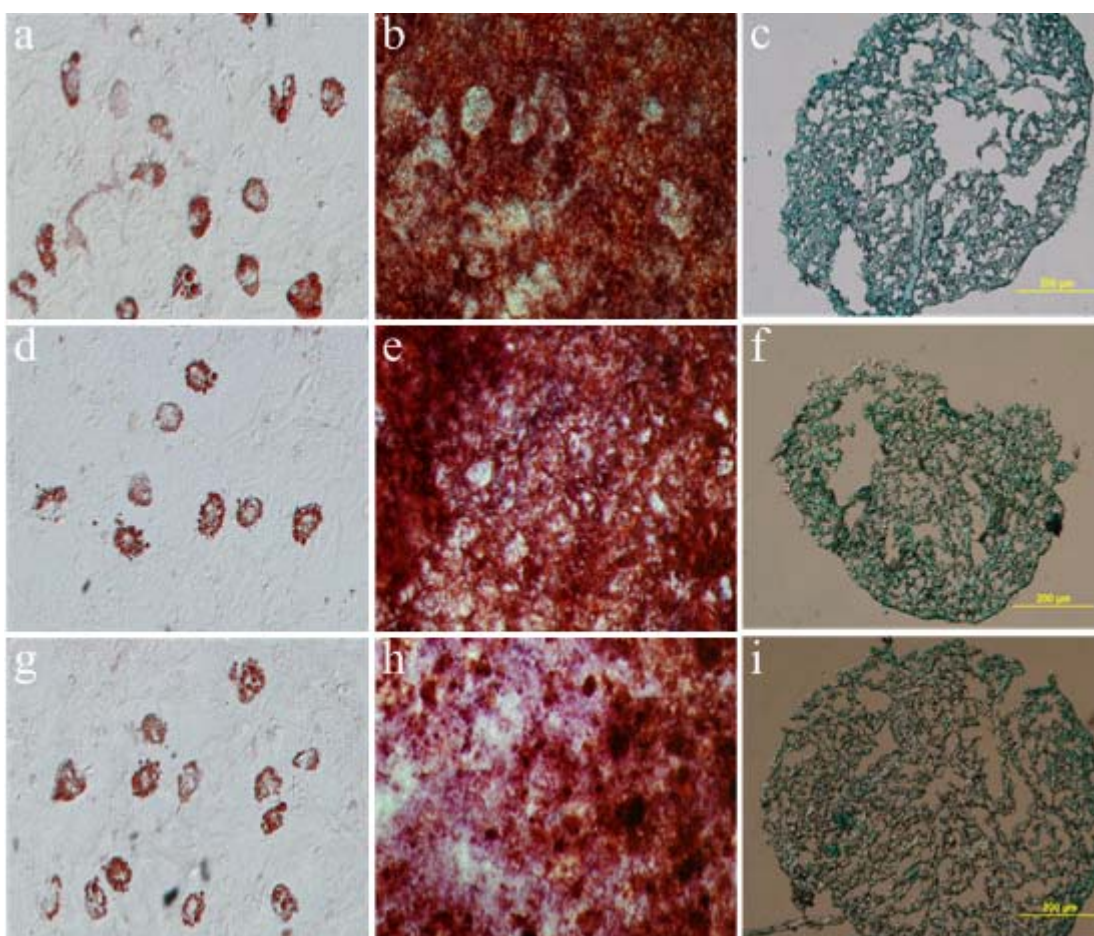


Figure 3.6 Differentiation potential of rBM-MSCs. The rBM-MSCs at passage 1 (a, b and c), passage 5 (d, e and f) and passage 10 (g, h and i) were subjected to adipogenesis, osteogenesis, chondrogenesis and assays by Oil Red-O staining (a, d and g), Alizarin Red staining (b, e and h) and Alcian blue staining (c, f and i), respectively. Original magnification, (b, e and h) 40 \times ; (c, e and i) 100 \times ; (a, d and g) 200 \times .

3.7 Reference

- Abdallah, B. M. and Kassem, M. (2009). The use of mesenchymal (skeletal) stem cells for treatment of degenerative diseases: current status and future perspectives. **J. Cell Physiol.** 218: 9-12.
- Azizi, S. A., Stokes, D., Augelli, B. J., DiGirolamo, C. and Prockop, D. J. (1998). Engraftment and migration of human bone marrow stromal cells implanted in the brains of albino rats--similarities to astrocyte grafts. **Proc. Natl. Acad. Sci. U S A** 95: 3908-3913.
- Baxter, M. A., Wynn, R. F., Jowitt, S. N., Wraith, J. E., Fairbairn, L. J. and Bellantuono, I. (2004). Study of telomere length reveals rapid aging of human marrow stromal cells following in vitro expansion. **Stem Cells** 22: 675-682.
- Berry, L., Grant, M. E., McClure, J. and Rooney, P. (1992). Bone-marrow-derived chondrogenesis in vitro. **J. Cell Sci.** 101: 333-342.
- Bieback, K., Kern, S., Kluter, H. and Eichler, H. (2004). Critical parameters for the isolation of mesenchymal stem cells from umbilical cord blood. **Stem Cells** 22: 625-634.
- Bonab, M. M., Alimoghaddam, K., Talebian, F., Ghaffari, S. H., Ghavamzadeh, A. and Nikbin, B. (2006). Aging of mesenchymal stem cell *in vitro*. **BMC Cell Biol.** 7:14.

- Brooke, G., Cook, M., Blair, C., Han, R., Heazlewood, C., Jones, B., Kambouris, M., Kollar, K., McTaggart, S., Pelekanos, R., Rice, A., Rossetti, T. and Atkinson, K. (2007). Therapeutic applications of mesenchymal stromal cells. **Semin. Cell Dev. Biol.** 18: 846-858.
- Campagnoli, C., Roberts, I. A., Kumar, S., Bennett, P. R., Bellantuono, I. and Fisk, N. M. (2001). Identification of mesenchymal stem/progenitor cells in human firsttrimester fetal blood, liver, and bone marrow. **Blood** 98: 2396-2402.
- Caplan, A. I. (2007). Adult mesenchymal stem cells for tissue engineering versus regenerative medicine. **J. Cell Physiol.** 213: 341-347.
- Colter, D. C., Class, R., DiGirolamo, C. M. and Prockop, D. J. (2000). Rapid expansion of recycling stem cells in cultures of plastic-adherent cells from human bone marrow. **Proc. Natl. Acad. Sci. U S A** 97: 3213-3218.
- Colter, D. C., Sekiya, I. and Prockop, D. J. (2001). Identification of a subpopulation of rapidly self-renewing and multipotential adult stem cells in colonies of human marrow stromal cells. **Proc. Natl. Acad. Sci. U S A** 98: 7841-7845.
- Conget, P. A. and Minguell, I. I. (1999). Phenotypical and functional properties of human bone marrow msenchymal progenitor cells. **J. Cell Physiol.** 181: 67-73.
- Devine, S. M., Bartholomew, A. M., Mahmud, N., Nelson, M., Patil, S., Hardy, W., Sturgeon, C., Hewett, T., Chung, T., Stock, W., Sher, D., Weissman, S., Ferrer, K., Mosca, J., Deans, R. and Moseley, A. (2001). Mesenchymal stem cells

are capable of homing to the bone marrow of non-human primates following systemic infusion. **Exp. Hematol.** 29: 244-255.

Digirolamo, C. M., Stokes, D., Colter, D., Phinney, D. G., Class, R. and Prockop, D. J. (1999). Propagation and senescence of human marrow stromal cells in culture: a simple colony-forming assay identifies samples with the greatest potential to propagate and differentiate. **Br. J. Haematol.** 107: 275-281.

Goodwin, H. S., Bicknese, A. R., Chienm, S. N., Bogucki, B. D., Quinn, C. O. and Wall, D. A. (2001). Multilineage differentiation activity by cells isolated from umbilical cord blood: expression of bone, fat, and neural markers. **Biol. Blood Marrow Transplant** 7: 581-588.

Gregory, C. A., Ylostalo, J. and Prockop, D. J. (2005). Adult bone marrow stem/progenitor cells (MSCs) are preconditioned by microenvironmental “niches” in culture: a two-stage hypothesis for regulation of MSC fate. **Sci. STKE** 294: 37.

Javazon, E. H., Colter, D. C., Schwarz, E. J. and Prockop, D. J. (2001). Rat marrow stromal cells are more sensitive to plating density and expand more rapidly from single-cell-derived colonies than human marrow stromal cells. **Stem Cells** 19: 219-225.

Jessop, H. L., Noble, B. S. and Cryer, A. (1994). The differentiation of a potential mesenchymal stem cell population within ovine bone marrow. **Biochem. Soc. Trans.** 22: 248S.

- Jiang, Y., Jahagirdar, B. N., Reinhardt, R. L., Schwartz, R. E., Keene, C. D., Ortiz-Gonzalez, X. R., Reyes, M., Lenvik, T., Lund, T., Blackstad, M., Du, J., Aldrich, S., Lisberg, A., Low, W. C., Largaespada, D. A, and Verfaillie, C. M. (2002). Pluripotency of mesenchymal stem cells derived from adult marrow. **Nature** 418: 41-49.
- Johnstone, B., Hering, T. M., Caplan, A. I., Goldberg, V. M. and Yoo, J. U. (1998). *In vitro* chondrogenesis of bone marrow-derived mesenchymal progenitor cells. **Exp. Cell Res.** 238: 265-272.
- Kadiyala, S., Young, R. G., Thiede, M. A. and Bruder, S. P. (1997). Culture expanded canine mesenchymal stem cells possess osteochondrogenic potential *in vivo* and *in vitro*. **Cell Transplant** 6: 125-134.
- Martin, D. R., Cox, N. R., Hathcock, T. L., Niemeyer, G. P. and Baker, H. L. (2002). Isolation and characterization of multipotential mesenchymal stem cells from feline bone marrow. **Exp. Hematol.** 30: 879-886.
- Mets, T. and Verdonk, G. (1981). *In vitro* aging of human bone marrow derived stromal cells. **Mech. Ageing Dev.** 16: 81-89.
- Meuleman, N., Tondreau, T., Delforge, A., Dejeneffe, M., Massy, M., Libertalis, M., Bron, D. and Lagneaux, L. (2006). Human marrow mesenchymal stem cell culture: serum-free medium allows better expansion than classical alpha-MEM medium. **Eur. J. Haematol.** 76: 309-316.
- Mosca, J. D., Hendricks, J. K. and Buyaner, D. (2000). Mesenchymal stem cells as

vehicles for gene delivery. **Clin. Orthop.** (suppl 379): S71-S90.

Muraglia, A., Cancedda, R. and Quarto, R. (2000). Clonal mesenchymal progenitors from human bone marrow differentiate in vitro according to a hierarchical model. **J. Cell Sci.** 113: 1161-1166.

Neuhuber, B., Swanger, S. A., Howard, L., Alastair Mackay, A. and Fischer, I. (2008). Effects of plating density and culture time on bone marrow stromal cell characteristics. **Exp. Hematol.** 36: 1176-1185.

Pal, R., Hanwate, M., Jan, M. and Totey, S. (2009). Phenotypic and functional comparison of optimum culture conditions for upscaling of bone marrow-derived mesenchymal stem cells. **J. Tissue Eng. Regen. Med.** 3:163-174.

Parach, D., Fellenberg, J., Brummendorf, T. H. Eschlbeck, A. M., Richter, W. (2004). Telomere length and telomerase activity during expansion and differentiation of human mesenchymal stem cells and chondrocytes. **J. Mol. Med.** 82: 49-55.

Peister, A., Mellad, J. A., Larson, B. L., Hall, B. M., Gibson, L. F. and Prockop, D. J. (2004). Adult stem cells from bone marrow (MSCs) isolated from different strains of inbred mice vary in surface epitopes, rates of proliferation, and differentiation potential. **Blood** 103:1662-1668.

Phinney, D. G., Kopen, G., Isaacson, R. L. and Prockop, D. J. (1999a). Plastic adherent stromal cells from the bone marrow of commonly used strains of

- inbred mice: variations in yield, growth, and differentiation. **J. Cell Biochem.** 72: 570-585.
- Phinney, D. G., Kopen, G., Righter, W., Webster, S., Tremain, N. and Prockop, D. J. (1999b). Donor variation in the growth properties and osteogenic potential of human marrow stromal cells. **J. Cell Biochem.** 75: 424-436.
- Pittenger, M. F., Mackay, A. M., Beck, S. C., Jaiswal, R. K., Douglas, R., Mosca, J. D., Moorman, M. A., Simonetti, D. W., Craig, S. and Marshak, D. R. (1999). Multilineage potential of adult human mesenchymal stem cells. **Science** 284:143-147.
- Reyes, M. and Verfaillie, C. M. (2001). Characterization of multipotent adult progenitor cells, a subpopulation of mesenchymal stem cells. **Ann. NY Acad. Sci.** 938: 231-233; discussion 233-235.
- Ringe, J., Kaps, C., Schmitt, B., Buscher, K., Bartel, J., Smolian, H., Schultz, O., Burmester, G.R., Haupl, T. and Sittinger, M. (2002). Porcine mesenchymal stem cells. Induction of distinct mesenchymal cell lineages. **Cell Tissue Res.** 307: 321-327.
- Sekiya, I., Larson, B. L., Smith, J. R., Pochampally, R., Cui, J. G. and Prockop, D. J. (2002). Expansion of human adult stem cells from bone marrow stroma: conditions that maximize the yields of early progenitors and evaluate their quality. **Stem Cells** 20: 530-541.
- Shahdadfar, A., Fronsdal, K., Haug, T., Reinholt, F. P. and Brinckmann, J. E. (2005).

In vitro expansion of human mesenchymal stem cells: choice of serum is a determinant of cell proliferation, differentiation, gene expression, and transcriptome stability. **Stem Cells** 23: 1357-1366.

Smith, J. R., Pochampally, R., Perry, A., Hsu, S. C., Prockop, D. J. (2004). Isolation of a highly clonogenic and multipotential subfraction of adult stem cells from bone marrow stroma. **Stem Cells** 22: 823-831.

Stenderup, K., Justesen, J., Talebian, F. Ghaffari, S. H., Ghavamzadeh, A. and Nikbin, B. (2003). Aging is associated with decreased maximal life span and accelerated senescence of bone marrow stromal cells. **Bone** 33: 919-926.

Wakitani, S., Saito, T. and Caplan, A. I. (1995). Myogenic cells derived from rat bone marrow mesenchymal stem cells exposed to 5-azacytidine. **Muscle Nerve** 18: 1417-1426.

Wexler, S. A., Donaldson, C., Denning-Kendall, P., Rice, C., Bradley, B. and Hows, J. M. (2003). Adult bone marrow is a rich source of human mesenchymal stem cells but umbilical cord and mobilized adult blood are not. **Br. J. Haematol.** 121: 368-374.

Yu, D. and Silva, G. A. (2008). Stem cell sources and therapeutic approaches for central nervous system and neural retinal disorders. **Neurosurg. Focus** 24: E11.

CHAPTER IV

DISCRIMINATION OF FUNCTIONAL MESENCHYMAL STEM CELLS DERIVED HEPATOCYTE USING FTIR MICROSPECTROSCOPY

4.1 Abstract

Applying mesenchymal stem cells (MSCs) to therapy liver disease, carefully monitor and fully characterizes of functional hepatocyte differentiated *in vitro* are needed. This study employed Fourier transform infrared (FTIR) microspectroscopy to investigate the characteristics of rat bone marrow mesenchymal stem cells (rBM-MSCs) derived hepatocytes by detecting biochemical and molecular composition changes during hepatogenesis process. Principal Component Analysis (PCA) enables us to discrimination the maturation stage of rBM-MSCs derived hepatocytes from undifferentiation rBM-MSCs, the induction and the differentiation stage of rBM-MSCs derived hepatocytes by their FTIR “marker bands”. The predominant discriminating factors responsible for this separation were identified at the following vibrational frequencies: 3012 cm^{-1} (*cis* C=C stretch), 2952 cm^{-1} (vas CH_3), 2854 cm^{-1} (vs CH_2) and 1722 cm^{-1} (C=O stretching of unsaturated acid), which possible associated with triglyceride and unsaturated fatty acid accumulation in hepatocytes for attaining their function. Base on these finding, we suggested that the

rBM-MSCs derived hepatocytes are characterized by high lipid content which facilitates a means of identifying hepatocytes from their derived stem cells by using FTIR microspectroscopy. These results supported that FTIR microspectroscopy is sensitive for monitoring the differentiation state of stem cells under hepatogenic induction particularly at late stage. It provides biochemical information that is complimentary to that obtained from conventional techniques, and may give unambiguous results. In addition, this approach is more straightforward, non-destruction and requires less sample preparation compared with the conventional methodologies.

4.2 Introduction

Practical application of stem cells for regenerative medicine, a number of normal cells differentiated from stem cells are needed to carefully characterize prior to their use for clinical transplantation by rapid low-cost assays. However, in existence methods assay, such as immunocytochemistry, flow cytometry, gene expression studies for functional end cells have been showed to have their restrictions use in practical since time consuming as well as requiring biomarker or label. In addition, these established methods could not monitor various cell types originating from stem cells at the same time. New methods which can be applied both on the single cell level and large populations of cells would be established by monitoring stem cells differentiation *in vitro*.

The emergence of biospectroscopy in cell biology gives a promising tool for stem cell research (Heraud and Tobin, 2009). This biospectroscopy analyses stem cells by using Fourier transform infrared (FTIR) microspectroscopy which have been employed to study human (Krafft et al., 2005; Bentley et al., 2007; Hoshino et al., 2007; Heraud et al., 2010) and murine stem cells (Ami et al., 2008; Tanthanuch et al., 2010) characterization and differentiation by detecting and defining biochemical changes occurring during the differentiation process in the cells. These studies demonstrated that different cell types possessed distinct IR spectral phenotypes, which can be used to distinguish between stem cells and their derivatives. This approach has an ability to characterize difference cell type by sensitive IR spectroscopic fingerprints and give the information changes in macromolecular cellular components such as lipids, proteins nucleic acids and carbohydrates which seen as an easy, rapid, sensitive, nondestructive, noninvasive, label-free method which can be applied to monitoring or sorting large populations of cells (Miler et al., 2003; Downes et al., 2010).

Due to the ethic controversy of embryonic stem cells research and the problem of sources shortages in other adult stem cells, mesenchymal stem cells (MSCs) have been regarded as one of the most promising cell therapeutics for liver disease (Xu et al., 2008). More recently, an *in vitro* direct differentiation model employing growth factors and cytokines know to induce hepatic from MSCs has been developed (Schwartz et al., 2002; Lee et al., 2004). As the liver plays a central role in metabolism, the stem cells derived hepatocytes are needed to be carefully

characterized including the function assay *in vitro*.

The process of embryonic liver development includes the early stage, mid stage and late stage *in vivo*. In this study we have used the hepatic differentiation protocol which mimics the embryonic liver development *in vivo* to induce rBM-MSCs differentiation to hepatocyte and distinguish each differentiation stage by using FTIR microspectroscopy. Aim to determine FTIR markers to characterization of each stage with an easy way.

4.3 Materials and Methods

4.3.1 Isolation, culture and characterization of rBM-MSCs

rBM-MSCs isolation, culture and characterization implemented employing the same protocol as in chapter 3.

4.3.2 Hepatic differentiation

Passage 4 rBM-MSCs culturing at 100% confluence were used for hepatocyte differentiation assays. Hepatic differentiation from rBM-MSCs was performed as described with some modifications (Talens-Visconti et al., 2006). rBM-MSCs were serum deprived for 2 days (conditioning step) in Iscove's Modified Dulbecco's Medium (IMDM) supplemented with 10 ng/ml basic fibroblast growth factor (bFGF) and 20 ng/ml epidermal growth factor (EGF). Then a 2 step protocol was performed. Step 1 medium consisting of IMDM supplemented with 20 ng/ml hepatocyte growth factor (HGF), 10 ng/ml bFGF and 4.9 mmol/L nicotinamide for 7

days. Step 2 medium consisting of IMDM supplemented with 10 $\mu\text{mol/ml}$ ITS (insulin, transferrin and selenous acid, BD), 1 $\mu\text{mol/ml}$ dexamethasone (Dex) and 20 ng/ml oncostatin M (OSM) for 14 days. Medium were changed twice weekly. The different differentiation stages were defined as follow: step 1 (induction stage); step 2 for 7 days (differentiation stage) and 14 days (maturation stage).

4.3.3 Immunocytochemistry for hepatocyte specific marker.

At the last day of differentiation, the cells were fixed with 4% paraformaldehyde solution for 30 minutes at room temperature, and then washed three times with PBS (-), followed by incubation in blocking solution for 2 hours. The cells were subsequently incubated with the following primary antibody mouse anti- α -Fetoprotein (AFP; 1:200), rabbit anti-mouse albumin (ALB; 1:100, Abcan, Cambridge, UK), rabbit anti-hapatocyte nuclear factor 3 β (HNF3 β ; 1:200, Santa), goat anti-hapatocyte nuclear factor 1 α (HNF1 α ; 1:200, Santa), mouse anti-cytokeratin 18 (CK18, 1:200, Santa), goat anti-CCAAT/enhancer-binding proteins α (C/EBP α ; 1:200, Santa) at 4°C overnight. Afterword, the excess primary antibodies were washed out, the cells were treated with second antibody Alexa 488 donkey anti-mouse IgG (1:1000, Molecular probes) or Rhodamine RedTM-goat anti-rabbit IgG (1:1000, Molecular probes) or Alexa 594 donkey anti-goat IgG (1:1000, Molecular probes) respectively for 1 hour. The cells were co-stained with DAPI for 5 minutes and then examined under florescence stereomicroscopy.

4.3.4 Indocyanine green (ICG) uptake study.

ICG (25 mg) was dissolved in 5 ml of solvent in a sterile vial and then added to 20 ml of DMEM containing 10% FBS. The final concentration of the resulting ICG solution was 1 mg/ml. The ICG solution was added to the cell culture dish and incubated at 37°C for 15 minutes. The dishes were rinsed three times with PBS (-), the cellular uptake of ICG was examined with a stereomicroscope.

4.3.5 Periodic Acid-Shiff (PAS) histochemical staining.

Differentiated hepatocytes were immersed in periodic acid solution for 5 minutes at room temperature and rinsed three times with distilled water. Cells were treated with Schiff's reagent for 15 minutes at room temperature, washed in running tap water for 5 minutes, and examined with light microscope.

4.3.6 Albumin ELISA.

Cell culture medium at the induction stage, the differentiation stage and the maturation stage was collected as samples for albumin ELISA following manufacture's instructions. Sample from 5 separate cultures were analyzed in triplicate for each group.

4.3.7 Urea production

The cells of each stage that is the induction stage, the differentiation stage and the maturation stage were incubated with medium containing 5 mM NH₄Cl for 24 hours and the supernatant were measured colometrically in the culture media according to the manufacture's instructions (Quantichrom Urea assay kit, Bioassay

Systems). Fresh culture media supplemented with 5 mM NH₄Cl was used as negative controls. Sample from 5 separate cultures were analyzed in triplicate for each group.

4.3.8 Reverse transcription-polymerase chain reaction (RT-PCR) analysis

The total cellular RNA was extracted from cells using the Trizol reagent according to standard protocols and its purity was assessed by the absorbance ratio 260/280 nm. RNA integrity was examined by agarose gel electrophoresis. cDNA samples were synthesized from 1 µg of total RNA by using a Super Script II first-strand synthesis system (Invitrogen, Carlsbad, CA) with a-oligo(dT)-adaptor primer according to the manufacturer's instructions. The cDNA preparation template was used for subsequent PCR amplification by using Taq DNA polymerase. PCR amplifications were performed using specific primers (Table 4.1) in a final volume of 25 µl. The PCR conditions were: 1) 95°C for 3 minutes; 2) 30 cycles of 30 seconds at 95°C, 30 seconds at 54°C for and 30 seconds at 72°C. Samples were electrophoresed on a 1.5% agarose gel and nucleic acids were visualized by ethidium bromide staining.

Table 4.1 Primers used for RT-PCR characterization

Primer	Sequence	Size (bp)	References
AFP	S: 5'-GAGAGTTGCCAGCATAACGAA-3'	198	Hasuike et al., 2005
	A: 5'-CCTTGTCATACTGAGCGGCTA-3'		
ALB	S: 5'-GAGACTGCCCTGTGTGGAAGA-3'	186	Hasuike et al., 2005
	A: 5'-CTTCCACCAAGGACCCACTA-3'		
HNF-3 β	S: 5'-CCTACTCGTACATCTCGCTCATCA-3'	178	Li et al., 2008
	A: 5'-CGCTCAGCGTCAGCATCTT-3'		
CYP2B1	S: 5'-GAGTTCTTCTCTGGGTTTCCTG-3'	196	Li et al., 2008
	A: 5'-ACTGTGGGTCATGGAGAGCTG-3'		
GAPDH	S: 5'-TGCCCCCGACCGTCTAC-3'	180	Hasuike et al., 2005
	A: 5'-ATGCGGTTCCAGCCTATCTG-3'		

4.3.9 Sample preparation for FTIR microspectroscopy

Samples were collected at different culturing point as follows: the undifferentiated rBM-MSCs, the induction stage, the differentiation stage and the maturation stage. The sample were washed with PBS (-) for three times and removed from the culture dishes after treatment with 0.05% trypsin/0.5 mM EDTA for 3 minutes. The suspension were centrifuged at 600 \times g for 5 minutes and washed three times in a physiological solution (0.9% NaCl in distilled water). The number of cells

was counted with a hemacytometer and adjusted the concentration of $1 \times 10^6/\text{ml}$, then deposited onto indium tin oxide-coated, silver-doped glass slide (MirriIR, Yienta Sciences, OH, USA) air-dried, and stored in the desiccators until spectra were acquired.

4.3.10 FTIR microspectroscopy and data analysis

FTIR measurement was carried out on the IR end station at Synchrotron Light Research Institute (Public Organization), Thailand. The IR data acquisition was performed by the Bruker Hyperion 2000 microscope (Bruker Optics Inc., Ettlingen, Germany) equipped with a nitrogen cooled MCT (HgCdTe) detector with a $36\times$ IR objective, coupled to the Bruker Vertex 70 spectrometer. IR spectra were obtained from a reflection mode by collecting 64 scans, $68\times 68 \mu\text{m}$ aperture size at a resolution of 4 cm^{-1} over a measurement range of $4000\text{-}600 \text{ cm}^{-1}$. Spectral acquisition and instrument control was performed using OPUS 6.5 (Bruker) software.

The Principal Component Analysis (PCA) was conducted on spectra in the range of $3050\text{-}2800 \text{ cm}^{-1}$ and $1750\text{-}750 \text{ cm}^{-1}$ by using Unscrambler 9.7 software (CAMO, Oslo, Norway). All the original IR spectra were processed by taking the second derivative using the Savitzky–Golay algorithm with nine points of smoothing which allow to minimizing the effects of variable baselines and normalized with multiplicative signal correction (EMSC) which normalizes spectra, accounting for differences in sample thickness. Six PCs were chosen for analysis, and loading for each PC were plotted for each sample. Scores plots were used to visualize any

clustering of spectra, and loading plots were used to explain which spectral region most account to the variance in the dataset.

Unsupervised hierarchical cluster analysis (UHCA) was performed in the spectral range of 3050-2800 cm^{-1} and 1750-750 cm^{-1} by using Ward's algorithm, which express a matrix defining inter-spectral distances and merge the similar IR spectra into groupings.

4.3.11 Statistical analysis

Data are presented as mean \pm SEM. The results were analyzed by Student's t-test. $P < 0.05$ was considered statistically significant.

4.4 Results

4.4.1 Characterization of rBM-MSC derived hepatocyte

Upon hepatic differentiation medium, rBM-MSCs underwent a drastic morphological change, which developed a hepatocyte-like morphology, defined as a round or polygonal shape, cytoplasmic granulation and a central nucleus with prominent nucleolus, fibroblastic cells, however, persisted through the differentiation process (Fig.4.1). To determine whether differentiated cells showed the characteristic expression of hepatic phenotype markers, total RNA from cells was isolated at the induction step, the differentiation stage and the maturation stage. RNA transcripts of a number of hepatocyte-specific genes such as HNF3 β , AFP (early hepatic markers), ALB (mid-late hepatic marker) and CYP2B1 (late hepatic marker) were examined by

RT-PCR (Fig. 4.2). Undifferentiated rBM-MSCs were used as negative controls and the rat adult liver cells were used as positive control. Evident AFP and HNF3 β expression appeared at the induction stage and continued to expression through out the whole differentiation stages. Albumin expression appeared at the differentiation stage and continued to expression until the maturation stage. CYP2B1 only expressed at the maturation stage. The change in key liver-enriched factors indicated that the differentiation protocol was effective in driving rBM-MSCs toward a hepatic phenotype. To confirm the homogeneous expression of HNF3 β , AFP (early hepatic markers), ALB (mid-late hepatic marker) and HNF1 α (late hepatic marker) in differentiated cell populations, immunocytochemistry was used to examine the expression of these markers in the differentiated cells. The results showed that the cells expression of these liver specific marker at the maturation stage (Fig. 4.3). The results demonstrate that the levels of hepatic protein markers increased in rBM-MSCs in response to the differentiation protocol, which consistent with mRNA expression analysis.

In order to test whether the differentiated cells possessed liver cell function, we measured liver function of the differentiated cells. Albumin and urea synthesis, as well as glycogen production and ICG uptake, are unique characteristics of hepatocyte. We assayed glycogen storage of the differentiated cells using PAS staining. Glycogen staining was present in the cell at the maturation stage (Fig. 4.4 a). ICG uptake showed that the differentiated cells could uptake ICG at the maturation

stage (Fig. 4.4 b). rBM-MSCs showed no activity of albumin and urea synthesis, glycogen production or ICG uptake in their undifferentiated stage. At the differentiation stage, rBM-MSCs cultured in hepatic differentiation media gained urea synthesizing capabilities. At the induction stage, the induced cells began to secrete albumin at a level of 0.32 ± 0.87 $\mu\text{l/ml}$. At the maturation stage, the albumin concentration of the medium significantly increased up to 3.12 ± 0.25 $\mu\text{l/ml}$, significant higher than that at the differentiation stage ($P < 0.05$, Fig. 4.4 c). The urea concentration of the media was 0.56 ± 0.17 ng/cell/hour at the induction stage ($P < 0.05$), and increased up to 1.98 ± 0.51 ng/cell/hour at the differentiation stage ($P < 0.05$, Fig. 4.4 d). The results suggested that rBM-MSCs derived hepatocyte produce liver-specific protein and are functional *in vitro*.

4.4.2 FTIR microspectroscopy

The hepatic differentiation processes of rBM-MSCs were followed by spectral changes using FTIR microspectroscopy. In order to eliminate individual bands that may overlap in the unprocessed spectra to be visualized, the spectra were converted to the second derivatives and following normalization to correct for differences in sample thickness (Schmid et al., 1997). The average second derivative FTIR spectra presented significant spectral changes in bands associated with lipid region ($3050\text{-}2800$ cm^{-1}), protein region ($1760\text{-}1350$ cm^{-1}) and nucleic acid region ($1350\text{-}900$ cm^{-1}) (Fig. 4.5). Existing literature was used to tentatively assign some of the main peaks contributing to the variance (Table 4.2).

The spectral differences between culturing stages were observed in 3050-2800 cm^{-1} region, which is dominated by acyl chain stretching vibrations with fatty acids of lipids as showed in Fig. 4.5 a. This region are assigned to C-H stretching modes, the symmetric and asymmetric C-H stretching vibrations of CH_2 occur at 2852 cm^{-1} and 2923 cm^{-1} , while the symmetric and asymmetric mode of CH_3 fall at 2873 cm^{-1} and 2958 cm^{-1} , respectively. The spectral profile of this region is similar excepting the bands intensity, thus reflects the degree of lipid content in cells. From the undifferentiated rBM-MSCs to the induction stage, the lipid content remained approximately constant. However, the lipid bands were observed to increase dramatically along differentiation, which reached the highest intensity at the maturation stage of differentiation. It is interesting to note that the main lipid head group ($\nu\text{C}=\text{O}$ stretching at 1740 cm^{-1}) of all differentiation stages showed close spectral position and intensity. Beside, the extra peak at 1712-1722 cm^{-1} corresponding to the C=O stretching of ester group of α and β unsaturated acids was observed to increase along differentiation stages, whereas the strong band shift from 1712 to 1722 cm^{-1} was observed upon the maturation stage. Noteworthy, the *cis* double bond C=C at 3010 cm^{-1} associated with unsaturated fatty acids was observed to dramatically increase throughout the hepatic differentiation process. The band at 1170 cm^{-1} (C-O stretch of esters) was observed to increase during differentiation. The results demonstrated that the maturation stage cells showed highest lipid concentration compare with the undifferenatiation rBM-MSCs, the induction stage and the

differentiation stage cells, which might be reflected to the producing of the new lipid species.

The region from 1760 to 1350 cm^{-1} (Fig.4.5 b) gives information to the total cell protein content in each differentiation stage. The amide I region (1700-1600 cm^{-1}) provides information of protein secondary structure, containing four predominate components: intermolecular β -sheet (1639 cm^{-1}), α -helix (1652 cm^{-1}), β -turn (1681 cm^{-1}) and β -sheet (1695 cm^{-1}). The relative intensity of these components was observed to change when hepatic differentiation took place, indicating that different proteins were expressed during differentiation process. Undifferentiated rBM-MSCs presented highest intensity of α -helix structure (1652 cm^{-1}), β -turn (1681 cm^{-1}) and β -sheet (1695 cm^{-1}). These bands intensity showed sequentially decrease through differentiation stage, suggesting that protein content was likely to be reduced along differentiation process. In addition, the spectral profile of amide II region (1511 cm^{-1} to 1580 cm^{-1}) presented significant changed at the maturation stage. It was found the random coil position of amide II showed duplex peak at 1546 cm^{-1} and 1552 cm^{-1} in all differentiation stage, except the maturation stage cells found absent of 1552 cm^{-1} band. Moreover, undifferentiated rBM-MSCs presented strongly band at 1511 cm^{-1} which give highest intensity over all differentiation stage. This band represents aromatic C=C stretching that might be reflected to protein containing high aromatic amino group. Therefore, the observation of different amide II structure might be connected to the transition of protein species to served hepatic function.

In the nucleic acid region from 1350-900 cm^{-1} , three principal bands were identified and assigned. As can be seen in Fig. 4.5 c, these bands respectively occurred at 1240 cm^{-1} ($\nu_{\text{as}}\text{PO}_4^{2-}$), 1085 cm^{-1} ($\nu_{\text{s}}\text{PO}_4^{2-}$) and 970 cm^{-1} (RNA ribose phosphate main chain), which were found to changes in intensity during hepatic differentiation. The band at 1240 cm^{-1} were observed to change in peak position and intensity during differentiation, which was the peak position shift to 1232 cm^{-1} at the induction stage and backed to 1240 cm^{-1} at the differentiation stage and the maturation stage. The band intensity at 1240 cm^{-1} and 1085 cm^{-1} decreased at the maturation stage of differentiation indicating that the differentiation finish and the band intensity at 970 cm^{-1} which assigned to RNA, seen to increases in the induction stage and the differentiation stage of differentiation, indicating that mRNA translation take place and active to produce the proteins that the new phenotype are expressed, which in line with the protein secondary structure change.

4.4.3 Multivariate analysis

To identify the significant spectral variation upon differentiation process, principal component analysis (PCA) was applied to identify potential rBM-MSCs derived hepatocyte markers. PCA is a widely accepted method that enables the similarities and differences of spectral to be more readily identified. The scores indicate which objects are responsible variety spaces, while loading plot is used to highlight the contribution of each spectral frequency to each PC. PCA decomposition performed on the second derivative spectra from each differentiation stage. The results

showed that the first two PCs explained the best variance in experimental datasets in PCA models. These PCs accounting for 86% total variance (Fig. 4.6 a). PCA analysis provides the potential FTIR marker for discriminate cell stage of differentiation. The distinct separation between the differentiation stage cells and the undifferentiated rBM-MSCs, the induction stage cells is observed in the PCA scores plot along PC1, which explained 51% total variance (Fig 4.6 b), except the maturation stage cells, which was separated along PC2 from other stages (explaining 35% total variances). The PC1 loading plot shows the differences in α -helix protein secondary structure (positive loading at 1648 cm^{-1}) and aromatic C=C stretching (at 1511 cm^{-1}), employed to differentiate the undifferentiated rBM-MSCs, the induction stage cells from the differentiation stage cells, is important discriminator. Meanwhile, the major contributing peak for the differentiation stage cells separated from others stages cells was 1658 cm^{-1} (α -helix), with further peaks of 2915 cm^{-1} ($\nu_{\text{as}}\text{CH}_2$), 2850 cm^{-1} ($\nu_{\text{s}}\text{CH}_2$), 1618 cm^{-1} (amide I), 970 cm^{-1} (RNA ribose phosphate main chain), which revealed in the PC1 negative loading.

The difference between the maturation stage cells and the undifferentiated rBM-MSCs, the induction stage cells in term of lipid, protein secondary structure and nucleic acid were revealed in the PC2 loading plot, which explained 35% total variance (Fig. 4.6 b). The absorption band at 2925 cm^{-1} ($-\text{CH}_3$, $-\text{CH}$ asymmetrical stretch), 2854 cm^{-1} ($-\text{CH}_2$, $-\text{CH}$ symmetrical stretch) and 1722 cm^{-1} ($\text{C}=\text{O}$ stretch) are highly positively correlated with PC2, indicating high lipid content in this stage of cell,

which could be used as marker bands to separate the undifferentiated rBM-MSCs from other stage. Importantly, the band at 1722 cm^{-1} associated to C=O stretch only appeared in maturation stage cells and was hence highly correlated to this stage. The negative loading at lipid bands (2946 cm^{-1} , 2912 cm^{-1} and 2842 cm^{-1}), protein bands (1658 cm^{-1} , 1552 cm^{-1} , 1469 cm^{-1}) and nucleic acid band (1087 cm^{-1}) was employed to discriminate undifferentiated rBM-MSCs and the induction stage cells from other stages, indicating different lipid content, protein secondary structure and DNA/RNA content in these stage.

UHCA was used to study the similarity of spectra between rBM-MSCs and rBM-MSCs derived hepatocytes in the regions of $3050\text{-}2800\text{ cm}^{-1}$ and $1750\text{-}800\text{ cm}^{-1}$. Second derivative FTIR spectra were vector normalized and UHCA applied using Ward's algorithm. The dendrogram represented in the Fig 4.7 permits to identify three major clusters of spectra. There was no misclassification among each group. The spectra of the maturation stage cells were clearly separated from other stages. The induction stage cells and the differentiation stage cells have the similar spectra. This is further evidence for the distinct FTIR spectral profiles corresponding to the three cell types as revealed by PCA, and described above.

4.5 Discussions

The induce hepatocyte protocol used in this study have been demonstrated to efficient and convenient way to induce rBM-MSCs to hepatic lineage, the results

showed that the differentiated cells displayed the hepatocyte like morphology, expressed of hepatic specific gene and protein, functioned as adult liver cells, in accordance with previous studies (Wang et al., 2004; Seo et al., 2005; Chien et al., 2006; Sgodda et al., 2007).

Conventional method to characterization of stem cell derived hepatocyte has been demonstrated that the cells we attained were genuine hepatocyte. We wanted to found the easy way to characterization of stem cell derived hepatocyte, in this aim, we employed FTIR microspectroscopy to detect the process of differentiation and identify FTIR “marker bands” related to biochemical changes that occurred during the differentiation of rBM-MSCs to hepatocytes. The spectral feature we attained from the maturation stage of rBM-MSCs derived hepatocytes were showed to similar to that from human HepG2 cells (Najbjerg et al., 2011). Our results showed that lipid content increase dramatically along differentiation, which reached the highest intensity at the maturation stage of rBM-MSCs derived hepatocyte during differentiation. This increasing in lipid content was consistent with the hepatocyte function: synthesis of lipoproteins, storage of triglycerides by carbohydrates metabolism (Dentin et al., 2006). Moreover, insulin and glucose were added as basic components in hepatogenic differentiation medium might play a key role on induction of gene involving hepatic lipogenesis and lipogenic enzyme activity (Guillen and Cabo, 1997; Han et al., 2009). In addition, the *cis* double bond C=C at 3010 cm^{-1} associated with unsaturated fatty acids was also observed to dramatically increase through hepatic differentiation

process. Observation of both C=O and C=C stretching confirm the accumulation of unsaturated fatty acid by hepatocytes. Previous research has shown that the unsaturated fatty acids protect normal cells against the damage induced by saturated fatty acids, since the excess fatty acids are toxic to cells (Listenberger et al., 2003). Therefore, the unsaturated fatty acid in hepatocyte might play a key role on lipotoxicity prevention (Walker, 2004). In addition, an increase in unsaturated fatty acids band might be attribute to remodeling of phosphatidylcholine (PC) which need to acquire their appropriate fatty acid composition (Zhao et al., 2008).

Important insights to the protein region showed that undifferentiated rBM-MSCs presented highest intensity of α -helix structure (1652 cm^{-1}), β -turn (1681 cm^{-1}) and β -sheet (1695 cm^{-1}). These bands intensity showed to sequentially decrease through differentiation stage, suggesting protein content was likely to reduce along differentiation process. As we know, during the process of hepatic differentiation *in vitro*, AFP begin to expression at the early-stage and through at mid-stage, while ALB expression begin at mid and late stage (Aurich et al., 2007). These two proteins have been showed to contain high α -helix secondary structure (Laskowski et al., 1997). The α -helix band intensity at the maturation stage were observed to decrease compared with the differentiation stage, indicating that the number of AFP positive cells decreased, which consist with previous study (Lee et al., 2004, Sato et al., 2005). Moreover, we found that undifferentiated rBM-MSCs presented strongly band at 1511 cm^{-1} which give highest intensity over all differentiation stage. This band represents

aromatic C=C stretching that might be reflected to protein containing high aromatic amino group (Barth, 2000). Blondheim and his group reported the expression of 8 genes in adult human MSCs relating to the dopamine synthesis which up rise to the tyrosine level in cells as dopamine precursor (Blondheim et al, 2006). Thus, rBM-MSCs might probably have similar pathway that reflect the accumulation of aromatic tyrosine in cells. Therefore, the observation of different amide II structure might be connected to the transition of protein species to served hepatic function.

Furthermore, the intensity of bands in the nucleic acid region, at 1240 cm^{-1} (ν_{asPO}^{2-}), 1085 cm^{-1} (ν_{sPO}^{2-}) and at 970 cm^{-1} (RNA ribose phosphate main chain) was observed to decrease. Symmetric and asymmetric modes of PO^{2-} have been attributed to DNA backbone structure (Chiriboga et al., 2000), were decreased at the maturation stage of differentiation indicating that the differentiation finish and the hepatocytes possessed low proliferation rate (LeCluyse et al., 1995; Rogiers and Vercruyse, 1998). The band at 970 cm^{-1} assigned to RNA, increased from undifferentiated rBM-MSCs to the induction stage and the differentiation stage, finally decreased at the maturation stage, indicating that mRNA translation take place and active to produce the proteins that the new phenotype are expressed, which in line with the protein secondary structure changes.

4.6 Conclusions

The results show that the FTIR microspectroscopy is a powerful approach to

directly probe the biochemical changes observed in the process of rBM-MSCs differentiation into hepatocyte. Combining FTIR spectra with PCA and UHCA, provide an efficiency method to discrimination of hepatocyte from their origins. PCA analysis provided information of possible biochemical changes occurring during the differentiation processes, whereas, UHCA methods could used to discriminate and classify the different differentiation stages. The most promising marker located at lipid region, which appears important for segregation IR spectral of rBM-MSCs derived hepatocyte. FTIR microspectroscopy has been showed to be a sensitive method to discriminate differentiated cell from their stem cells origins, which represent a simple, reagent-free, for monitoring and characterization of the process of stem cell differentiation and would potential be an alternative technique which complementary to other immunocytochemistry methods.

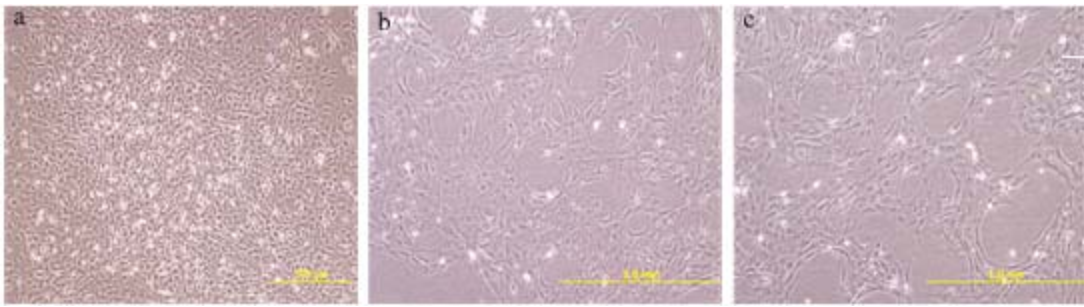


Figure 4.1 Changes in cell morphology during hepatic differentiation of rBM-MSCs.

Cells exhibited fibroblast like morphology at conditioning stage (a), small round, oval islands morphology at the induction stage (b), and hepatocyte like morphology at the maturation stage (c), respectively. Original magnification, 40 ×.

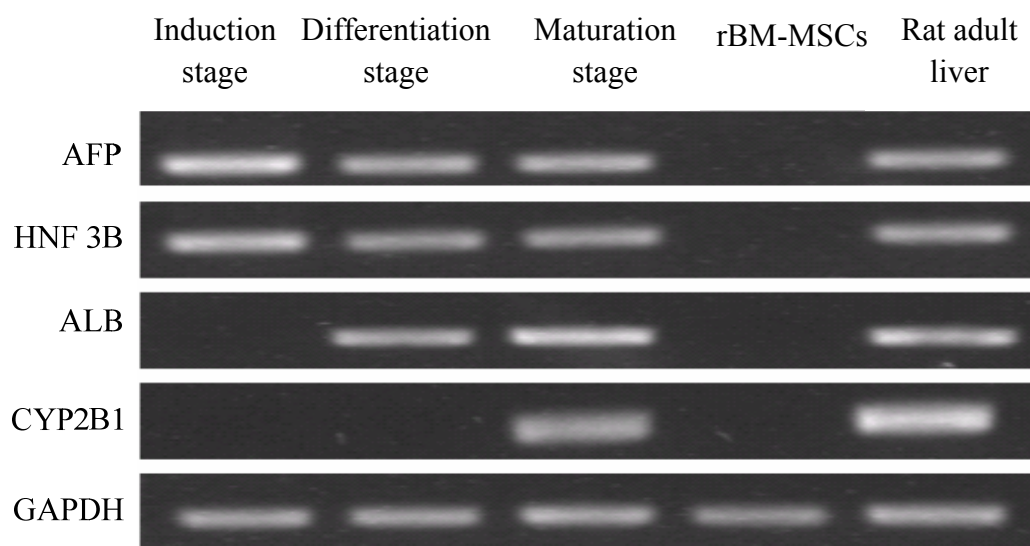


Figure 4.2 RT-PCR analyses of the temporal expression pattern of selected

hepatocyte specific gene during hepatic differentiation of rBM-MSCs. AFP, HNF 3 β , ALB and CYP2B1 expression were analyzed at the induction stage, differentiation stage and maturation stage.

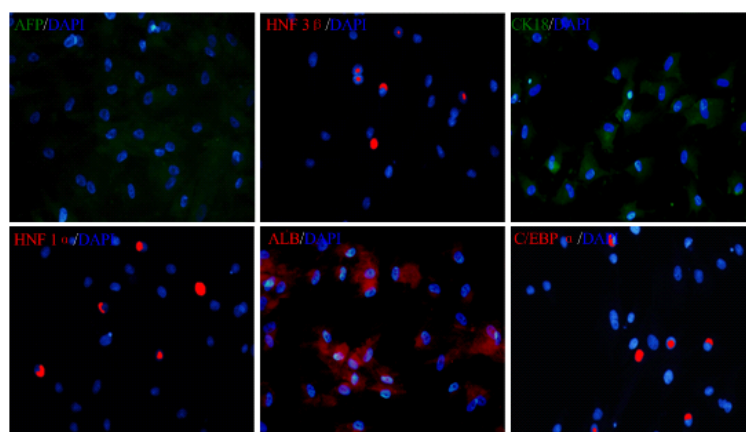


Figure 4.3 The expression of AFP, HNF 3 β , CK18, HNF 1 α , ALB and C/EBP α at the maturation stage of differentiation by immunocytochemistry. Original magnification, 100 \times .

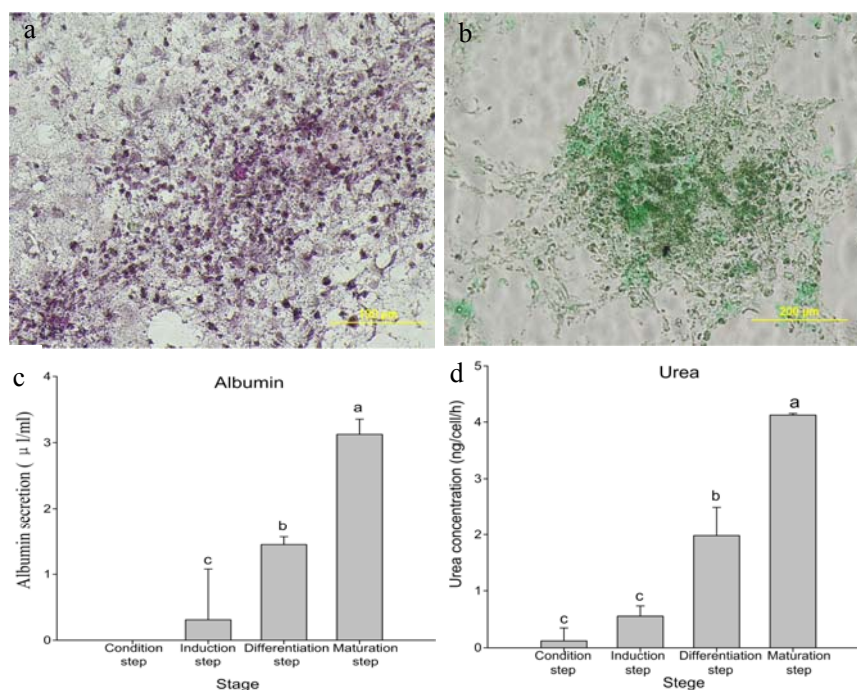


Figure 4.4 The induced rBM-MSCs showed liver function. Glycogen staining (a), ICG uptake (b), albumin secretion (c) and urea concentration (d) at the maturation stage of differentiation. Values represent means \pm SD. Significance was set at $P < 0.05$. Original magnification, 40 \times .

Table 4.2 FTIR frequencies and tentative band assignments

Wavenumber (cm⁻¹)	Assignment	Reference
~3010	<i>cis</i> =CH stretch	Guillen and Cabo, 1997
~2958	CH asym. stretch of -CH ₃	Socrates, 2001
~2923	CH asym. stretch of -CH ₂	Socrates, 2001
~2873	CH sym. stretch of -CH ₃	Socrates, 2001
~2852	CH sym. stretch of -CH ₂	Socrates, 2001
~1743	C=O stretch (ester)	Guillen and Cabo, 1997
~1722	C=O stretch (ester)	Nara et al., 2002
~1695	aggregated β-sheet structures	Bocker et al., 2007
~1681	antiparallel β-sheet structures	Bocker et al., 2007
~1639	antiparallel β-sheet structures	Bocker et al., 2007
~1627	antiparallel β-sheet structures	Bocker et al., 2007
~1580~1511	Amide II	Socrates, 2001
~1240	PO ²⁻ asym. stretch	Diem et al., 2008
~1085	PO ²⁻ sym. stretch	Bocker et al., 2007
~970	RNA ribose phosphate main chain	Wood et al., 2000

asym: asymmetric; sym: symmetric.

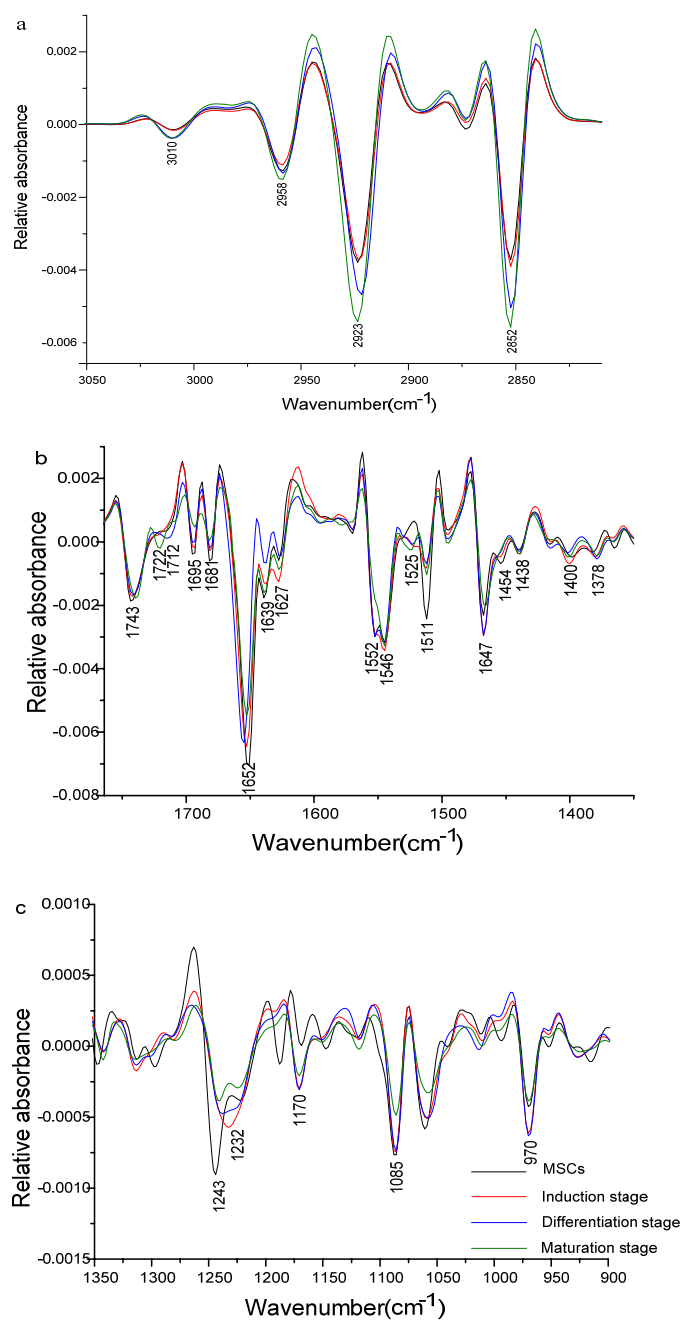


Figure 4.5 Average second derivative FTIR spectra of rBM-MSCs differentiation into hepatocyte-like cell. (a) Shows an enlargement of lipid region (3000-2800 cm^{-1}); (b) shows an enlargement of the protein region (1760-1350 cm^{-1}); (c) shows an enlargement of nucleic acid region (1350-900 cm^{-1}).

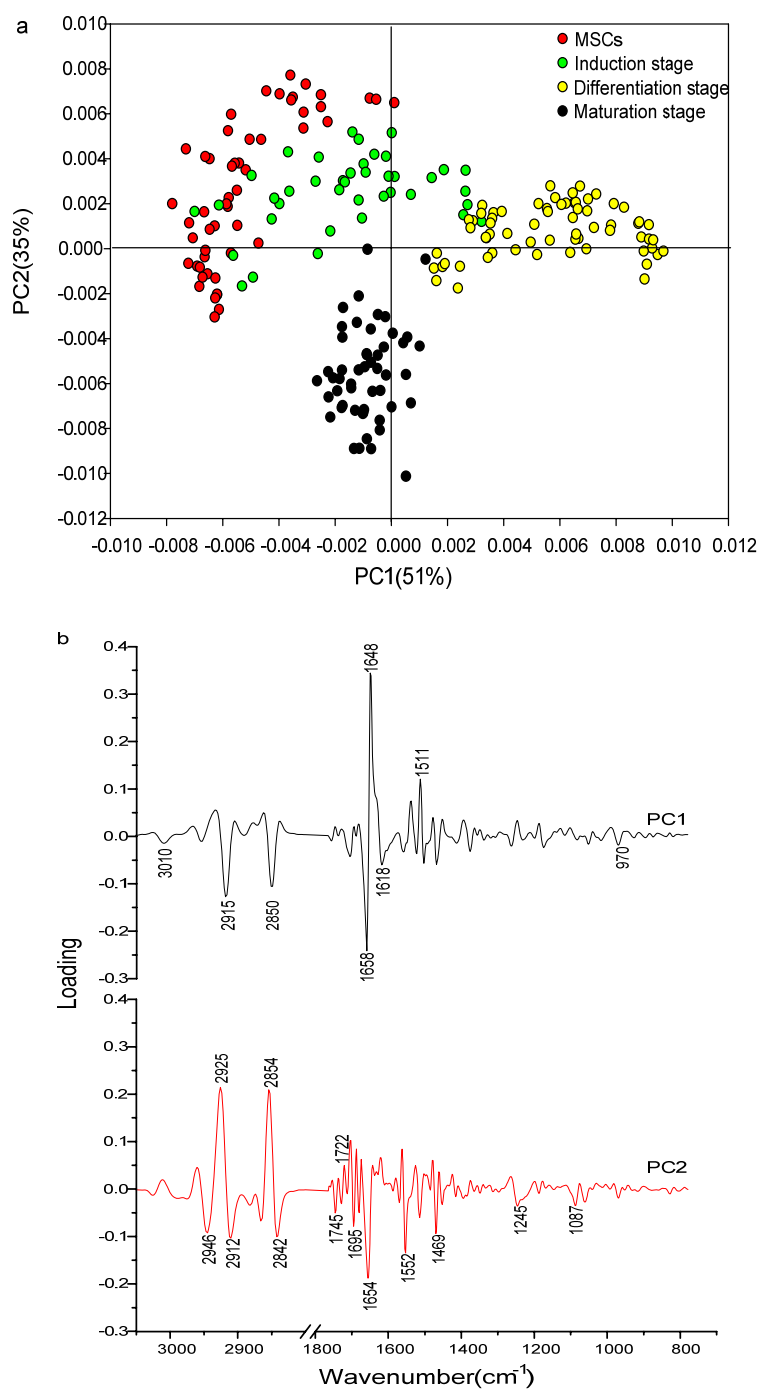


Figure 4.6 PCA scores plots (a) and loading plot (b) of rBM-MSCs differentiation into hepatocytes. Spectra were processed to the 2nd derivative over the spectral range between 3000-2800 cm⁻¹ and 1800-800 cm⁻¹.

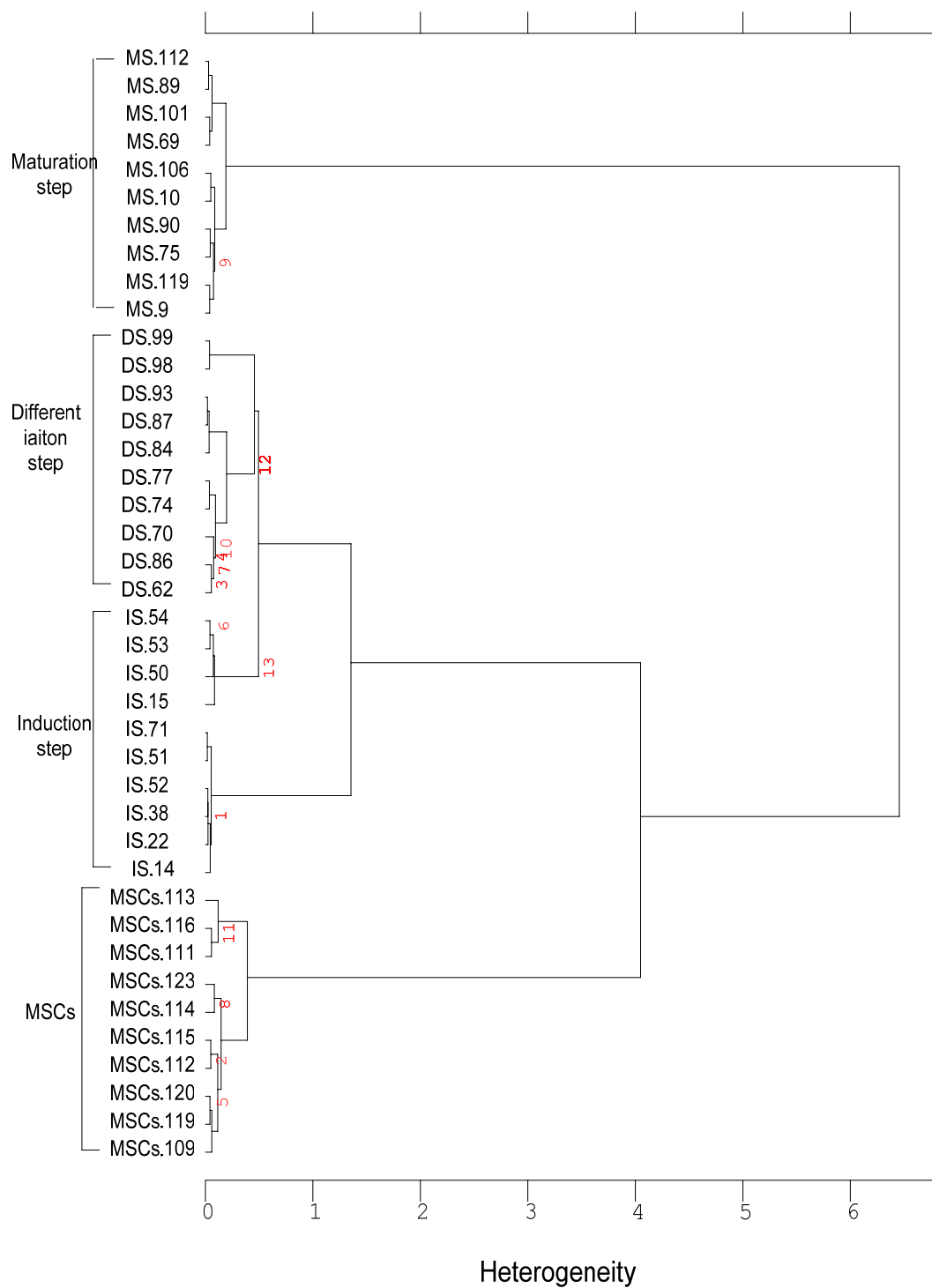


Figure 4.7 Cluster analysis of different stage of rBM-MSCs differentiation to hepatocytes.

4.7 Reference

- Ami, D., Neri, T., Natalello, A., Mereghetti, P., Doglia, S. M., Zanoni, M., Zuccotti, M., Garagna, S. and Redi, C. A. (2008). Embryonic stem cell differentiation studied by FT-IR spectroscopy. **Biochim. Biophys. Acta.** 1783: 98-106.
- Aurich, I., Mueller, L. P., Aurich, H., Luetzkendorf, J., Tisljar, K., Dollinger, M., Schormann, W., Walldorf, J., Hengstler, J., Fleig, W. E. and Christ, B. (2007). Functional integration of hepatocytes derived from human mesenchymal stem cells into mouse livers. **Gut.** 56: 405-415.
- Barth, A. (2000). The infrared absorption of amino acid side chains. **Prog. Biophys. Mol. Biol.** 74: 141-173.
- Bentley, A. J., Nakamura, T., Hammiche, A., Pollock, H. M., Martin, F. L., Kinoshita, S. and Fullwood, N. J. (2007). Characterization of human corneal stem cells by synchrotron infrared micro-spectroscopy. **Mol. Vis.** 13: 237-242.
- Blondheim, N. R., Levy, Y. S., Ben-Zur, T., Burshtein, A., Cherlow, T., Kan, I., Barzilai, R., Bahat-Stromza, M., Barhum, Y., Bulvik, S., Melamed, E. and Offen, D. (2006). Human mesenchymal stem cells express neural genes, suggesting a neural predisposition. **Stem Cells Dev.** 15: 141-164.
- Bocker, U., Ofstad, R., Wu, Z., Bertram, H. C., Sockalingum, G. D., Manfait, M., Egelanddal, B. and Kohler, A. (2007). Revealing covariance structures in fourier transform infrared and Raman microspectroscopy spectra: a study on pork muscle fiber tissue subjected to different processing parameters. **Appl.**

Spectrosc. 61: 1032-1039.

Chien, C. C., Yen, B. L., Lee, F. K., Lai, T. H., Chen, Y. C., Chan, S. H. and Huang, H.

I. (2006). In vitro differentiation of human placental derived multipotent cells into hepatocyte-like cells. **Stem Cells** 24: 1759-1768.

Chiriboga, L., Yee, H. and Diem, M. (2000). Infrared Spectroscopy of Human Cells

and Tissue. Part VII: FT-IR Microspectroscopy of DNase- and RNase-Treated Normal, Cirrhotic, and Neoplastic Liver Tissue. **Appl.**

Spectrosc. 54: 480-485.

Dentin, R., Denechaud, P. D., Benhamed, F., Girard, J. and Postic, C. (2006). Hepatic

gene regulation by glucose and polyunsaturated fatty acids: a role for ChREBP. **Nutrition** 136: 1145-1149.

Diem, M., Griffiths, P. R. and Chalmers, J. M. (Eds). (2008). Vibration Spectroscopy

for Medical Diagnosis. Wiley, UK.

Downes, A., Mouras, R. and Elfick, A. (2010). Optical spectroscopy for noninvasive

monitoring of stem cell differentiation. **J. Biomed. Biotechnol.** 101864.

Guillen, M. D. and Cabo, N. (1997). Characterization of edible oils and lard by

Fourier transform infrared spectroscopy. Relationships between composition and frequency of concrete bands in the fingerprint region. **J. Am. Oil Chem.**

Soc. 74: 1281-1286

Han, C., Wang, J., Li, L., Zhang, Z., Wang, L. and Pan, Z. (2009). The role of insulin

and glucose in goose primary hepatocyte triglyceride accumulation. **J. Exp.**

Biol. 212: 1553-1558.

Hasuike, S., Ido, A., Uto, H., Moriuchi, A., Tahara, Y., Numata, M., Nagata, K., Hori, T., Hayashi, K. and Tsubouchi, H. (2005). Hepatocyte growth factor accelerates the proliferation of hepatic oval cells and possibly promotes the differentiation in a 2-acetylaminofluorene/partial hepatectomy model in rats.

J. Gastroenterol. Hepatol. 20: 1753-1761.

Heraud, P. and Tobin. M. J. (2009). The emergence of biospectroscopy in stem cell research. *Stem cell research* 3: 12-14.

Heraud, P., Ng, E. S., Caine, S., Yu, Q. C., Hirst, C., Mayberry, R., Bruce, A., Wood, B. R., McNaughton, D., Stanley, E. G. and Elefanty, A.G. (2010). Fourier transform infrared microspectroscopy identifies early lineage commitment in differentiating human embryonic stem cells. **Stem Cell Res.** 4: 140-147.

Hoshino, K., Ly, H. Q., Frangioni, J. V. and Hajjar, R. J. (2007). *In vivo* tracking in cardiac stem cell-based therapy. **Prog. Cardiovasc. Dis.** 49: 414-420.

Krafft, C., Salzer, R., Seitz, S., Ern, C. and Schieker, M. (2007). Differentiation of individual human mesenchymal stem cells probed by FTIR microscopic imaging. **Analyst** 132: 647-653.

Laskowski, R. A., Hutchinson, E. G., Michie, A. D., Wallace, A. C., Jones, M. L. and Thornton, J. M. (1997). PDBsum: a Web-based database of summaries and analyses of all PDB structures. **Trends Biochem. Sci.** 22: 488-490.

LeCluyse, E. L., Bullock, P. L. and Parkinson, A. (1995). Strategies for restoration

and maintenance of normal hepatic structure and function in long-term cultures of rat hepatocytes. **Adv. Drug Del. Rev.** 22: 133-186.

Lee, K. D., Kuo, T. K., Whang-Peng, J., Chung, Y. F., Lin, C. T., Chou, S. H., Chen, J. R., Chen, Y. P. and Lee, O. K. (2004). *In vitro* hepatic differentiation of human mesenchymal stem cells. **Hepatology** 40: 1275-1284.

Li, T. Z., Shin, S. H., Cho, H. H., Kim J. H. and Suh, H. (2008). Growth factor-free cultured rat bone marrow derived mesenchymal stem cells towards hepatic progenitor cell differentiation. **Biotechnology and Bioprocess Engineering** 13: 659-665.

Listenberger, L. L., Han, X., Lewis, S. E., Cases, S., Farese Jr., R. V., Ory, D. S. and Schaffer, J. E. (2003). Triglyceride accumulation protects against fatty acid-induced lipotoxicity. **Proc. Natl. Acad. Sci. U S A** 100: 3077-3082.

Miler, L. M., Smith, G. D. and Carr, G. L. (2003). Synchrotron-based biological microspectroscopy: From the mid- to the far-infrared regimes. **J. Biol. Phys.** 29: 219-239.

Najbjerg, H., Afseth, N. K., Young, J. F., Bertram, H. C., Pedersen, M. E., Grimmer, S., Vogt, G. A. and Kohler, G. (2011). Monitoring cellular responses upon fatty acid exposure by Fourier transform infrared spectroscopy and Raman spectroscopy. **Analyst** 136: 1649-1658.

Nara, M., Okazaki, M. and Kagi, H. (2002). Infrared study of human serum very-low-density and low-density lipoproteins. Implication of esterified lipid

C=O stretching bands for characterizing lipoproteins. **Chem. Phys. Lipids** 117: 1-6.

Rogiers, V. and Vercruyse, A. (1998). Hepatocyte cultures in drug metabolism and toxicological research and testing. **Methods Mol. Biol.** 107: 279-294.

Sato, Y., Araki, H., Kato, J., Nakamura, K., Kawano, Y., Kobune, M., Sato, T., Miyanishi, K., Takayama, T., Takahashi, M., Takimoto, R., Iyama, S., Matsunaga, T., Ohtani, S., Matsuura, A., Hamada, H. and Niitsu, Y. (2005). Human mesenchymal stem cells xenografted directly to rat liver differentiated into human hepatocytes without fusion. **Blood** 106: 756-763.

Schmid, P. C., Spimrova, I. and Schmid, H. H. (1997). Incorporation of exogenous fatty acids into molecular species of rat hepatocyte phosphatidylcholine. **Archives of Biochemistry and Biophysics** 32: 1181-1187.

Schwartz, R. E., Reyes, M., Koodie, L., Jiang, Y., Blackstad, M., Lund, T., Lenvik, T., Johnson, S., Hu, W. S. and Verfaillie, C. M. (2002). Multipotent adult progenitor cells from bone marrow differentiate into functional hepatocyte-like cells. **J. Clin. Invest.** 109: 1291-1302.

Seo, M. J., Suh, S. Y., Bae, Y. C. and Jung, J. S. (2005). Differentiation of human adipose stromal cells into hepatic lineage *in vitro* and *in vivo*. **Biochem. Biophys. Res. Commun.** 328: 258-264.

Sgodda, M., Aurich, H., Kleist, S., Aurich, I., Konig, S, Dollinger, M. M., Fleig, W. E. and Christ, B. (2007). Hepatocyte differentiation of mesenchymal stem cells

- from rat peritoneal adipose tissue *in vitro* and *in vivo*. **Exp. Cell Res.** 313: 2875-2886.
- Socrates, G. (2001). Infrared and Raman Characteristic agaroup afarequencies. Wiley and Sons Ltd, Chinchester, UK.
- Talens-Visconti, R., Bonora, A., Jover, R., Mirabet, V., Carbonell, F., Castell, J. V. and Gomez-Lechon, M. J. (2006). Hepatogenic differentiation of human mesenchymal stem cells from adipose tissue in comparison with bone marrow mesenchymal stem cells. **World J. Gastroenterol.** 12: 5834-5845.
- Tanthanuch, W., Thumanu, K., Lorthongpanich, C., Parnpai, R. and Heraud, P. (2010). Neural differentiation of mouse embryonic stem cells studied by FTIR spectroscopy. **J. Mol. Structure** 967: 189-195.
- Walker, W. A. (2004). Pediatric gastrointestinal disease: pathophysiology diagnosis, management, B C Decker Inc, Hamilton, USA.
- Wang, P. P., Wang, J. H., Yan, Z. P., Hu, M. Y., Lau, G. K., Fan, S. T. and Luk, J. M. (2004). Expression of hepatocyte-like phenotypes in bone marrow stromal cells after HGF induction. **Biochem. Biophys. Res. Commun.** 320: 712-716.
- Wood, B. R., Tait, B. and McNaughton, D. (2000). Fourier transform infrared spectroscopy as a method for monitoring the molecular dynamics of lymphocyte activation. **Appl. Specreosc.** 54: 353-359.
- Xu, Y. Q. and Liu, Z. C. (2008). Therapeutic potential of adult bone marrow stem cells in liver disease and delivery approaches. **Stem Cell Rev.** 4: 101-112.

Zhao, Y., Chen Y. Q., Bonacci, T. M., Brecht, D. S., Li, S., Bensch, W. R., Moller, D. E., Kowala, M., Konrad, R. J. and Cao, G. (2008). Identification and characterization of a major liver lysophosphatidylcholine acyltransferase. **Biological Chemistry** 283: 8258-8265.

CHAPTER V

**CHROMATIN REMODELING AGENTS IN HEPATIC
DIFFERENTIATION OF BONE MARROW
MESENCHYMAL STEM CELLS AND ANALYSIS BY
FTIR MICROSPECTROSCOPY**

5.1 Abstract

Epigenetic events, including covalent histone modifications and DNA methylation, are acknowledged to play fundamental roles in the determination of lineage-specific gene expression and cell fate decisions. This study was aimed to investigate whether the DNA methyl transferases inhibitors (DNMTi) 5-Aza-2'-deoxycytidine (5-Aza-dC) and histone deacetylases inhibitors (HDACi) Trichostatin A (TSA) could promote the hepatic differentiation potential of rat bone marrow mesenchymal stem cells (rBM-MSCs). This study also employed the Fourier Transform Infrared (FTIR) microspectroscopy to monitor the biochemical and molecular composition changes upon 5-Aza-dC and/or TSA exposure during hepatic differentiation. Results demonstrated that exposure of rBM-MSCs to 1 μ M TSA in both the differentiation and the maturation stage considerably improved hepatic differentiation. More specifically, TSA enhanced the hepatocyte-shape development, and promoted chronological expression of hepatic proteins, such as α -Fetoprotein (AFP), albumin (ALB), hepatocyte nuclear factor 3 β (HNF3 β), hepatocyte nuclear

factor 1 α (HNF1 α), cytokeratin 18 (CK18) and CCAAT/enhancer-binding proteins α (C/EBP α). In addition, TSA improved the hepatic function, including glycogen storage, Indocyanine green (ICG) uptake, albumin and urea secretion. Meanwhile, the treatment of rBM-MSCs with 20 μ M 5-Aza-dC only or in combination with TSA ineffectively improved hepatic differentiation. The major spectral differences between 5-Aza-dC and/or TSA treated cells and untreated cells were identified at the following vibrational frequencies: 3012 cm^{-1} (*cis*C=C stretch), 2958 cm^{-1} (*vas*CH₃), 2923 cm^{-1} (*vas*CH₂), 2852 cm^{-1} (*vs*CH₂), 1743 cm^{-1} (*vs*C=O stretch), 1722 cm^{-1} (C=O stretching of unsaturated acid), 1652 cm^{-1} (α -helix), 1627 cm^{-1} (intramolecular β -sheet), 1085 cm^{-1} (DNA/RNA) and 970 cm^{-1} (DNA/RNA). These differences suggested that 5-Aza-dC and/or TSA affect the biochemical composition of the cells, which indicated that FTIR microspectroscopy provides an explorative method in monitoring how the chromatin remodeling agent functions on the cells.

5.2 Introduction

Liver development from the endodermal layer is known to proceed via several distinct steps that involve extracellular signals induced by growth factors and cytokines. Numerous cytokines and growth factors have been shown to have potent effects on hepatic growth and differentiation *in vitro* (Lee et al., 2004; Snykers et al., 2006; Talens-Visconti et al., 2007). The importance of the sequential addition of liver-specific factors in a time-dependent manner that resembles the secretion pattern during liver embryogenesis was demonstrated (Snykers et al., 2006). A variety of biochemical cocktails have been developed for promoting the differentiation of adult stem cells into hepatocytes (Snykers et al., 2006; Talens-Visconti et al., 2007;

Kinoshita and Miyajima, 2002; Lee et al., 2004). However, the potential of differentiation attained in existing methods is still low. Mechanisms underlying MSCs overcoming lineage borders and trans-differentiation to hepatocyte is unclear. Initial attempts for improvement were mainly focused on mimicking the *in vivo* situation and addition of soluble medium components. Recently, epigenetic modifications on the procedures of differentiation have received much more attention. This is due to their fundamental role on the controlling of differentiation (Snykers et al. 2009). Epigenetic modifier including DNA methyltransferases inhibitors (DNMTi), such as 5-Aza-2'-deoxycytidine (5-Aza-dC), 5-azacytidine (5-Azac) and histone deacetylases inhibitors (HDACi), such as trichostatin A (TSA) and dimethylsulfoxide (DMSO) were commonly used.

Trichostatin A (TSA) is an organic compound that specifically inhibits classes I and II mammalian histone deacetylase (HDAC) by binding directly to the catalytic site of HDAC (Finnin et al. 1999). The TSA function has interfered with the removal of acetyl groups from histones (histone deacetylases, HDAC) and therefore altered the ability of DNA transcription factors to access the DNA molecules inside chromatin (Medina et al. 1997). Histone acetylating is generally associated with gene activation. The previous studies showed that exposure to TSA, the phenotype of normal primary rat hepatocytes were maintained *in vitro* culture, implying that epigenetic alterations could represent a method to develop phenotypically stable primary hepatocyte cultures (Papeleu et al. 2003; Henkens et al. 2007). Consequently, the hypothesis was made that epigenetic alterations could represent a novel approach to develop phenotypically stable primary hepatocyte cultures. Since chromatin remodeling also plays a central role during organogenesis in regulating differentiation

and stem cell functions. The further reports demonstrated that, exposure of 1 μM TSA to culture human BM-MSC and rat mesenchymal progenitor cells (rMPC) pre-treated for 6 days with hepatogenic stimulating agents, the functional hepatocytes were achieved, indicating that TSA could function as a stimulant during or post-differentiation of hepatic differentiation (Snykers et al. 2007b; De Kock et al. 2008).

5-Aza-2'-deoxycytidine (5-Aza-dC) is a strong inducer of DNA de-methylation. It is an analogue of cytosine, that when incorporated into DNA, irreversibly binds the methyltransferase enzymes as they attempt to methylate the cytosine analogue. This depletion of methyltransferase in the cell results in passive de-methylation, which is known to reactivate epigenetically silenced genes (Mossman et al. 2010). 5-Aza-dC was applied to maintain differentiation in normal mouse primary hepatocyte (Rogiers et al. 2008). Exposure 5-Aza-dC for 24 hours prior to hepatic stimulation which is needed to be successful to induce hepatic differentiation of murine BM-MCS (Yamazaki et al. 2003), rat ADSC (Sgodda et al. 2007), human BM-MSC (Aurich et al. 2007), human umbilical cord blood MSC (Yoshida et al. 2007). In the context, the results showed that 5-Aza-dC could be function as precondition agent prior to hepatic differentiation (Snykers et al., 2009).

FTIR microspectroscopy has been extensively used for the study of conformational changes of molecules and molecular interactions. This method provides specific information regarding the biochemical composition of the sample. The unique characteristics of IR absorption bands of cellular components such as proteins (amide I band at 1650 cm^{-1} , amide II at 1545 cm^{-1} and amide III at 1300 cm^{-1}), lipids (CH stretching bands at $3000\text{-}2800\text{ cm}^{-1}$, CO stretching from ester groups at

1730 cm^{-1}) and nucleic acids (asymmetric PO_2 stretching from nucleic acids at 1240 cm^{-1} , symmetric PO_2 stretching from nucleic acids at 1080 cm^{-1}) can be used for the identification or characterization of biomolecular samples. Moreover, changes in these absorbance bands (e.g. changes in shape, intensity or shifts in peak position) are useful to pinpoint the differences or changes in samples, structures and states of biological specimens.

Up to now, such HDMTi and DNMTi are mostly applied separately, and there is no report comparing the effect of both combined and single exposure to 5-Aza-dC and TSA on the process of hepatogenesis. We were interested to evaluate and compare the effect of such chromatin remodeling agent on the rBM-MSCs differentiation to hepatocyte and employed FTIR microspectroscopy to monitor biochemical and molecular composition changes of the cell upon such chromatin remodeling agent treatment during hepatogenesis.

5.3 Materials and Methods

5.3.1 Isolation and culture of rBM-MSCs

rBM-MSCs isolation and culture was implemented employing the same protocol as in chapter 3.

5.3.2 Hepatic differentiation

The standard hepatogenic protocol was done using the same protocol as in chapter 4. The different chromatin remodeling agents were added to the standard hepatogenic medium at different points of time. These culture conditions included (Table 5.1): (1) group 1: rBM-MSCs were pretreated 20 μM 5-Aza-dC for 24 hours and 1 μM TSA was added to both of the differentiation and maturation steps. (2)

Group 2: rBM-MSCs were pretreated 20 μ M 5-Aza-dC for 24 hours and 1 μ M TSA was added to the maturation step. (3) Group 3: rBM-MSCs were pretreated 20 μ M 5-Aza-dC for 24 hours. (4) Group 4: 1 μ M TSA was added to both of the differentiation and maturation steps. (5) Group 5: 1 μ M TSA was added to the maturation step. (6) Group 6: the standard hepatogenic medium as the control group.

Table 5.1 Chromatin remodeling agent inducing hepatic differentiation protocols

Step	Time	Condition					
		G1	G2	G3	G4	G5	G6
Pre-treatment	24 hours	5-Aza-dC	5-Aza-dC	5-Aza-dC			
Conditioning	48 hours						
Induction	7 days						
Differentiation	7days	TSA			TSA		
Maturation	7days	TSA	TSA		TSA	TSA	

5.3.3 Characterization of hepatocyte-like cells

The liver specific proteins and genes expression, as well as the liver functional assays were implemented using the same protocol and methodology of chapter 4. Positive cell numbers were obtained by counting the number of positive cells out of 1000 culture cells. The data is presented as mean \pm SEM. The results were analyzed by Student's t-test. $P < 0.05$ was considered statistically significant.

5.3.4 FTIR microspectroscopy and data acquisition

Cell samples were collected from different groups at different cultural

points as follows: the induction step, the differentiation step and the maturation step. The sample preparations were using the same methods as in chapter 4.

Spectra were collected by the Bruker Hyperion 2000 microscope equipped with a nitrogen cooled MCT detector with a 36×IR objective, coupled to the Bruker Vertex 70 spectrometer. IR spectra were obtained from a reflection mode by collecting 64 scans, 68×68 μm aperture size at a resolution of 4 cm⁻¹ over a measurement range of 4000-600 cm⁻¹. Spectral acquisition and instrument control was performed using OPUS 6.5 software.

5.3.5 Statistical analysis

The PCA was performed with The Unscrambler 9.7 using the spectra in the range of 3050-2800 cm⁻¹ and 1750-750 cm⁻¹. All the original IR spectra were processed by taking the second derivative using the Savitzky–Golay algorithm with nine points of smoothing which allow for minimizing the effects of variable baselines and normalized with multiplicative signal correction (EMSC) which normalizes spectra, accounting for differences in sample thickness. Six PCs were chosen for analysis, and loading for each PC were plotted for each sample. Scores plots were used to visualize any clustering of spectra, and loading plots were used to explain which spectral regions most accounted for the variances in the dataset.

The relative areas (in percent) were calculated by the integral area of the curve for lipid (*cis* double bond C=C from 3020-3000 cm⁻¹, C-H stretching vibration from 3000-2800 cm⁻¹ and C=O stretching vibration from 1750-1720 cm⁻¹), for amide I protein (1700-1600 cm⁻¹), for DNA/RNA (1336-944 cm⁻¹). The relative integrated area (in percent) of the macromolecular component was calculated in normalized second-derivative infrared spectra by using OPUS 6.5 software. Data was given as

means \pm SD; $P < 0.05$ and was considered significantly different. Error bars indicate standard errors of the means.

5.4 Results

5.4.1 The effect of 5-Aza-dC and TSA on the hepatogenic process

5.4.1.1 Morphological features

To determine the differentiation efficacy of the chromatin remodeling agent, rBM-MSCs culture were exposed to 5-Aza-dC and TSA separately or in combination at different inducing time points (Table 5.1). Results reveal that 5-Aza-dC did not effect the changes of cell morphology in the treatment groups (G 1, 2 and 3) during the pretreatment and the conditioning step, which presented fibroblastic shape (Fig 5.1). At the induction step, cell morphology of all experimental groups has developed to be epithelioid shape. The cells in 5-Aza-dC treated groups (G 1, 2 and 3) were found to have three days delay in morphological changes, compared to those in control group 6. As the differentiation progressed, the change in cellular morphology was gradual in all experimental groups. At the differentiation step, islands of adherence round or polygonal-shaped cells surrounded by spindle-shape cells were observed in all experimental groups. Remarkable changes in cell morphology were observed in group 4 at this step, which displayed hepatocyte-like morphology, defined as cytoplasmic granulation and a central nucleus with prominent nucleolus, but was not observed in control group 6, indicating TSA promoted the hepatic differentiation. At the maturation step, cells underwent a drastic morphological change in all experimental groups compared with those at the beginning of differentiation. However, the sizes of such islands were observed to be

different in each group. Group 4, with exposure of TSA at both the differentiation and the maturation steps, showed the largest size of such islands. The smallest sizes were observed in group 3 which were exposed to 5-Aza-dC only. In addition, the same sizes were observed in group 1, 2, 5 and 6.

5.4.1.2 Liver-specific protein expression

To evaluate whether the morphological changes in 5-Aza-dC and/or TSA treated cells were associated with the changes in expression patterns at the protein level, the expressions of early (HNF3 β , AFP), mid-late (ALB, CK18) and late (HNF1 α , C/EBP α) hepatic markers were performed by immunocytochemistry. The cells from all experimental groups chronologically expressed HNF3 β , AFP, ALB, CK18, HNF1 α and C/EBP α (Fig 5.2), but the patterns and the levels of expression were different in each group (Fig 5.3). The positive rate was calculated by counting the positive cells out of 1000 total cells for each experimental group. At the induction step, the number of HNF3 β positive cells in 5-Aza-dC treated groups (G1, 2 and 3) were significantly lower than that in control group 6 (10 \pm 12%, 6 \pm 11% and 8 \pm 21% vs. 13 \pm 12%, respectively), while, the number of AFP positive cells were not significantly different, which consisted with the result of morphology change, indicating 5-Aza-dC delay the hepatic differentiation. By comparison, the cells in all experimental groups did not express or low express of ALB, CK18, HNF1 α and C/EBP α . At the differentiation step, the positive cell numbers of all analyzed markers were observed to increase except AFP. In TSA only treated Group 4, the number of HNF3 β , ALB, CK18, HNF1 α and C/EBP α positive cells were significantly higher comparing with control group 6 (45 \pm 6% vs. 33 \pm 7%; 35 \pm 6% vs. 18 \pm 12%; 32 \pm 5% vs. 14 \pm 1%; 25 \pm 19% vs. 18 \pm 20%; 24 \pm 3% vs. 18 \pm 5%, respectively). The numbers of positive cells of all

analyzed markers were significantly lower in 5-Aza-dC only treated group 2 and 3 compared with control group 6. There was no significant difference of ALB ($17\pm 16\%$ vs. $18\pm 21\%$), CK18 ($15\pm 2\%$ vs. $14\pm 1\%$), HNF1 α ($18\pm 13\%$ vs. $18\pm 1\%$) and C/EBP α ($12\pm 1\%$ vs. $18\pm 5\%$) positive cells between combination of TSA and 5-Aza-dC group (G1) and control group 6. At the maturation step, the cells in control group 6 expressed AFP, ALB, CK18, HNF1 α , C/EBP α and low levels of HNF3 β , indicating a complete hepatocyte differentiation. The number of positive cells express HNF3 β , AFP, ALB, CK18, HNF1 α , C/EBP α were significantly higher in group 4 comparing with that in control group 6 ($10\pm 2\%$ vs. $4\pm 1\%$; $49\pm 1\%$ vs. $32\pm 4\%$; $41\pm 1\%$ vs. $30\pm 4\%$; $45\pm 9\%$ vs. $27\pm 3\%$; $34\pm 5\%$ vs. $25\pm 14\%$; $33\pm 3\%$ vs. $28\pm 1\%$, respectively). There was no significant difference of the positive cell number expression of all analyzed markers between group 1, 2, 5 and control group 6. 5-Aza-dC treated only group 3, however, was found to have a lower expression of all analyzed markers compared with control group 6.

5.4.1.3 Liver-specific gene expression

To determine whether morphologic changes were sustained and associated with the induction of hepatocyte-specific genes, the total RNA was isolated at the induction step, the differentiation step and the maturation step. RT-PCR was used to analyze the expression of early (HNF 3 β and AFP) and mid-late (ALB and CYP2B1) genes (Fig 5.4). Undifferentiated rBM-MSCs and rat adult liver cells were used as negative and positive controls, respectively. At the induction step, the cells expression of HNF 3 β and AFP, but not expression of ALB and CYP2B1 were detected in all experimental groups. At the differentiation step, the ALB expression was detected in control 6, as well as group 1, 4 and 5, but not in group 2 and 3. In

addition, the CYP2B1 expression was only found in group 4. Moreover, HNF 3 β and AFP continued to be expressed in all experimental groups. At the maturation step, the cell in control group 6 lost to expression of HNF 3 β and began to express CYP2B1. Meanwhile, the expression patterns of all genes in group 1, 4 and 5 cells were observed as the same as adult liver cells. Moreover, the cells continued to the expression of AFP in all experimental groups and ALB expression was detected in all experimental groups.

5.4.1.4 Hepatic functionality

To evaluate whether these rBM-MSC-derived hepatocyte-like cells also acquired typical functional hepatic features, ALB and urea secretion, glycogen production and storage and ICG uptake were analyzed at the last day of hepatic differentiation (Fig 5.5). TSA, added to both of the differentiation and maturation step (G4) significantly increased glycogen production, ICG uptake, ALB and urea secretion when compared with control group 6, while, the lowest level of these were found in 5-Aza-dC only treated group 3, in accord with the previous results that TSA promoted hepatic differentiation and 5-Aza-dC failed to improve hepatic differentiation potential.

5.4.2 Macromolecular changes identified by FTIR microspectroscopy

In an attempt to monitor the cell response to 5-Aza-dC and TSA using FTIR microspectroscopy, the spectra from each group at each step was analyzed. The average FTIR absorbance spectra proved difficult to observe spectral differences among each group, so the second derivative spectrum was performed, which gives a minimum peak for vibration bands and allows easier identification of individual peaks that may be superimposed in the raw spectra. Assignment of biological bands for the

IR spectrum was showed in Table 4.2.

5.4.2.1 Cellular responses monitoring by FTIR microspectroscopy during induction step

5-Aza-dC was added to the pretreatment medium of group 1, 2 and 3 in order to determine their effect on hepatic differentiation of rBM-MSCs. The spectra were collected at the induction step of rBM-MSCs differentiation to hepatocyte. The results demonstrated significant spectral differences between 5-Aza-dC treated cells (G1, 2 and 3) and untreated cells (G4, 5 and 6) (Fig 5.6). The *cis* double bond C=C at 3010 cm^{-1} associated with unsaturated fatty acids (Guillen and Cabo, 1997) was shown to have lower relative absorbance intensity in 5-Aza-dC treated cells (G1, 2 and 3) than untreated cells (G4, 5 and 6) (Fig 5.6a). Moreover, the bands location at 2958 cm^{-1} ($\nu_{\text{as}}\text{CH}_3$), 2923 cm^{-1} ($\nu_{\text{as}}\text{CH}_2$), 2852 cm^{-1} ($\nu_{\text{s}}\text{CH}_2$) which associated with long chain fatty acid of lipid (Socrates, 2001) and the main lipid head group ($\nu_{\text{s}}\text{C}=\text{O}$ stretching at 1743 cm^{-1}) (Guillen and Cabo, 1997) were found to have lower content in 5-Aza-dC treated cells. Bands attributed to proteins ($1700\text{-}1350\text{ cm}^{-1}$) showed more subtle variation differences between the 5-Aza-dC treated and untreated cells, only the band at 1627 cm^{-1} which assigned to intramolecular β -sheet (Bocker et al., 2007) was observed to absent in 5-Aza-dC treated cells (Fig 5.6b). The DNA/RNA regions (1085 cm^{-1} assigned to $\nu_{\text{s}}\text{PO}_2^-$) (Bocker et al., 2007) showed higher intensity in 5-Aza-dC treated cells (Fig 5.6c). The integrated area of C=C unsaturated fatty acids, CH_3 lipid and C=O lipid head were less intense in 5-Aza-dC treated cells comparing with untreated cells, whilst, the integrated area of DNA/RNA was more intense in 5-Aza-dC treated cells comparing with untreated cells. The spectra profiles of protein were shown to be different between 5-Aza-dC treated cells

and 5-Aza-dC treated cells, but not significantly different in their content, indicating the different protein species were expressed. The results indicated that 5-Aza-dC affected the lipid and DNA/RNA content but not the protein content of the cells.

The PCA model was used to examine the variability of all FTIR spectra data set acquired from the 5-Aza-dC treated cells (G1, 2 and 3) and untreated cells (G4, 5 and 6). Distinct clustering of spectra from 5-Aza-dC treated cells and untreated cells were observed in the PCA scores plot along PC2 (explaining 34% total variance, Fig 5.7a). The correlation loading plot was shown in Fig. 5.7b. Lipid bands at 3010 cm^{-1} (*cis*C=C stretch), 2923 cm^{-1} (*vs*CH₂), 2852 cm^{-1} (*vs*CH₂), 1740 cm^{-1} (*vs* C=O stretch) and proteins at 1621 cm^{-1} (intramolecular β -sheet), were strongly negative correlated with 5-Aza-dC untreated cells, indicating that higher intensity of these bands in 5-Aza-dC untreated cells, corroborating the difference in relative absorbance observed in the average spectra. Other bands associated with proteins (α -helix at 1656 cm^{-1} and intermolecular β -sheet at 1639 cm^{-1} , positive loading) and nucleic acid (*vs*PO²⁻ at 1085 cm^{-1} , positive loading) which were highly positive correlated with PC2 were important marker bands for 5-Aza-dC treated cells, confirming the results observed in the second derivative spectra.

5.4.2.2 Cellular responses monitoring by FTIR microspectroscopy during differentiation step

At the differentiation step of rBM-MSCs differentiation to hepatocyte, TSA were added to the medium and the spectra were collected from each experimental group upon exposure with the separation or combination of 5-Aza-dC and TSA. In general, the bands of *cis* double bond C=C (3010 cm^{-1}), CH₃ lipid ($300\text{-}2800\text{ cm}^{-1}$), *vs*C=O stretching (1740 cm^{-1}) and amide I ($1700\text{-}1600\text{ cm}^{-1}$) were

increased and DNA/RNA (1100-950 cm^{-1}) were decreased during differentiation in all experimental groups. The integrated area of *cis* double bond C=C of unsaturated fatty acids band were observed significantly lower in 5-Aza-dC treated cells (G1, G2 and 3) than that of the control cells (G6) (Fig. 5.6a). Even though, the cells in group 1 were further treated with TSA at the differentiation step, there was no significant difference in the integrated area of this band between 5-Aza-dC only treated cells (G2 and 3) and the cells that combine with 5-Aza-dC and TSA were treated (G1). There was no significant difference in the integrated area of this band between TSA only treated cells (G4) and control cells. The intensity of lipid bands at 2958 cm^{-1} (νsCH_3), 2923 cm^{-1} (νsCH_2) and 2852 cm^{-1} (νsCH_2) were significantly lower in 5-Aza-dC and/or TSA treated cells (G1, 2, 3 and 4) compared with the control cells (G6) (Fig 5.6a). The band at 1743 cm^{-1} assigned to $\nu\text{sC=O}$ stretching mainly associated with lipid head group was more intense in 5-Aza-dC and/or TSA treated cells (G1, 2, 3 and 4) than the control cells (Fig 5.6b). Interestingly, the band at 1722 cm^{-1} corresponding to the C=O stretching of ester group of α and β unsaturated acids (Nara et al., 2002) was not observed in 5-Aza-dC or/and TSA treated cells (Group 1, 2, 3, and 4) but in control cells. The integrated area of amide I was observed significantly higher levels in 5-Aza-dC only and a combination with TSA treated cells (G 1 and 3) than that of the control cells. More specifically, the predominate components of amide I attribute to these differently than those that were located at 1695 cm^{-1} (aggregated β -sheet), 1681 cm^{-1} (β -turn), 1652 cm^{-1} (α -helix), 1639 cm^{-1} (antiparallel β -sheet) and 1627 cm^{-1} (antiparallel β -sheet) (Bocker et al., 2007). The integrated area of DNA/RNA which was centered at 1085 cm^{-1} (νsPO_2^-) and 970 cm^{-1} (RNA ribose phosphate main chain) (Wood et al., 2000) showed high intense in 5-Aza-dC or/and TSA treated cells (G 1, 2,

3, and 4). It is interesting to mention that the spectra profile and content of unsaturated fatty acid in TSA treated cells (G4) were similar to that of control group (G6), however, the spectra profile and content of fatty acid, protein and DNA/RNA were similar to that of 5-Aza-dC treated cells (G1, 2 and 3).

The PCA score showed that the spectra extracted from 5-Aza-dC and/or TSA treated cells (G1, 2, 3 and 4) and untreated cells (G5 and 6), clustered separately along PC1, which explained 67% variance (Fig 5.7 c). The PC1 loading plot (Fig 5.7 d) showed that lipid band at 3010 cm^{-1} (*cis*C=C stretch), 2958 cm^{-1} ($\nu_{\text{as}}\text{CH}_3$), 2923 cm^{-1} ($\nu_{\text{as}}\text{CH}_2$), 2852 cm^{-1} ($\nu_{\text{s}}\text{CH}_2$), 1722 cm^{-1} (C=O stretch) and protein band at 1685 cm^{-1} (β -turn), which were highly negative correlated with PC1 correlated with untreated cells. Other bands associated with lipid at 1743 cm^{-1} ($\nu_{\text{s}}\text{C}=\text{O}$ stretching), proteins at 1695 cm^{-1} (β -sheet), 1656 cm^{-1} (α -helix) and nucleic acid at 1085 cm^{-1} ($\nu_{\text{s}}\text{PO}_4^{2-}$) and 970 cm^{-1} (RNA ribose phosphate main chain), which were positive loading in PC1 correlated with 5-Aza-dC and/or TSA treated cells. The PC results indicated that the spectra profile was similar in 5-Aza-dC and/or TSA treated cells at the differentiation step.

5.4.2.3 Cellular responses monitoring by FTIR microspectroscopy during maturation step

At the maturation step, TSA was further added to the hepatogenic medium. The spectra of each experimental group were collected at the end of rBM-MSCs differentiation to hepatocyte. The spectra of CH_3 lipid ($300\text{-}2800\text{ cm}^{-1}$) and amide I ($1700\text{-}1600\text{ cm}^{-1}$) were increased, in addition, $\nu_{\text{s}}\text{C}=\text{O}$ stretching (1740 cm^{-1}) and DNA/RNA ($1100\text{-}950\text{ cm}^{-1}$) were decreased during hepatogenic in all experimental groups. Fig 5.6 a showed that the integrated area of the *cis* double bond

C=C (3010 cm^{-1}) was not significantly different between treated cells (G1, 2, 4 and 5) and the control cells (G6), except 5-Aza-dC only treated cells (G3) which were found significantly lower of this band. The intensity of lipid bands at 2958 cm^{-1} (νasCH_3), 2923 cm^{-1} (νasCH_2) and 2852 cm^{-1} (νsCH_2) were found significantly lower in 5-Aza-dC only treated cells (G3) than the control cell. Meanwhile, TSA only (G4 and 5) or a combination with 5-Aza-dC treated cells (G1 and 2) were found to be lower than the control group but significantly higher than 5-Aza-dC only treated cells (G3) of these bands. The intensity of the main lipid head group ($\nu\text{sC=O}$ stretching at 1743 cm^{-1}) was significantly higher in TSA only treated cells (G4) than the control cells. 5-Aza-dC only treated cells (G3) showed the lowest content of this band. The band at 1722 cm^{-1} corresponding to the C=O stretching of ester group of α and β unsaturated acids appeared in all treated cells except 5-Aza-dC only treated cells. In the protein amide I region, the main component at 1695 cm^{-1} (aggregated β -sheet), 1681 cm^{-1} (antiparallel β -turn), 1652 cm^{-1} (α -helix), 1639 cm^{-1} (antiparallel β -sheet) and 1627 cm^{-1} (antiparallel β -sheet) were significantly higher in 5-Aza-dC only treated cells than control cells. There was no significant difference among the other treated cells (G1, 2, 4 and 5) of these bands they but showed higher intensity than the control cells. In DNA/RNA ($1300\text{-}900\text{ cm}^{-1}$), the bands at 1085 cm^{-1} (νsPO_2^-) and 970 cm^{-1} (RNA ribose phosphate main chain) were observed to be significantly higher in 5-Aza-dC only treated cells than control cells. There was no significant difference in TSA only or a combination with 5-Aza-dC treated cells of these bands.

The PCA scores plot (Fig 5.7e) shows that the spectra extracted from 5-Aza-dC only treated cells (G3) and from other treated cells (G1, 2, 4, 5 and 6), clustered separately along PC1 (explained 84% variance). The major peaks for

identifying the 5-Aza-dC only treated cells were protein band at 1654 cm^{-1} (α -helix) with other bands at 1085 cm^{-1} (νSPO_2^-) and 970 cm^{-1} (RNA ribose phosphate main chain) which associated with nuclei acid (Fig 5.7f), indicating that high intensity of these bands in 5-Aza-dC only treated cells at the maturation step. The negative PC1 loading plot belonging to group1, 2, 4, 5 and 6 shows higher levels in lipid bands at 3010 cm^{-1} (*cis*C=C stretch), 2921 cm^{-1} (νasCH_2), 2852 cm^{-1} (νsCH_2) and 1722 cm^{-1} (C=O stretch) than that of group 3, corroborating the large difference of profile in second derivative spectra.

5.5 Discussions

The objective of this study was to determine the effect of 5-Aza-dC and TSA separately or in combination on the rBM-MSCs differentiation to hepatocyte. In addition, we proposed to use FTIR microspectroscopy to obtain very specific information regarding the biochemical composition and changes in response of the cells upon 5-Aza-dC and/or TSA exposure during hepatogenesis. Results of conventional techniques showed that $1\text{ }\mu\text{M}$ TSA could improve and enhance the hepatic differentiation when it was added at both the differentiation and the maturation steps (G4). Especially, TSA found to induce early hepatocyte-like cells apparent, increased, prolonged and stabilized the overall expression level of typical hepatic protein and enhance hepatic function, such as albumin and urea secretion, glycogen production and ICG uptake. However, the degree of improvement is time dependent. When the cells were exposed of TSA at the maturation step (G5) neither improvement of the hepatic maturation degree, nor hepatic functionality. Our results were consistent with a previous study reported by Snykers and colleagues (2007a).

Addition of TSA to cultured human bone marrow MSCs, pre-treated for 6 days with hepatogenic stimulating agents, triggers their 'trans' differentiation into cells with similar phenotypic and functional characteristics as primary hepatocytes. Similar results have showed that rat bone marrow derived mesenchymal progenitor cells (rMPCs) that were exposed to TSA from day 6 of hepatic differentiation onwards. Significant hepatic differentiation was found. TSA seems a potential to overcome cell fate determinism, cross lineage borders and favor lineage-specific differentiation (Snykers et al., 2009). TSA that was added to the stimulating condition failed to promote oligodendrocyte differentiation in rat neural progenitors, while it could trigger differentiation into neural cells in a neural stimulating condition, which indicated that timing is one of the important factors that affect the TSA function (Hsieh et al., 2004). Our results showed that exposure TSA only at the maturation step failed to promote hepatic differentiation. This may be because of incorrect exposure time. Although mechanistic insights in how TSA regulate transcription of lineage-specific genes are, at present, largely unresolved, previous studies including our results demonstrated that pre-stimulation of the cells towards the intended selected direction prior to introduction of TSA, may comprise a key determinate to cross lineage boundaries and achieve promoted transdifferentiation into a specific lineage by means of TSA inhibition.

We also found that 5-Aza-dC exposure only failed to improve hepatic differentiation potential (G3) with the evidence that lower hepatic maturation degree and functionality, which opposite to the previously studies that 5-Aza-dC function as preconditioning agents prior to hepatic differentiation (Yamazaki et al. 2003; Aurich et al. 2007; Sgodda et al., 2007; Yoshida et al., 2007; Stock et al., 2008). In addition,

TSA more or less compensated the function of 5-Aza-dC treatment (G1 and 2) with time independent, the improvement of hepatic maturation degree and hepatic functionality were found, indicating that the synergetic or synergistic behavior of 5-Aza-dC and TSA respect to hepatic differentiation processes (Rogiers et al. 2008). The reasons underlying these controversial results are unknown. However, it might be due to the different sources of MSCs and difference in microenvironment. Successful cell fate manipulation highly relies on the microenvironment (cell-cell contact, cell densities), the appropriate type of epigenetic modifier and optimal fine-tuning of its dose and timing- onset and duration- of exposure (Shen et al., 2005; Seo-Gutierrez et al., 2005; Snykers et al., 2007b; De Kock et al., 2008). The suitability of HDACi and/or DNMTi to promote hepatic (trans) differentiation requires a delicate balance between proliferation and differentiation, biological activity, pharmacokinetic properties and toxicological characteristics, and finally apoptosis and cell survival (Snykers et al., 2007b). At least in some cases, failure of lineage-specific differentiation could be ascribed to inaccurate timing of exposure and dosage of chromatin modulating agents. Basically, although not generally, pre-stimulation of the cells towards the intended selected direction prior to introduction of HDACi, may comprise a key determinant to cross lineage boundaries and achieve promoted transdifferentiation into a specific lineage by means of HDAC inhibition (Enright et al., 2005; Kawamura et al., 2005; Seo-Gutierrez et al., 2005; Soto-Gutierrez et al., 2006; Snykers et al., 2007a; De Kock et al., 2008; Hay et al., 2008; Mizumoto et al., 2008).

We further investigated the biochemical changes upon 5-Aza-dC and/or TSA exposure by using FTIR microspectroscopy. Exposure TSA at both the differentiation

and the maturation step (G4), in general, the changes of spectra profile were similar to the control groups, but the level of changes were found to be different. The expression pathway of *cis* double bond C=C (3010 cm^{-1}) was found similar to control group (G6), however, C=O stretching of ester group of α and β unsaturated acids, CH₃ lipid of fatty acid, protein amide I secondary structure and DNA/RNA were shown to be significantly different. C=O stretching of ester group of α and β unsaturated acids was found to have higher intensity in group 4 than control group (G6) indicated the accumulation of unsaturated fatty acids in the cells. Unsaturated fatty acids protect normal cells against the damage induced by saturated fatty acids, since the excess fatty acids are toxic to cells (Listenberger et al., 2003). Therefore, the unsaturated fatty acid in hepatocyte may play a key role in lipotoxicity prevention (Walker, 2004). This result confirmed that TSA enhances the hepatocyte function which has been shown in conventional testing. The lower intensity of lipid bands at 2958 cm^{-1} ($\nu_{\text{as}}\text{CH}_3$), 2923 cm^{-1} ($\nu_{\text{as}}\text{CH}_2$) and 2852 cm^{-1} ($\nu_{\text{s}}\text{CH}_2$) were found in group 4 compared with control group (G6) at the end of the hepatic differentiation, which is relative to the function of the cell. Functional hepatocytes have the ability not only to accumulate triglycerides by carbohydrate metabolism but also to oxidize fatty acids produced by the cells (Dentin et al., 2006). The possible reason for the lower intensity of lipid bands may be because fatty acids produced by cells are being oxidized rather than those accumulated in the cell as triglycerides, which further confirms the conventional text. We observed the changes of protein secondary structure of the cells, which was observed significantly higher in group 4 than control group. This indicates the changes in protein composition of the TSA treated cells. The conventional method indicated that the different levels of liver specific protein were expressed in TSA

treated cells, which result in the protein content being different as shown in the IR spectra. The higher intensity of DNA/RNA bands at 1085 cm^{-1} and 970 cm^{-1} in TSA treated cells than control group (G6) were observed. The possible reason may be that TSA induces a hyperacetylation state of chromosome which enhances gene expression (Snyker et al., 2009). Furthermore, after exposing TSA to the maturation step (G5), the lipid and C=O stretching bands were found to have subtle difference to group 4, which reflect the different degree of functional hepatocyte, conforming the result that the TSA exposure is time dependent.

In 5-Aza-dC only treated cells (G3), the changes of spectral profile in lipid, protein and the DNA/RNA region were found to have a large difference compared with the control group. In 5-Aza-dC only treated cells, the lower intensity of band at 3010 cm^{-1} and 1743 cm^{-1} associated with unsaturated fatty acids indicated a low intensity of unsaturated fatty acids, confirming the results that 5-Aza-dC only treated fail to induce the functional hepatocyte differentiation. The content of bands at 2958 cm^{-1} (ν_{asCH_3}), 2923 cm^{-1} (ν_{asCH_2}) and 2852 cm^{-1} (ν_{sCH_2}) were significantly lower in 5-Aza-dC only treated cells, suggesting low lipid content in the cells. This spectral feature also demonstrated that 5-Aza-dC only fail to function hepatocyte differentiation, which consisted with the conventional characterization results. The confirmed evidence also seem absent of band at 1722 cm^{-1} which have been defined as a marker band in chapter 4. The high level of protein region maybe attributes the large proportion of undifferentiated rBM-MSCs which are rich in protein content (Blondheim et al, 2006). In addition, 5-Azac-dC have been shown to unmethylated DNA and active transcription (Sfzy, 2005), this may be the possible reason that the higher intensity of DNA (at 1240 cm^{-1} and 1085 cm^{-1}) content was observed in

5-Azac-dC treated cells. Combined exposure 5-Aza-dC and TSA (G1 and 2), regardless TSA exposure time, the spectral profile were similar to the control group but different to that of 5-Aza-dC or TSA only treated group. The results confirm the conventional analysis.

5.6 Conclusion

The results of conventional biochemistry tests suggesting that 1 μ M TSA enhance the improvement of hepatic differentiation. On the other hand, exposure with 5-Azac-dC only or combined exposure of 5-Azac-dC and TSA failed to improve hepatic differentiation. The changes in the observed FTIR absorbance bands upon 5-Azac-dC and TSA treated attributed to lipid, protein secondary structure and DNA/RNA. The observation of these biochemical changes contributed to the understanding of cell responded to chromatin remodeling agent. FTIR microspectroscopy are shown to be useful tools for tracking the alteration of biochemical molecular in cells during exposed to chromatin remodeling agent.

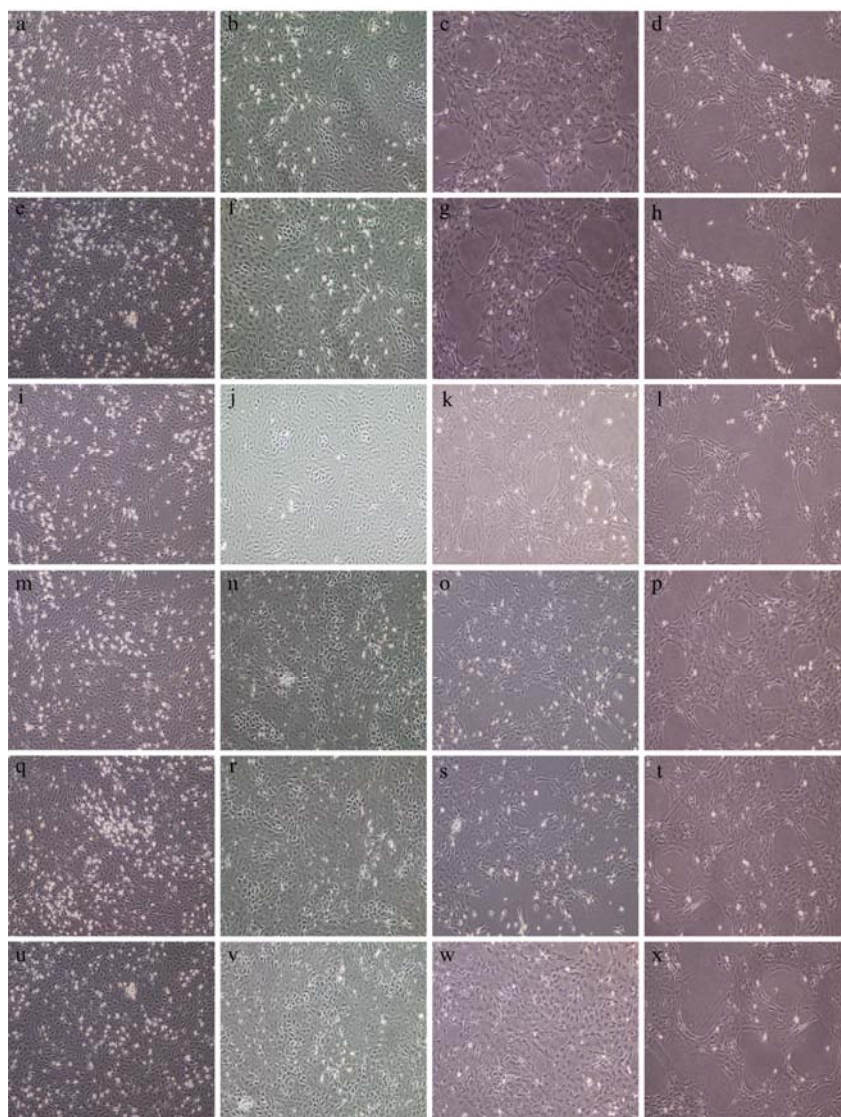


Figure 5.1 Changes in cell morphology during hepatic differentiation of rBM-MSCs. The cells in Group 1 (a-d), Group 2 (e-h), Group 3 (i-l), Group 4 (m-p), Group 5 (q-t) and Group 6 (u-x) exhibited fibroblast like morphology at the conditioning stage (a, e, i, m, q and u), small round or oval morphology at the induction stage (b, f, j, n, r and v), islands morphology at the differentiation stage (c, g, k, o, s and w) and hepatocyte like morphology at the maturation stage (d, h, l, p, t and x), respectively. Original magnification, 40 \times .

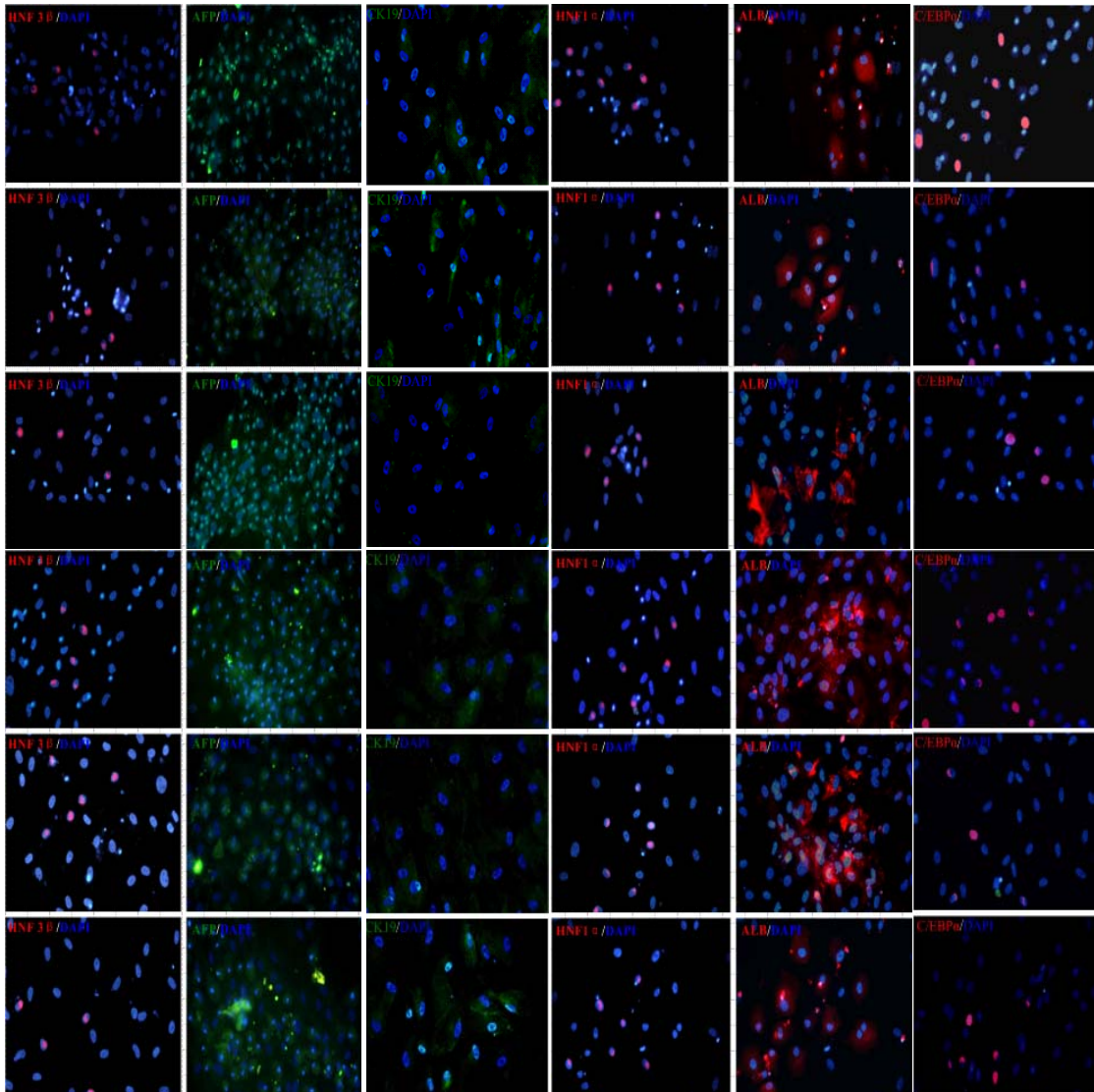


Figure 5.2 The expression of HNF 3 β , AFP, CK18, HNF 1 α , ALB and C/EBP α at the last day of hepatic differentiation of each experimental group by immunocytochemistry. The first row from the top to the sixth at the bottom represents Group1 to Group 6, respectively. Original magnification, 200 \times .

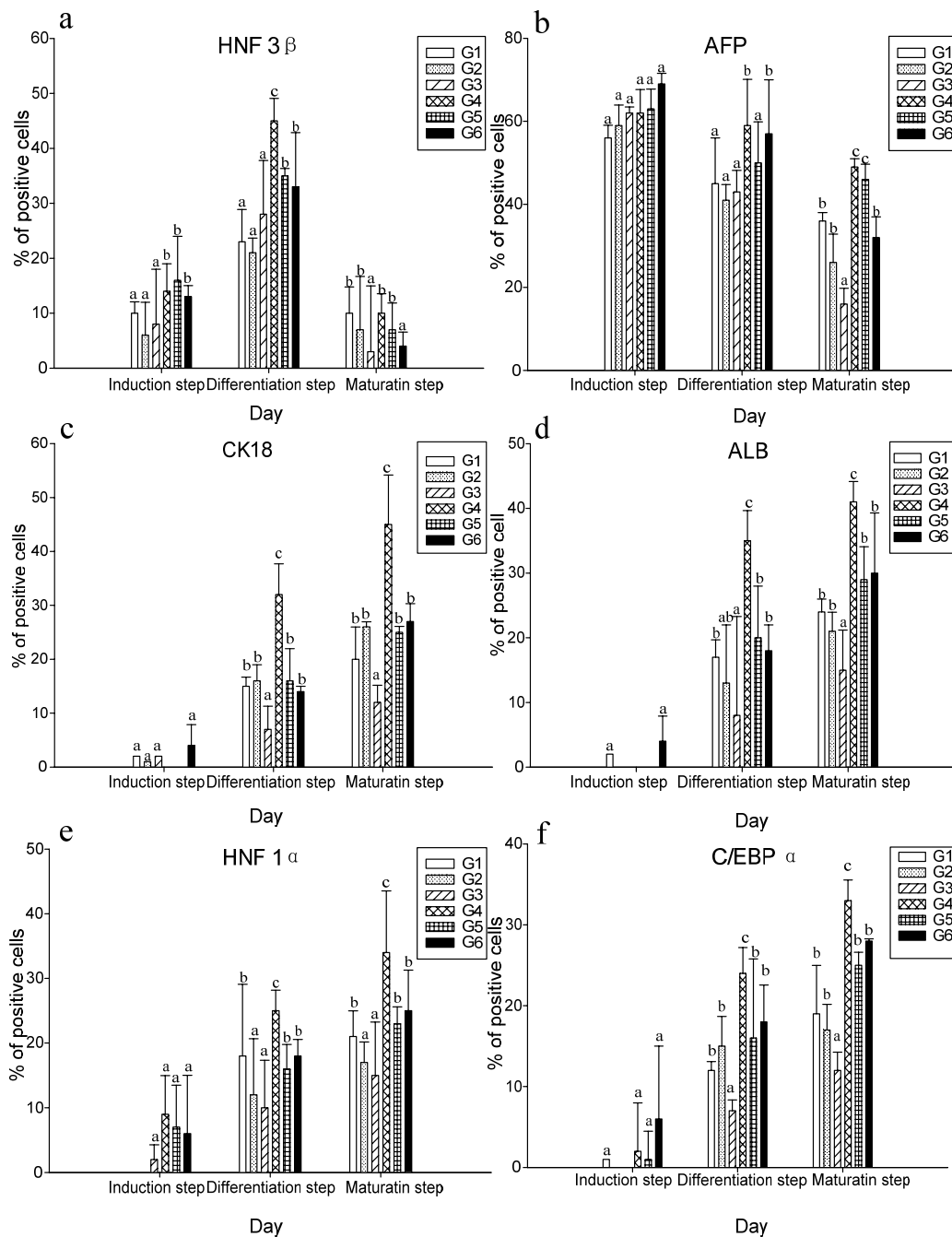


Figure 5.3 Comparative of hepatocyte specific proteins expression upon chromatin remodeling agent exposure. Immunocytochemistry was performed for HNF 3 β (a), AFP (b), CK18 (c), ALB (d), HNF 1 α (e), C/EBP α (f). Values represent means \pm SD. Significance was set at $P < 0.05$.

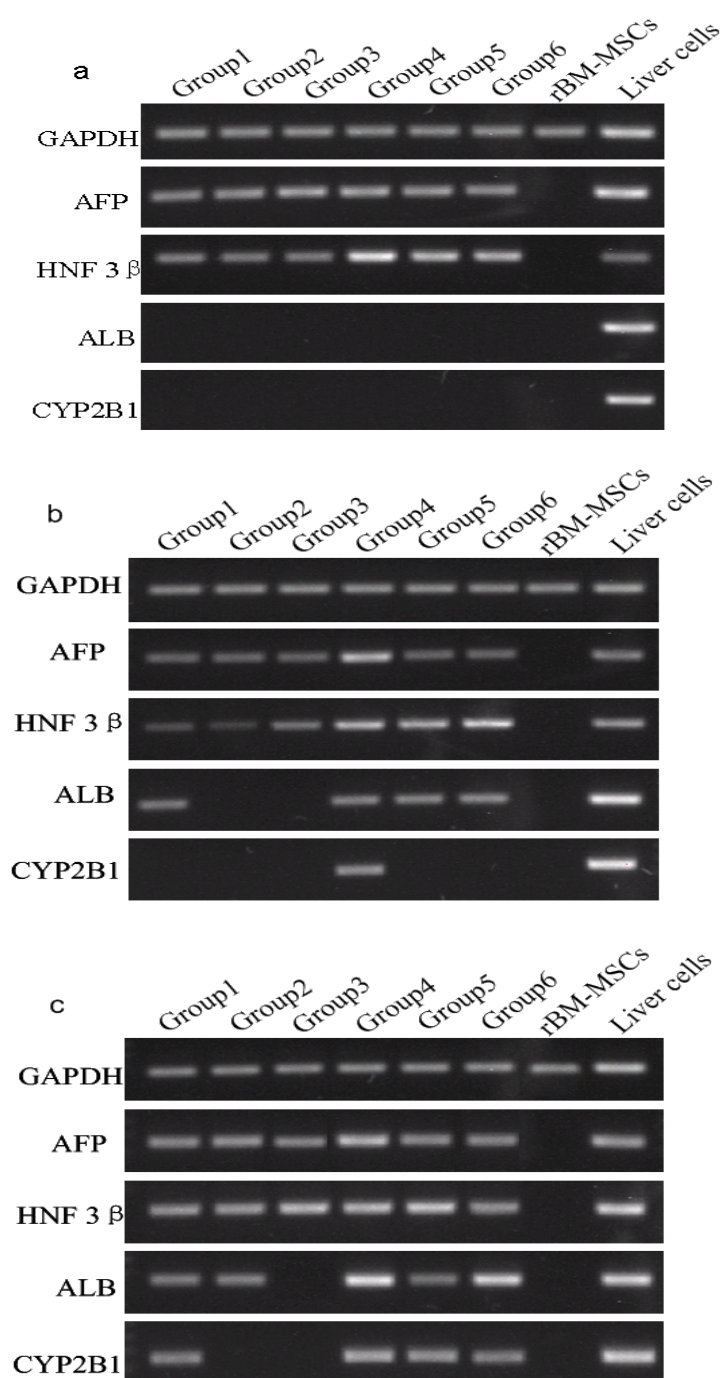


Figure 5.4 RT-PCR analyses of the temporal expression pattern of selected hepatocyte specific gene during hepatic differentiation of rBM-MSCs. AFP, HNF 3 β , ALB and CYP2B1 expression were analyzed at the induction step (a), the differentiation step (b) and maturation step (c), respectively.

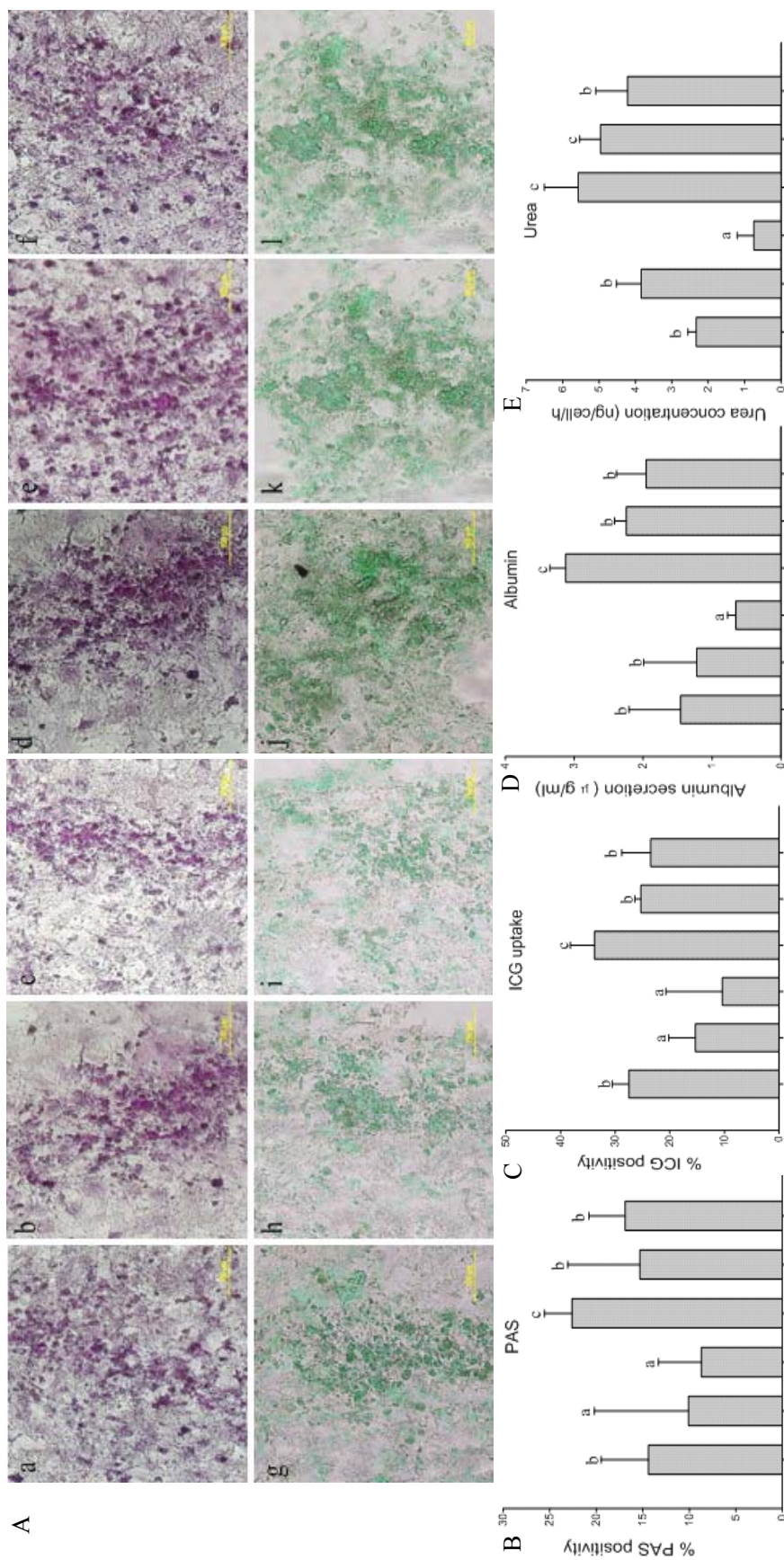
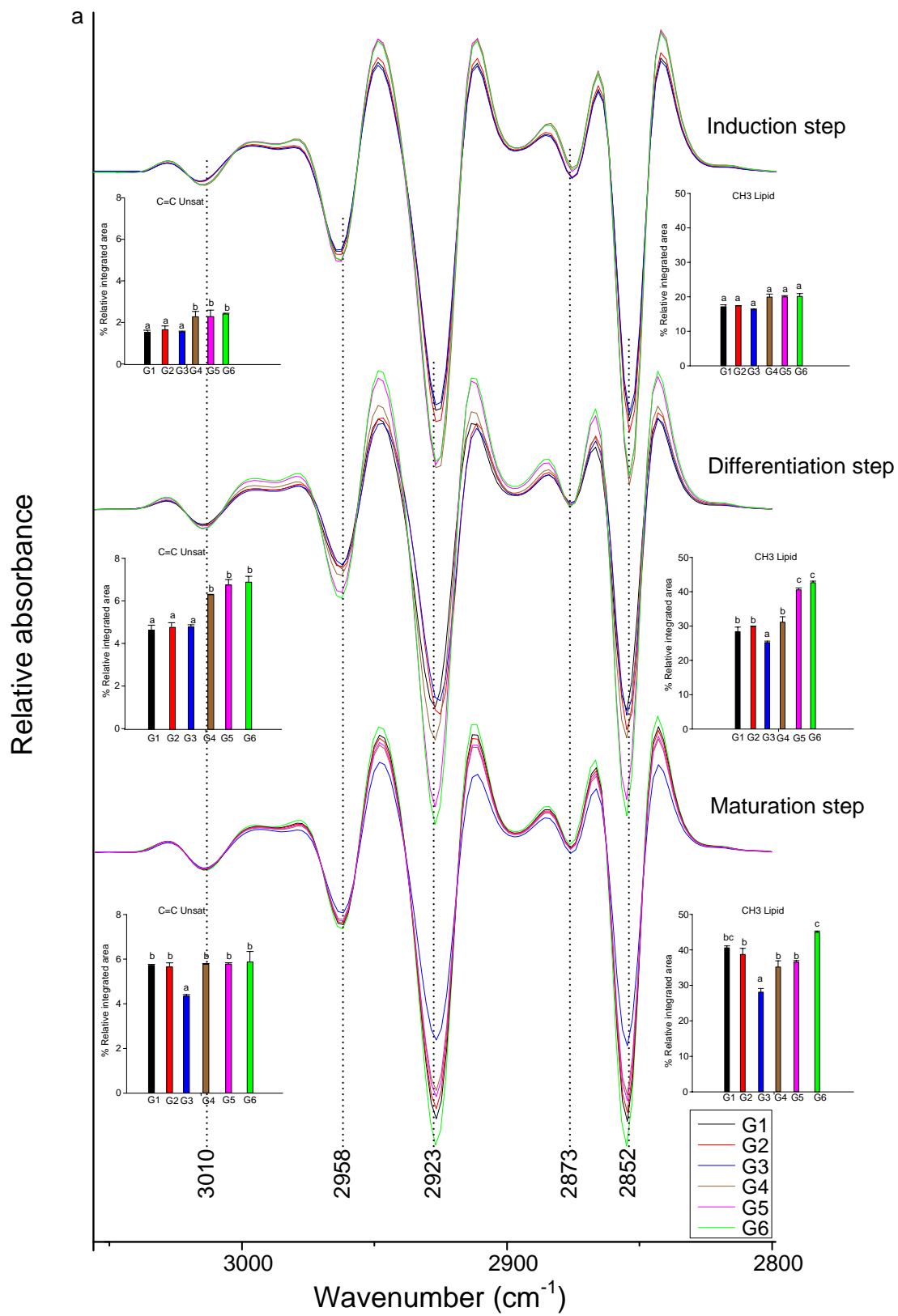
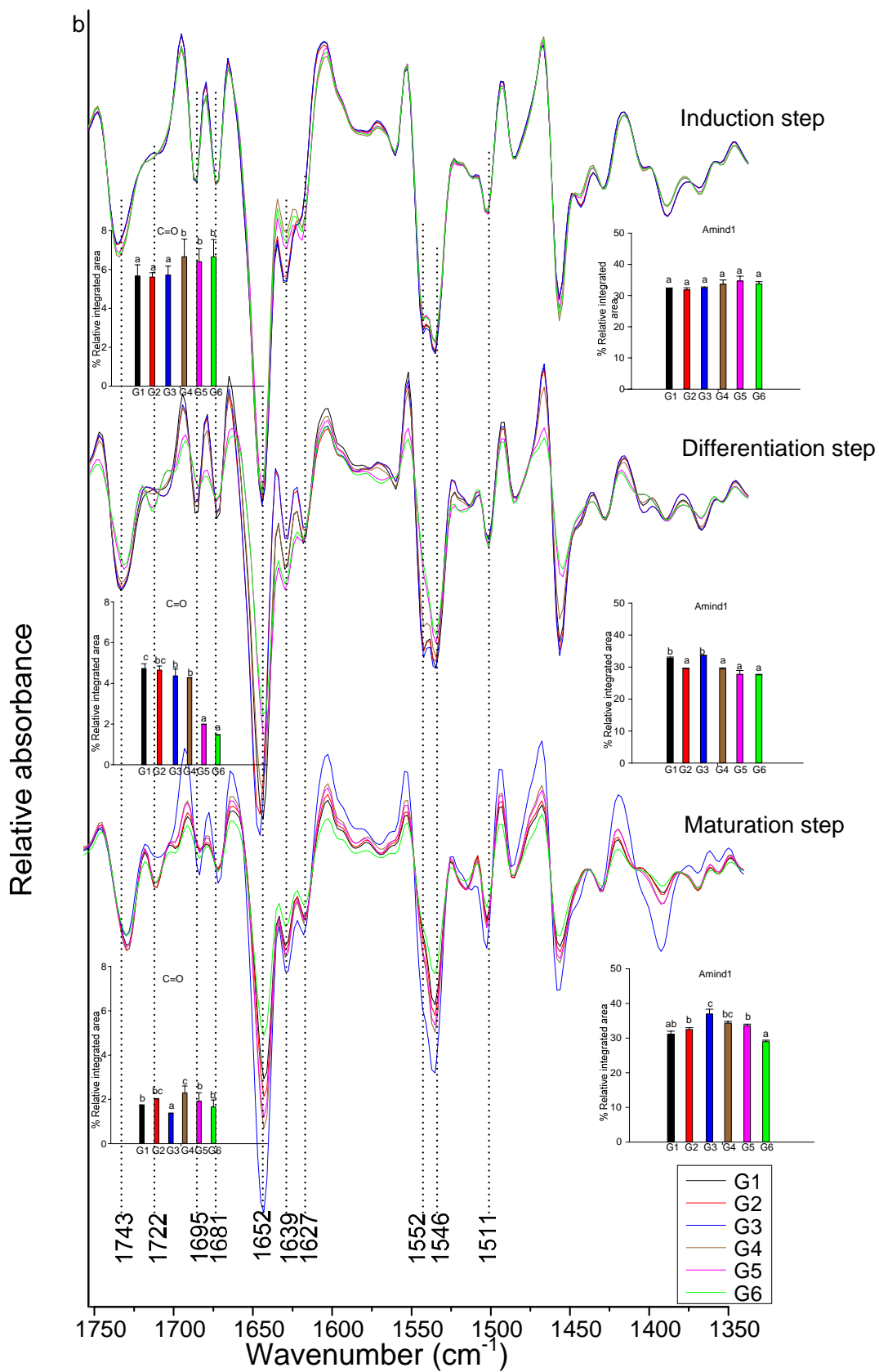


Figure 5.5 Comparative analysis of hepatocyte like functionality at the last day of hepatic differentiation. (A) PAS (a-f) assays showing glycogen-positive cells and ICG uptake (g-l) in each experimental group. (B) Level of glycogen positive cells. (C) ALB secretion. (D) Urea production. (E) Urea concentration. Original magnification, 40 ×. Significance was set at $P < 0.05$.





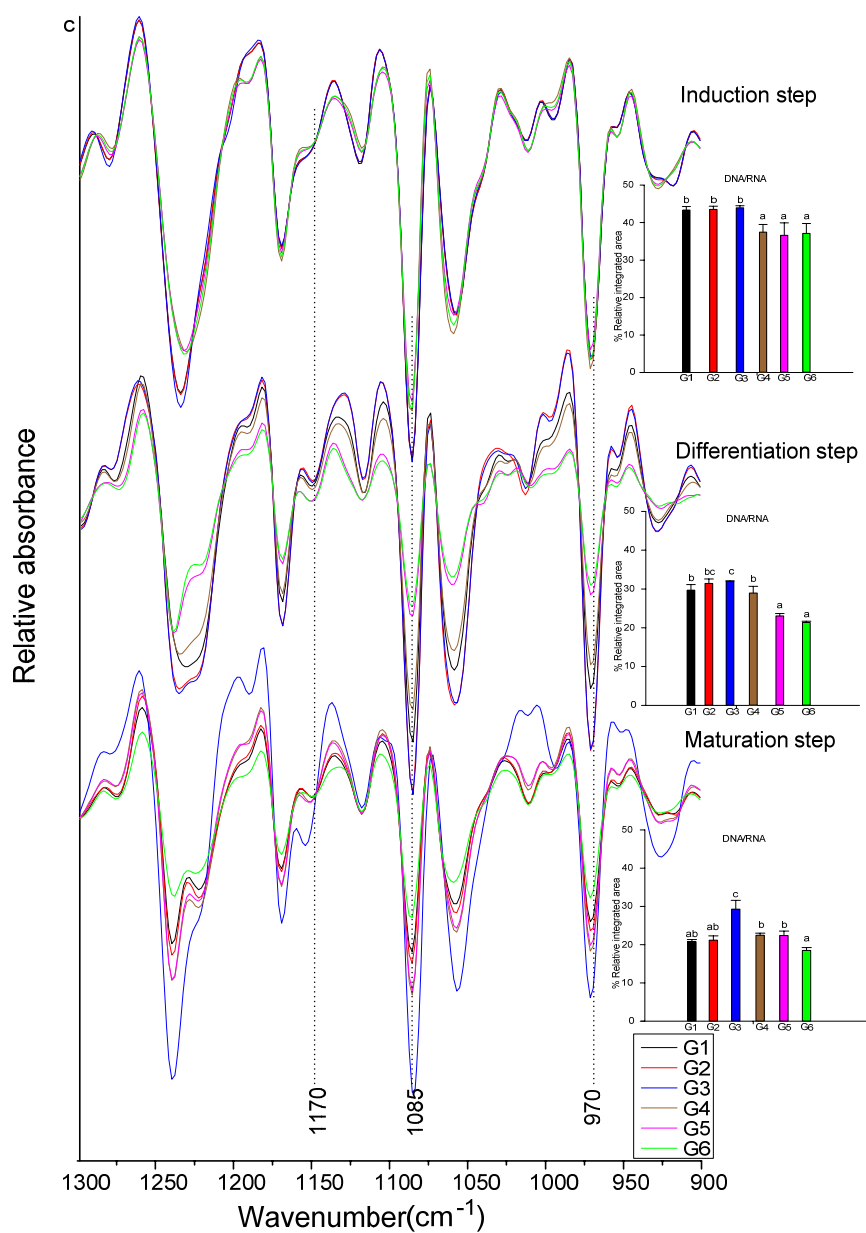


Figure 5.6 Average second derivative FTIR spectra of rBM-MSCs differentiation into hepatocyte-like cell upon exposure of chromatin remodeling agent at different stages. (a) Shows an enlargement of the lipid region (3000-2800 cm⁻¹); (b) shows an enlargement of the protein region (1760-1350 cm⁻¹); (c) shows an enlargement of nucleic acid region (1350-900 cm⁻¹). Significance was set at $P < 0.05$.

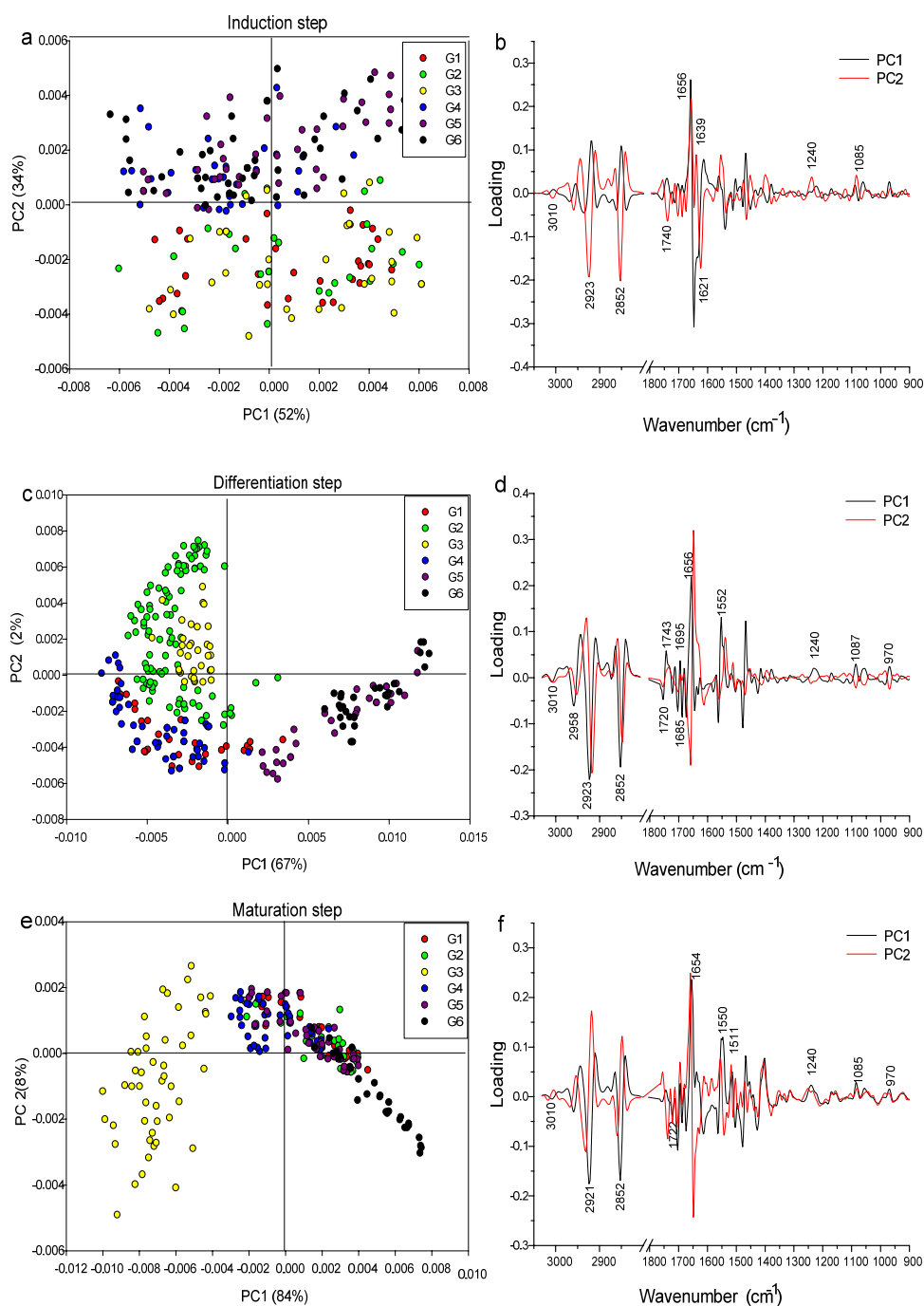


Figure 5.7 PCA scores plots (a, c and e) and loading plot (b, d and f) of rBM-MSCs differentiation into hepatocytes upon exposure of chromatin remodeling agent at difference stages. Spectra were process to the 2nd derivative over the spectral range between 3000-2800 cm^{-1} and 1800-800 cm^{-1} .

5.7 References

- Aurich, I., Mueller, L. P., Aurich, H., Luetzkendorf, J., Tisljar, K., Dollinger, M., Schormann, W., Walldorf, J., Hengstler, J., Fleig, W. E. and Christ, B. (2007). Functional integration of hepatocytes derived from human mesenchymal stem cells into mouse livers. **Gut**. 56: 405-415.
- Bocker, U., Ofstad, R., Wu, Z., Bertram, H. C., Sockalingum, G. D., Manfait, M., Egelanddal, B. and Kohler, A. (2007). Revealing covariance structures in fourier transform infrared and Raman microspectroscopy spectra: a study on pork muscle fiber tissue subjected to different processing parameters. **Appl. Spectrosc.** 61: 1032-1039.
- De Kock, J., Vanhaecke, T., Rogiers, V. and Snykers, S. (2008). Chromatin remodelling, a novel strategy to expedite the hepatic differentiation of adult bone marrow stem cells in vitro. **AATEX** 14: 605-611.
- Dentin, R., Denechaud, P. D., Benhamed, F., Girard, J., Postic, C. (2006). Hepatic gene regulation by glucose and polyunsaturated fatty acids: a role for ChREBP. **Nutrition** 136: 1145-1149.
- Enright, B. P., Sung, L. Y., Chang, C. C., Yang, X. and Tian, X. C. (2005). Methylation and acetylation characteristics of cloned bovine embryos from donor cells treated with 5-aza-20-deoxycytidine. **Biol. Reprod.** 72: 944-948.
- Finnin, M. S., Donigian, J. R., Cohen, A., Lichon, V. M., Rifkind, R. A., Marks, P. A., Breslow, R. and Pavletich, N. P. (1999). Structure of a histone deacetylase homologue bound to TSA and SAHA inhibitors. **Nature** 401: 188-193.
- Guillen, M. D. and Cabo, N. (1997). Characterization of edible oils and lard by Fourier transform infrared spectroscopy. Relationships between composition

and frequency of concrete bands in the fingerprint region. **J. Am. Oil Chem. Soc.** 74: 1281-1286

Hay, D. C., Zhao, D., Fletcher, J., Hewitt, Z. A., McLean, D., Urruticoechea- Uriguen A, Black, J. R., Elcombe, C., Ross, J. A., Wolf, R. and Cui, W. (2008). Efficient differentiation of hepatocytes from human embryonic stem cells exhibiting markers recapitulating liver development *in vivo*. **Stem Cells** 26: 894-902.

Henkens, T., Papeleu, P., Elaut, G., Vinken, M., Rogiers, V. and Vanhaecke, T. (2007). Trichostatin A, a critical factor to maintain differentiation in primary cultures of rat hepatocytes. **Toxicol. Appl. Pharmacol.** 218: 64-71.

Hsieh, J., Nakashima, K., Kuwabara, T., Mejia, E. and Gage, F. H. (2004). Histone deacetylase inhibition-mediated neuronal differentiation of multipotent adult neural progenitor cells. **Proc Natl Acad Sci U S A** 101: 16659-16664.

Kawamura, T., Ono, K., Morimoto, T., Wada, H., Hirai, M., Hidaka, K., Morisaki, T., Heike, T., Nakahata, T., Kita, T. and Hasegawa, K. (2005). Acetylation of GATA-4 is involved in the differentiation of embryonic stem cells into cardiac myocytes. **J. Biol. Chem.** 280: 19682-19688.

Kinoshita, T. and Miyajima, A. (2002). Cytokine regulation of liver development. **Biochim. Biophys. Acta.** 1592: 303-312.

Lee, K. D., Kuo, T. K., Whang-Peng, J., Chung, Y. F., Lin, C. T., Chou, S. H., Chen, J. R., Chen, Y. P. and Lee, O. K. (2004). *In vitro* hepatic differentiation of human mesenchymal stem cells. **Hepatology** 40: 1275-1284.

Listenberger, L. L., Han, X., Lewis, S. E., Cases, S., Farese Jr., R. V., Ory, D. S. and Schaffer, J. E. (2003). Triglyceride accumulation protects against fatty

- acid-induced lipotoxicity. **Proc. Natl. Acad. Sci. U S A** 100: 3077-3082.
- Medina, V., Edmonds, B., Young, G. P., James, R., Appleton, S. and Zalewsky, P. D. (1997). Induction of caspase-protease activity and apoptosis by Butyrate and Trichostatin A (inhibitors of histone deacetylase): dependence on protein synthesis and synergy with a mitochondrial/cytochrome c dependent pathway. **Cancer Res.** 57: 3697-3707.
- Mizumoto, H., Aoki, K., Nakazawa, K., Ijima, H., Funatsu, K. and Kajiwarra, T. (2008). Hepatic differentiation of embryonic stem cells in HF/organoid culture. **Transplant Proc.** 40: 611-613.
- Nara, M., Okazaki, M. and Kagi, H. (2002). Infrared study of human serum very-low-density and low-density lipoproteins. Implication of esterified lipid C=O stretching bands for characterizing lipoproteins. **Chem. Phys. Lipids** 117: 1-6.
- Papeleu, P., Loyer, P., Vanhaecke, T., Elaut, G., Geerts, A., Guguen- Guillouzo, C. and Rogiers, V. (2003). Trichostatin A induces cell cycle arrests but does not induce apoptosis in primary cultures of mitogenstimulated rat hepatocytes. **J. Hepatol.** 39: 374-382.
- Rogiers, V., Vanhaecke, T., De Rop, E. and Fraczek, J. Title of invention: stabilisation of the phenotypic properties of isolated primary cells. International patent number: PCT/EP2008/056706.
- Seo-Gutierrez, M. J., Suh, S. Y., Bae, Y. C. and Jung, J. S. (2005). Differentiation of human adipose stromal cells into hepatic lineage *in vitro* and *in vivo*. **Biochem. Biophys. Res. Commun.** 328: 258-264.
- Sgodda, M., Aurich, H., Kleist, S., Aurich, I., Konig, S, Dollinger, M. M., Fleig, W. E.

- and Christ, B. (2007). Hepatocyte differentiation of mesenchymal stem cells from rat peritoneal adipose tissue *in vitro* and *in vivo*. **Exp. Cell Res.** 313: 2875-2886.
- Shen, S., Li, J. and Cassaccia-Bonnet, P. (2005). Histone modifications affect timing of oligodendrocyte progenitor differentiation in the developing rat brain. **J. Cell Biol.** 169: 577-589.
- Snykers, S., Henkens, T., De Rop, E., Vinken, M., Fraczek, J., De Kock, J., De Prins, E., Geerts, A., Rogiers, V. and Vanhaecke, T. (2009). Role of epigenetics in liver-specific gene transcription, hepatocyte differentiation and stem cell reprogramming. **J. Hepatol.** 51: 187-211.
- Snykers, S., Vanhaecke, T., De Becker, A., Papeleu, P., Vinken, M., Van Riet, I. and Rogiers, V. (2007a). Chromatin remodeling: a key-factor in the endogenic differentiation of human mesenchymal stem cells. **BMC Dev. Biol.** 7: 1-15.
- Snykers, S., Vanhaecke, T., Papeleu, P., Luttun, A., Jiang, Y., Vander Heyden, Y., Verfaillie, C. and Rogiers, V. (2006). Sequential exposure to cytokines reflecting embryogenesis: the key for *in vitro* differentiation of adult bone marrow stem cells into functional hepatocytelike cells. **Toxicol. Sci.** 94: 330-341.
- Snykers, S., Vinken, M., Rogiers, V. and Vanhaecke, T. (2007b) Differential role of epigenetic modulators in malignant and normal stem cells: a novel tool in preclinical *in vitro* toxicology and clinical therapy. **Archives of Toxicology** 8: 533-544.
- Socrates, G. (2001). Infrared and Raman Characteristic frequencies. Wiley and Sons Ltd, Chichester, UK.

- Soto-Gutierrez, A., Navarro-Alvarez, N., Rivas-Carrillo, J. D., Chen, Y., Yamatsuji, T., Tanaka, N. and Kobayashi, N. (2006). Differentiation of human embryonic stem cells to hepatocytes using deleted variant of HGF and poly-amino-urethane-coated nonwoven polytetrafluoroethylene fabric. **Cell Transplant** 15: 335-341.
- Stock, P., Staeger, M. S., Muller, L. P., Sgodda, M., Volker, A., Volkmer, I., Lützkendorf, J. and Christ, B. (2008). Hepatocytes derived from adult stem cells. **Transplant Proc.** 40: 620-623.
- Szyf, M. (2005). DNA methylation and demethylation as targets for anticancer therapy. **Biochemistry (Mosc)** 70: 533-549.
- Talens-Visconti, R., Bonora, A., Jover, R., Mirabet, V., Carbonell, F., Castell, J. V. and Gómez-Lechón, M. J. (2007). Human mesenchymal stem cells from adipose tissue: differentiation into hepatic lineage. **Toxicol. In Vitro** 21: 324-329.
- Walker, W. A. (2004). Pediatric gastrointestinal disease: pathophysiology diagnosis, management, B C Decker Inc, Hamilton, USA.
- Wood, B. R., Tait, B. and McNaughton, D. (2000). Fourier transform infrared spectroscopy as a method for monitoring the molecular dynamics of lymphocyte activation. **Appl. Spectrosc.** 54: 353-359.
- Yamazaki, S., Miki, K., Hasegawa, K., Sata, M., Takayama, T. and Makuuchi, M. (2003). Sera from liver failure patients and a demethylating agent stimulate transdifferentiation of murine bone marrow cells into hepatocytes in coculture with nonparenchymal liver cells. **J. Hepatol.** 39: 17-23.
- Yoshida, Y., Shimomura, T., Sakabe, T., Ishii, K., Gonda, K., Matsuoka, S., Watanabe, Y., Takubo, K., Tsuchiya, H., Hoshikawa, Y., Kurimasa, A., Hisatome, I.,

Uyama, T., Terai, M., Umezawa, A. and Shiota, G. (2007). A role of Wnt/beta-catenin signals in hepatic fate specification of human umbilical cord blood-derived mesenchymal stem cells. **Am. J. Physiol. Gastrointest Liver Physiol.** 293: 1089-1098.

CHAPTER VI

**THERAPEUTIC EFFECT OF BONE MARROW
DERIVED MESENCHYMAL STEM CELLS ON
EXPERIMENTAL LIVER DAMAGE AND
INVESTIGATION BY SYNCHROTRON FTIR
MICROSPECTROSCOPY**

6.1 Abstract

The transplantation of autologous bone marrow-derived mesenchymal stem cells (BM-MSCs) holds great potential for treating end-stage liver diseases. Multipotent BM-MSCs can differentiate into hepatocytes, but few reports addressed a direct comparison of relative efficiency of BM-MSCs and BM-MSCs derived hepatocyte. The aim of this study was to compare the efficiency of rat BM-MSCs (rBM-MSCs) line with that of its hepatogenic differentiation derivative for suppression of dimethylnitrosamine-injured liver diseases in rats, whilst, synchrotron radiation Fourier transform infrared (SR-FTIR) microspectroscopy was applied to investigate the biochemical molecular alteration of the liver tissue after transplantation of cells. Transplantation of the rBM-MSCs derived hepatocytes into liver-injured rats restored their serum albumin level and significantly suppressed transaminase activity and liver disease. In contrast, these effects were not observed in the transplantation of rBM-MSCs. The changes of average spectra located near

1190-970 cm^{-1} (1150 cm^{-1} , 1081 cm^{-1} and 1026 cm^{-1}) indicated decreased levels of glycogen and other carbohydrate, in rBM-MSCs derived hepatocytes treated liver compared with control group and rBM-MSCs treated liver. Principal component analysis (PCA) could distinguish rBM-MSCs derived hepatocytes treated liver and control group or rBM-MSCs treated liver. We conclude that the transplantation of rBM-MSCs derived hepatocytes effectively treats liver disease in rat and SR-FTIR microspectroscopy provides important insights into the fundamental biochemical alteration occurring during stem cells transplantation.

6.2 Introduction

Liver damage often leads to liver fibrosis and sometimes leads to subsequent liver cirrhosis. Liver transplantation is one of the most effective treatments for severe liver-associated diseases such as cirrhosis. However, due to the shortage in donated organs and the growing list of patients in need of such intervention, transplantation is often not common (Iredale et al. 2003). Current studies suggest that hepatocyte transplantation may develop into a feasible alternative to whole-organ transplantation, however, the efficiency of isolation of sufficient transplantable hepatocytes is very low and is restricted by the small number of marginal donor organs allocated for this purpose (Lagasse et al., 2000; Thorgerirsson et al., 2006; Jiang et al., 2002; Reyes et al., 2002). Hence, novel cell sources are required to deliver hepatocytes of adequate quality for clinical use. Most of the recent studies concentrate on stem cells of extrahepatic origin, because of their ready availability and unrestricted potential to propagate and differentiate.

The preeminent candidate stem cells for therapy of an injured liver are

mesenchymal stem cells (MSCs), which possess both multipotentiality and semi-infinite proliferation ability. MSCs *in vitro* have the potential to differentiate into hepatocytes (Lee et al. 2004; Schwartz et al. 2002). Moreover, studies have shown that rat or human mesenchymal stem cells can differentiate into hepatocyte-like cells when transplanted into rat liver (Baksh et al. 2004; Li et al. 2006; Zhan et al. 2006). Recently, transplantation of rat bone marrow mesenchymal stem cells has been shown to protect the rat liver from chemically induced liver fibrosis (Zhao et al. 2005). Oyagi et al. provided evidence that transplantation of bone marrow-derived mesenchymal cells cultured with HGF, but not those without HGF, improved some hepatic functions and suppressed liver fibrosis in rats injured by CCl₄ (Oyagi et al., 2006). Several other studies have shown that transplantation of bone marrow-derived mesenchymal stem cells could ameliorate liver fibrosis (Fang et al., 2004; Zhao et al., 2005), but their effects were marginal or characterization of the cells used was limited. Thus, it remains controversial which type(s) of cells among those derived from the bone marrow shows the most potent suppressive effect on fibrosis, although further evidence that bone marrow cells contribute to regression of liver fibrosis in mice has recently been provided (Higashiyama et al., 2007; Ishikawa et al., 2007).

FTIR microspectroscopy is a powerful technique, which has been widely used in biophysical research, proven to provide sensitive and precise measurement of biochemical changes in biological cells and tissue (Lasch and Boese, 2001). Recently, synchrotron infrared microspectroscopy has been used for the early detection of liver fibrosis (Liu et al., 2006). FTIR imaging analysis could become a valuable analytic method in brain tumor research and possibly in the diagnosis of human brain tumors (Bambery et al., 2006). Wang et al used FTIR microspectroscopy to study the

compositional changes in inflammatory cardiomyopathy and the results demonstrate chemical difference between the inflammatory responses in mouse model, providing insight into why the disease can be self-limiting in some cases while fatal in others (Wang et al., 2005). This approach provides structural information of biological molecules such as protein, nucleic acids, carbohydrates and lipids, allowing detection, identification and quantification of changes in these macromolecular cellular components.

This study, we aimed to compare the efficiency of rat BM-MSCs line with that of its hepatogenic differentiation derivative for suppression of dimethylnitrosamine injure liver diseases rats, whilst, synchrotron radiation Fourier transform infrared (SR-FTIR) microspectroscopy was applied to investigate the biochemical molecular alteration of the liver tissue after transplantation of cells.

6.3 Materials and methods

6.3.1 Preparation of cells

rBM-MSCs were isolated and cultured implemented employing the same protocol as chapter 3. rBM-MSCs were maintained in the same culture medium as chapter 3. For inducing differentiation of hepatogenic lineage, rBM-MSC were explored to conditioning medium containing IMDM, 10 ng/ml bFGF and 20 ng/ml EGF for 2 days; following differentiation medium consisting of IMDM, 20 ng/ml HGF, 10 ng/ml bFGF and 4.9 mmol/L nicotinamide for 7 days and differentiation and maturation medium consisting of IMDM, 10 μ mol/ml ITS, 1 μ mol/ml Dex, and 20 ng/ml OSM for 14 days.

6.3.2 Treatment of animals

Female Wistar rats were 3 weeks old, weighing between 180 and 200 g. Rats were bred and maintained in an air conditioned animal house with specific pathogen-free conditions, and were subjected to a 12:12-hours daylight/darkness and allowed unlimited access to chow and water. Liver damage was induced by dimethylnitrosamine (DMN) administration as follow: On day 0, rats were injected intraperitoneally at a dose of 100 μ L DMN (diluted 1:100 with 0.15 mol/L sterile saline) per 100 g body weight. The injection was given on three consecutive days of each week for 4 weeks.

6.3.3 Transplantation experiments

After being detached from the plate by trypsin/EDTA treatment, the cells were stained using the PKH Fluorescent Cell Linker kit. Cells were suspension in 1 ml phosphate buffer saline for each donor cells at the concentration of 1×10^6 cells/ml. Nine rats were randomly divided into three groups after 4 weeks DMN-induced: DMN/rBM-MSCs, n = 3, to inject intravenously a dose of rBM-MSCs 1×10^6 cells per rat; DMN/hepatocyte, n = 3, to inject intravenously a dose of hepatocytes 1×10^6 cells per rat; DMN/saline, n = 3, to inject the same volume of saline. On day 28, venous blood was collected and all rats were killed, and liver tissue harvested for analysis. Animal studies were carried out in compliance with the guidelines of the Institute for Laboratory Animal Reaesrch, Suranaree University of Technology.

6.3.4 Histopathologic staining

Frozen liver samples (approx. 0.5 cm^3) were randomly taken from the right, median and left lobes of each rat liver and embedded in optimal temperature cutting (OCT) compound, sectioned consecutively at 10 μ m in a cryostat at $-18 \text{ }^\circ\text{C}$. The liver section were mounted on slides for histopathologic staining and fluorescence

detection and also plated on MirrIR low-e infrared reflective slides for FTIR analysis. PKH26 derived fluorescence was observed using fluorescence microscope, and number of positive cells were counted in more than three different views for each liver sample. For Hematoxylin and Eosin staining (H&E), the liver sections were mounted on slides and air dried for at least 20 minutes followed by fixation in 10% Formalin for 30 seconds. Then these sections were stained with routine H&E according to regular staining procedure such as hydration, staining, dehydration and clearing. The stained slides were finally covered with a cover-slip using a mounting medium Entellen.

6.3.5 Assessment of liver function

Blood sample were obtained from each rat and centrifuged for 30 minutes at 600 ×g and serum was collected. Albumin (ALB), aspartate aminotransferase (AST) and alanine transaminase (ALT) were assessed using conventional laboratory methods.

6.3.6 Synchrotron infrared microspectroscopy (SR-FTIR)

High spatial resolution infrared spectral maps were collected at an infrared microspectroscopy beamline (2BM1B) at the Australian Synchrotron, Melbourne, Australia. SR-FTIR spectra were acquired using a Hyperion 2000 FTIR microscope (Bruker Optik GmbH, Ettlingen, Germany) with a narrow-band mercury cadmium telluride (MCT) detector coupled to a Bruker Vertex 80V FTIR spectrometer, which was connected to IR beamline at the Australian Synchrotron. The sample was mapped through the focused beam using a X-Y step size of 4 μm with a 4 μm aperture in the microscope focal plane with a spectral resolution of 8 cm⁻¹ with 64 interferograms coadded. All acquisition and control functions of the microscope were performed

though Bruker Opus version 6.5.

6.3.7 Data analysis

Spectra from all liver samples were extracted using CytoSpec™ (Cytospec Inc., Boston MA, USA) spectroscopic software after performing a quality test to assess the appropriate sample thickness, rejecting spectra with maximum absorbance less than 0.2 or greater than 0.8 absorbance units over the spectrum range of 3100-970 cm^{-1} . Spectra extracted using Cytospec were subsequently converted into galactic format by a macro converter in OPUS6.5 software in preparation for multivariate data analysis.

Representative spectra from all groups were processed and compared following multivariate analysis. Prior to multivariate analyses or classification the data was preprocessed by performing second derivative using the Savitzky-Golay algorithm with 9 smoothing points, and normalization using Extended Multiplicative Signal Correction (EMSC). The Unscrambler 9.7 software was used for multivariate data analysis.

6.4 Results

6.4.1 The liver-damaged rat model

Routine H&E staining was employed to characterize representative liver sections at 1 week, 2 weeks and 4 weeks following DMN injection and the normal liver section as control, as displayed in Fig. 6.1. The liver tissue from normal liver showed the normal histological cytoplasm of hepatocyte, i.e., they are polyhedral with eosinophilic cytoplasm and a usually central nucleus (Fig. 6.1a). However, for 1 week following DMN injection, necrosis areas appeared. Specifically, after 2 weeks of

DMN injection, the large areas of necrosis were found. At the fourth week of injection, the alteration of liver structure was even more evident, with more hemorrhagic necrosis and disruption of tissue architecture.

6.4.2 Tracing of transplanted cells in the DMN-injured liver

PKH26-stained rBM-MSCs and hepatocytes were transplanted into DMN-injured rats to examine what cell type is effective for the engraftment in the liver. Fig. 6.2 showed the fluorescence images and the positive engraftment cell number. The PKH26-stained cells were easily detected in the liver by fluorescence microscopy. The transplanted cells were located in blood vessels, the sinusoid, and the liver lobules. This result suggested that the transplanted cells entered sinusoid and liver parenchymal tissue. There was significant difference between the positive cell of liver that receive an rBM-MSCs derived hepatocyte transplant and that of liver receiving rBM-MSCs. Therefore, induction hepatic differentiation pre-transplantation was more effective for improving the engraftment of rBM-MSCs to the injured recipient liver.

6.4.3 Recovery of albumin production by stem cells transplantation

The normal level of rat serum albumin was 3.9 g/dL, while the DMN treatment rat serum albumin was 3.2 g/dL, which was significant lower than normal level (Fig. 6.3a). Liver-injured rats recovered serum albumin levels but still lower than that of normal level following by the transplantation of rBM-MSCs. In contrast, the transplantation of rBM-MSCs derived hepatocyte into liver damaged rats restored the serum albumin close to the normal level. Although it is not clear whether the transplanted rBM-MSCs differentiated into hepatocytes that produced albumin, or whether DMN-damaged liver regenerated in response to the rBM-MSCs derived

hepatocytes, induction hepatic differentiation pre-transplantation effectively led to restored albumin production after the transplantation.

6.4.4 Suppression of liver inflammation by stem cells transplantation

The normal AST and ALT levels in serum were 155 and 110 U/L, respectively. As shown in Fig. 6.3, the serum AST and ALT levels in the DMN-treated rats were 220 and 180 U/L, respectively, which were significantly higher than normal level. The transplantation of rBM-MSCs derived hepatocytes significantly suppressed the serum AST and ALT levels to the normal in the DNMI-injured rats. The transplantation of rBM-MSCs suppressed the serum AST and ALT level in the DNMI-injured rats but still could not suppress to the normal level. Induction hepatic differentiation pre-transplantation effectively suppressed liver inflammation.

The effects of rBM-MSCs and rBM-MSCs derived hepatocytes on DNMI-injured liver were evaluated by histopathologic examination of the liver sections by H&E staining. The control group (Fig. 6.4a), exhibited the hemorrhagic necrosis and disruption of tissue architecture. The changes of necrosis areas and the tissue architecture in the liver sections were observed in transplantation of rBM-MSCs group (Fig 6.4b). These alterations were remarkably changed in transplantation of rBM-MSCs derived hepatocytes group. Hemorrhagic necrosis was rarely observed and tissue architecture appears to be similar to that of normal rats (Fig 6.4c).

6.4.5 Synchrotron radiation Fourier Transform Infrared (SR-FTIR)

microspectroscopy investigation of liver tissue

SR-FTIR microspectroscopy was applied to investigate the biochemical molecule alteration of the liver tissue after transplantation of rBM-MSCs and

rBM-MSCs derived hepatocytes to DMN-injured rats. Fig 6.5 shows average second derivative IR spectra from 1800 to 950 cm^{-1} in each group. The average spectra showed difference in bands near 1658 cm^{-1} (α -helix), 1544 cm^{-1} (amide II), as well as IR absorbance bands at 1150 cm^{-1} , 1081 cm^{-1} , 1026 cm^{-1} which were assigned to glycogen and other carbohydrate (Camacho et al., 2001). The intensities of α -helix (1658 cm^{-1}) and amide II (1544 cm^{-1}) shown higher in rBM-MSCs injection liver tissue, followed by rBM-MSCs derived hepatocyte injection liver tissue than that in normal liver tissue, indicating the different protein content. It was also shown that the glycogen and other carbohydrate bands at 1150 cm^{-1} , 1081 cm^{-1} , 1026 cm^{-1} , were highest in DMN-injured liver tissue (control), and followed by rBM-MSCs liver tissue and rBM-MSCs derived hepatocyte injection liver tissue. The profile of these bands in rBM-MSCs derived hepatocyte injection liver tissue shown close to that of normal liver tissue.

PCA analysis of the SR-FTIR spectra was performed in the 1770-1500 cm^{-1} and 1190-970 cm^{-1} spectral region. The PCA score plot showed that the spectra extracted from control group, rBM-MSCs injection group, rBM-MSCs derived hepatocyte injected group and normal liver can be clustered separately along PC1 (69%) and PC2 (19%) (Fig 6.6a). Spectra from control liver tissue and rBM-MSCs injection liver tissue could be distinguished from rBM-MSCs derived hepatocyte injected liver tissue and normal liver tissue by having negative loading at 1666 cm^{-1} , 1157 cm^{-1} , 1083 cm^{-1} and 1027 cm^{-1} attributed to protein secondary structure and glycogen and other carbohydrate, in line with the average secondary spectra (Fig 6.6b). Spectra from control liver tissue could be separated from rBM-MSCs injected liver tissue by having negative loading at 1666 cm^{-1} , 1157 cm^{-1} ,

1083 cm^{-1} and 1027 cm^{-1} , showing the higher content of these bands in control liver tissue. These PC result showed that difference in bands associated with collagen were responsible for the separation of the clusters of the each group.

6.5 Discussion

In this study we showed the effectiveness of transplanting rBM-MSCs to treat liver failure in an experimental animal model, which consistent with previous study (Oyagi et al., 2006). Induction hepatic differentiation pre-transplantation enhanced the engraftment of rBM-MSCs in the recipient liver and caused clear therapeutic effects in DMN-injured rats. We found that the transplantation of rBM-MSCs derived hepatocytes significantly reduced the serum transaminase levels in DMN-injured rats. Induction hepatic differentiation pre-transplantation appeared to be effective for the suppression of liver inflammation. PKH staining showed that a significantly higher number of rBM-MSCs derived hepatocytes were engrafted in injured liver than rBM-MSCs. These rBM-MSCs derived hepatocytes which induced by hepatocyte growth factor (HGF) showed higher engraftment potential. Previous reported that HGF up-regulated C-X-C chemokine receptor type 4 (CXCR4), which is the chemokine receptor for stromal cell-derived factor-1 (SDF-1), in human hematopoietic stem cells (Horuk, 2001; Kollet et al., 2003). The SDF-1 is expressed in liver bile duct epithelium and the secretion is increased by the inflammation. The CXCR4 might be up-regulated in rBM-MSCs derived hepatocytes which induced by HGF and the engraftment in the injured liver could be enhanced by the interaction with SDF-1. The report has shown that CCl_4 -injured hepatocytes stimulated HGF secretion in the co-cultured BM-MSCs (Oyagi et al., 2006). HGF is well known to

suppress hepatocyte death and liver fibrosis (Sakaida et al., 2004). When transplanted into DMN-injured rat, engrafted rBM-MSCs derived hepatocytes could secrete HGF in the liver and suppress the inflammation. However, our result opposite to the previous result that undifferentiated rBM-MSCs were the most effective for suppression of liver fibrosis (Hardjo et al., 2009). It is still not clear why and how the undifferentiated rBM-MSCs most effectively suppressed liver fibrosis. The different results of our current study maybe attribute to the different approach of rBM-MSCs delivery. In our study, we chose intravenous injection, which is an easy and convenient way of stem cells delivery, with less invasive and traumatic (Xu and Liu, 2008). The reports had shown that intravenous injection of manipulation of the transplanted cells more efficient to migrate to the target areas, because the injured target organ may express specific receptor or ligands to facilitate trafficking of such manipulation transplanted cells (Xu and Liu, 2008).

We employed SR-FTIR microspectroscopic technique to obtain more insight into the biochemical molecule changing after transplantation of rBM-MSCs to the DMN-injured rat. The spectra profile of each group has shown significantly different in the region of $1770-980\text{ cm}^{-1}$ which associated with protein secondary structure and glycogen and other carbohydrate. The different in protein secondary structure of amide I and II indicated the different protein expression in each group. DMN could destroy protein and inhibit the protein synthesis as revealed by the lower protein absorbance in the control group (Villa-Trevino, 1967). The higher level protein absorbance was found in rBM-MSCs and rBM-MSCs derived hepatocyte injection group, suggesting the resume of protein synthesis after cells transplantation. However the mechanisms of how this transplanted cells resume the protein synthesis still

unclear. It was also shown that the absorbance of glycogen and other carbohydrate bands observed between 1190-970 cm^{-1} (1150 cm^{-1} , 1081 cm^{-1} , 1026 cm^{-1}), were observed to lower in rBM-MSCs derived hepatocyte treated liver than that in control group and rBM-MSCs treated group. Liver plays a major role in carbohydrate metabolism. DMN causes liver loses function particularly in destruction of glycogenolysis which leads to accumulation of glycogen in the liver. In control group, these bands were observed to have the highest level indicated the accumulation of glycogen in liver. However, these bands were shown to lower in rBM-MSCs and rBM-MSCs derived hepatocyte injection group, especially in rBM-MSCs derived hepatocyte injection group, suggesting the decrease of glycogen deposition in the liver, which results in resuming the carbohydrate metabolism in the liver after cells transplantation. In rBM-MSCs derived hepatocyte injection group, the profile of these bands were found to similar to that of normal liver tissue, indicating the same biochemical molecular between then, which confirm that rBM-MSCs derived hepatocyte effectively treats liver disease.

6.6 Conclusion

The transplantation of rBM-MSCs derived hepatocyte effectively treats liver injury in rats. They restored serum albumin level and significantly suppressed transaminase activity and liver disease. This is a promising technique for autologous transplantation in humans with liver injury. The changes of average spectra located near 1190-970 cm^{-1} in rBM-MSCs derived hepatocyte treated liver indicated the resume of protein synthesis and carbohydrate metabolism in the liver after cells transplatation. SR-FTIR microspectroscopy provides biochemical information that is

complimentary to that obtained from conventional technique to monitoring stem cell transplantation.

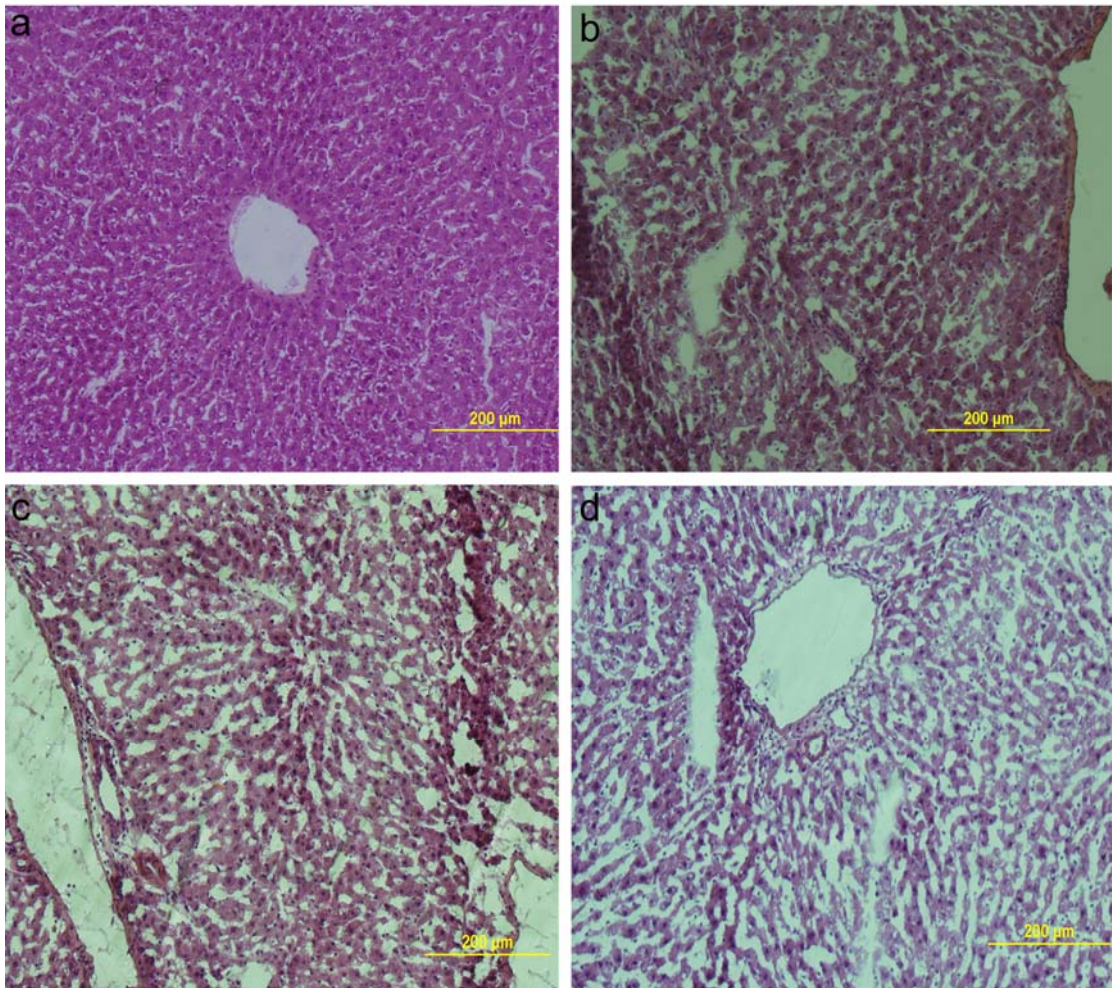


Figure 6.1 Representative liver tissues stained with hematoxylin and eosin. Normal liver (a); 1 week injection of DMN (b); 2 weeks injection of DMN (c); 4 weeks injection of DMN (d). Original magnification, 100 ×.

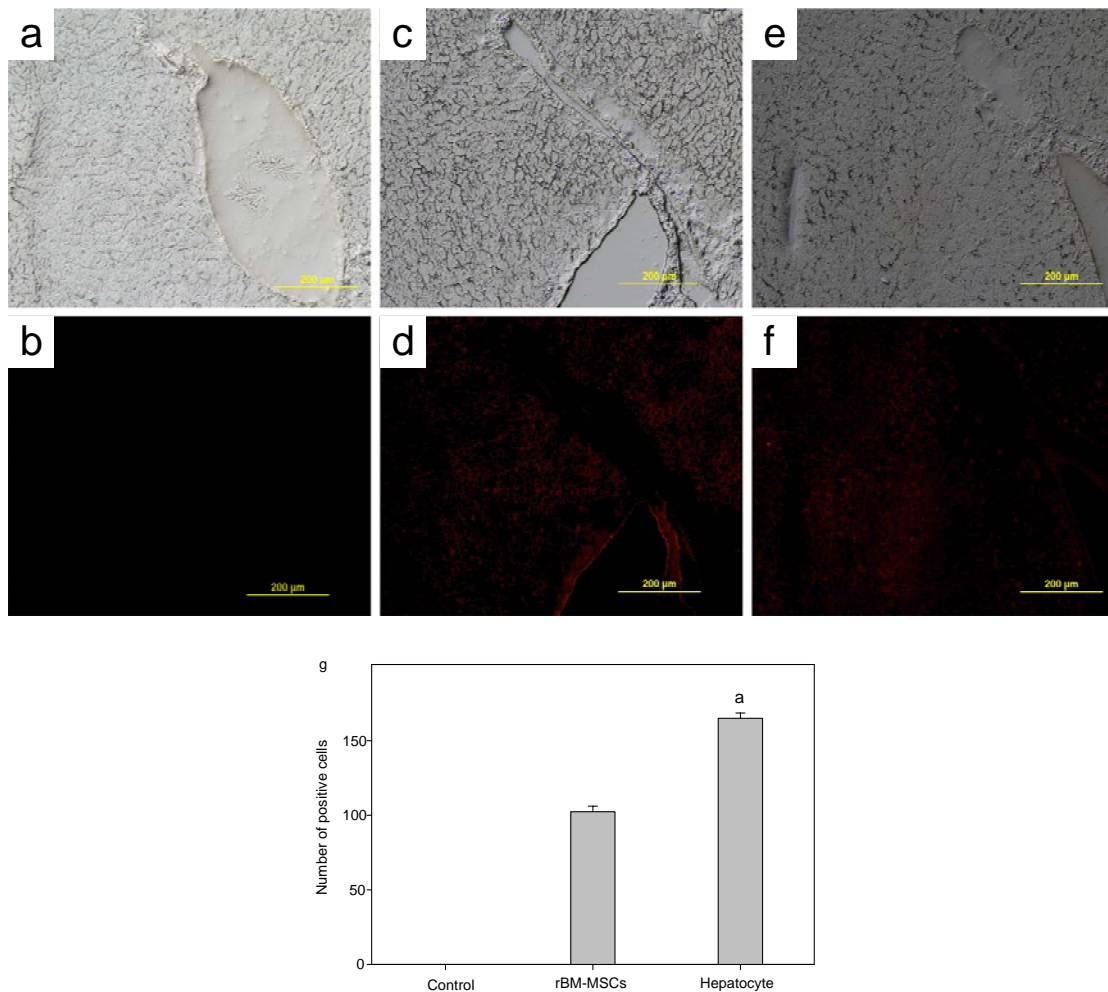


Figure 6.2 Engraftment of PKH-stained rBM-MSCs and hepatocyte in DMN-injured rat liver. Non-transplanted liver from DMN-treated rats was used as the control (a and b). rBM-MSCs (c and d) and hepatocyte (e and f) were transplanted into DMN-injured rats, and 4 weeks later liver sections were observed with fluorescence microscope. The left (a, c and e) and right (b, d and f) pictures are bright-field and fluorescence images, respectively. Positive number of PKH fluorescence (g). Significance was set at $P < 0.05$. Original magnification, $100\times$.

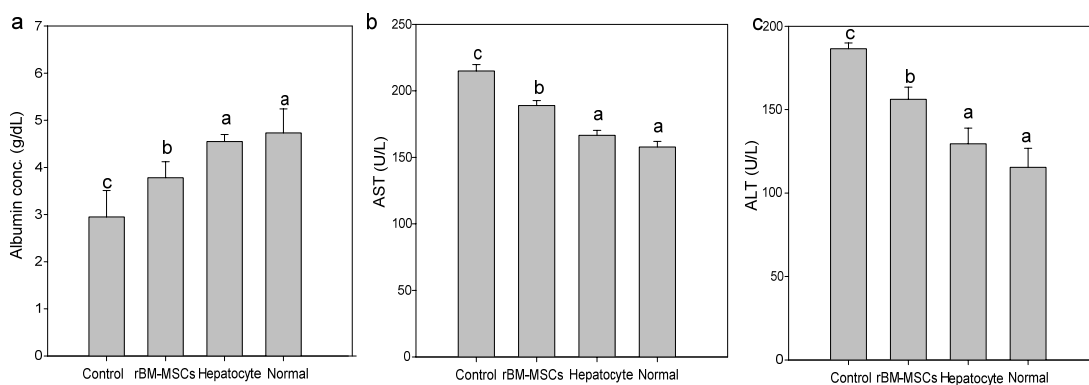


Figure 6.3 Biochemical analysis. Concentration of albumin, AST and ALT in blood serum of rat. Significance was set at $P < 0.05$.

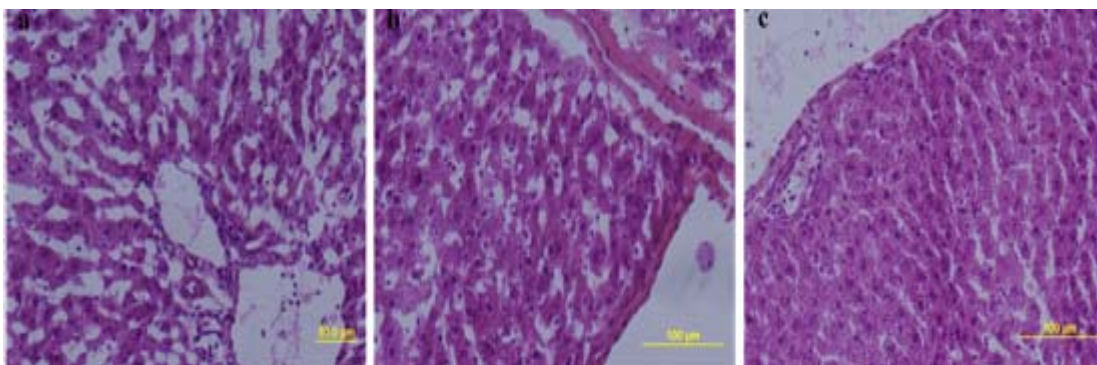


Figure 6.4 Hematoxylin and Eosin staining of liver sections from DNM-injured rats that received cell transplant. (a) Saline/DMN; (b) rBM-MSCs/DMN; (c) hepatocyte/DMN. Original magnification, 200 ×.

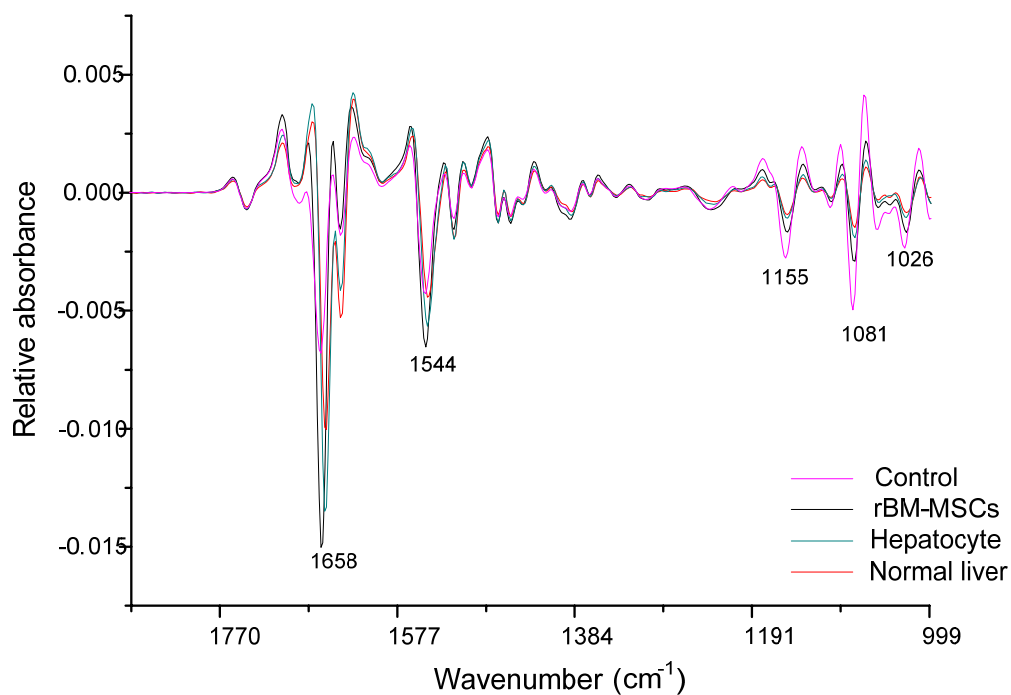


Figure 6.5 Average second derivative FTIR spectra from 1800 to 950 cm^{-1} .

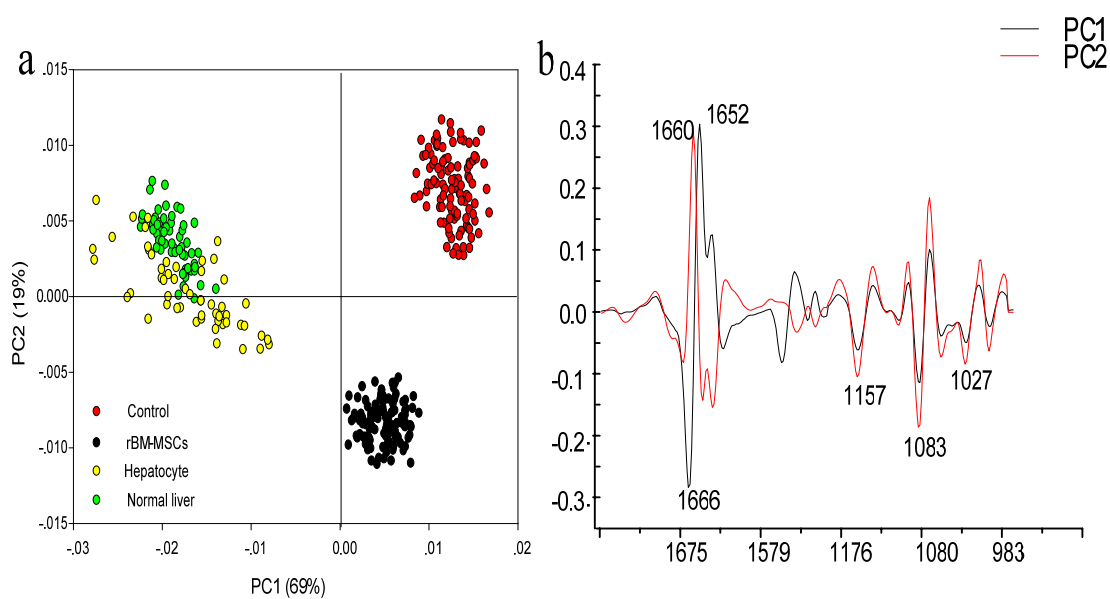


Figure 6.6 PCA scores plots (a) and loading plot (b). Spectra were processed to the 2nd derivative over the spectral range between 1770-1500 cm^{-1} and 1190-970 cm^{-1} .

6.7 References

- Baksh, D., Song, L. and Tuan, R. S. (2004). Adult mesenchymal stem cells: characterization, differentiation, and application in cell and gene therapy. **J. Cellular and Molecular Medicine** 8: 301-316.
- Bamberg, K. R., Schultke, E., Wood, B. R., MacDonald, S. T. R., Ataelmannan, K., Griebel, R. W., Juurlink, B. H. J. and McNaughton, D. (2006). A fourier transform infrared microspectroscopic imaging investigation into an animal model exhibiting glioblastoma multiforme. **Bioch. Biophys. Acta.** 1758: 900-907.
- Camacho, N. P., West, P., Torzilli, P. A and Mendelsohn, R. (2001). FTIR microscopic imaging of collagen and proteoglycan in bovine cartilage. **Biopolymers** 62:1-8.
- Fang, B., Shi, M., Liao, L., Yang, S., Liu, Y. and Zhao, R. C. (2004). Systemic infusion of FLK1(+) mesenchymal stem cells ameliorate carbon tetrachloride-induced liver fibrosis in mice. **Transplantation** 78: 83-88.
- Hardjo, M., Miyazaki, M., Sakaguchi, M., Masaka, T., Ibrahim, S., Kataoka, K. and Huh, N. H. (2009). Suppression of carbon tetrachloride-induced liver fibrosis by transplantation of a clonal mesenchymal stem cell line derived from rat bone marrow. **Cell Transplant.** 18: 89-99.
- Higashiyama, R., Inagaki, Y., Hong, Y. Y., Kushida, M., Nakao, S., Niioka, M., Watanabe, T., Okano, H., Matsuzaki, Y., Shiota, G. and Okazaki, I. (2007). Bone marrow-derived cells express matrix metalloproteinases and contribute to regression of liver fibrosis in mice. **Hepatology** 45: 213-222.
- Horuk, R. (2001). Chemokine receptors. **Cytokine Growth Factor Rev.** 12: 313-335.

- Iredale, J. P, Shiota, G. and Okazaki, I. (2003). Cirrhosis: new research provides a basis for rational and targeted treatments. **British Medical J.** 327: 143-147.
- Ishikawa, T., Terai, S., Urata, Y., Marumoto, Y., Aoyama, K., Murata, T., Mizunaga, Y., Yamamoto, N., Nishina, H., Shinoda, K. and Sakaida, I. (2007). Administration of fibroblast growth factor 2 in combination with bone marrow transplantation synergistically improves carbon-tetrachloride-induced liver fibrosis in mice. **Cell Tissue Res.** 327: 463-470.
- Jiang, Y., Jahagirdar, B. N., Reinhardt, R. L., Schwartz, R. E., Keene, C. D., Ortiz-Gonzalez, X. R., Reyes, M., Lenvik, T., Lund, T., Blackstad, M., Du, J., Aldrich, S., Lisberg, A., Low, W. C., Largaespada, D. A., and Verfaillie, C. M. (2002). Pluripotency of mesenchymal stem cells derived from adult marrow. **Nature** 418: 41-50.
- Kollet, O., Shivtiel, S., Chen, Y. Q., Suriawinata, J., Thung, S. N., Dabeva, M. D., Kahn, J., Spiegel, A., Dar, A., Samira, S., Goichberg, P., Kalinkovich, A., Arenzana-Seisdedos, F., Nagler, A., Hardan, I., Revel, M., Shafritz, D. A. and Lapidot, T. (2003). HGF, SDF-1, and MMP-9 are involved in stress-induced human CD34⁺ stem cell recruitment to the liver. **J. Clin. Invest.** 112: 160-169.
- Lagasse, E., Connors, H., Al-Dhalimy, M., Reitsma, M., Dohse, M., Osborne, L., Wang, X., Finegold, M., Weissman, I. L. and Grompe, M. (2000). Purified hematopoietic stem cells can differentiate into hepatocytes *in vivo*. **Nat. Med.** 6: 1229-1234.
- Lasch, P. and Boese, M. (2002). FT-IR spectroscopic investigations of single cells on

- the subcellular level. **Vibra. Spectroscopy** 28: 147-157.
- Lee, K. D., Kuo, T. K., Whang-Peng, J., Chung, Y. F., Lin, C. T., Chou, S. H., Chen, J. R., Chen, Y. P. and Lee, O. K. (2004). *In vitro* hepatic differentiation of human mesenchymal stem cells. **Hepatology** 40: 1275-1284.
- Li, W., Liu, S. N., Luo, D. D., Zhao, L., Zeng, L. L., Zhang, S. L. and Li, S. L. (2006). Differentiation of hepatocytoid cell induced from whole-bone-marrow method isolated rat myeloid mesenchymal stem cells. **World J. Gastroenterology** 12: 4866-4869.
- Oyagi, S., Hirose, M., Kojima, M., Okuyama, M., Kawase, M., Nakamura, T., Ohgushi, H. and Yagi, K. (2006). Therapeutic effect of transplanting HGF-treated bone marrow mesenchymal cells into CCl₄-injured rats. **J. Hepatol.** 44: 742-748.
- Reyes, M., Lund, T., Lenvik, T., Aguiar, D., Koodie, L. and Verfaillie, C. M. (2001). Purification and *ex vivo* expansion of postnatal human marrow mesodermal progenitor cells. **Blood** 98: 2615-2621.
- Rojkid, M., Giambrone, M. A. and Fuller, G. (1979). Collagen metabolism in the liver of normal and carbon tetrachloride treated rat. **Biomedicine** 31: 199-200.
- Sakaida, I., Terai, S., Yamamoto, N., Aoyama, K., Ishikawa, T., Nishina, H. and Okita, K. (2004). Transplantation of bone marrow cells reduces CCl₄-induced liver fibrosis in mice. **Hepatology** 40: 1304-1311.
- Schwartz, R. E., Reyes, M., Koodie, L., Jiang, Y., Blackstad, M., Lund, T., Lenvik, T., Johnson, S., Hu, W. S. and Verfaillie, C. M. (2002). Multipotent adult progenitor cells from bone marrow differentiate into functional hepatocyte-like cells. **J. Clinical Investigation** 109: 1291-1302.

- Surewicz, W. K., Mantsch, H. H. and Chapman, D. (1993). Determination of protein secondary structure by Fourier transform infrared spectroscopy: a critical assessment. **Biochemistry** 32: 389-394.
- Thorgeirsson, S. S., Lee, J. S. and Grisham, J. W. (2006). Functional genomics of hepatocellular carcinoma. **Hepatology** 43: 145-150.
- Villa-Trevino, S. (1967). A possible mechanism of inhibition of protein synthesis by dimethylnitrosamine. **Biochem. J.** 105: 625-631.
- Wang, Q., Sanad, W., Miller, L. M., Viogt, A., Klingel, K., Kandolf, R., Strangl, K. and Baumann, G. (2005). Infrared imaging of compositional changes in inflammatory cardiomyopathy. **Vibra. Spectroscopy** 38: 217-222.
- Xu, Y. Q. and Liu, Z. C. (2008). Therapeutic potential of adult bone marrow stem cells in liver disease and delivery approaches. **Stem Cell Rev.** 4: 101-112.
- Zhan, Y., Wang, Y., Wei, L., Chen, H., Cong, X., Fei, R., Gao, Y. and Liu, F. (2006). Differentiation of hematopoietic stem cells into hepatocytes in liver fibrosis in rats. **Transplant Proceedings** 38: 3082-3085.
- Zhao, D. C., Lei, J. X., Chen, R., Yu, W. H., Zhang, X. M., Li, S. N. and Xiang, P. (2005). Bone marrow-derived mesenchymal stem cells protect against experimental liver fibrosis in rats. **World J. Gastroenterology** 11: 3431-3440.

CHAPTER VII

OVERALL CONCLUSION

BM-MSCs are a population of self-renewing multipotent cells that have significant clinical potential in cellular therapies and tissue regeneration owing to their potential ease of *in vitro* culture and manipulation. The results from this thesis have demonstrated that rBM-MSCs could be isolated by selective plastic surface attached method and seeded at low initial seeding densities, resulting in higher yields and faster expansion. TSA but not 5-Aza-dC is essential to promote differentiation of rBM-MSCs towards functional hepatocyte-like cells *in vitro*. Transplantation of rBM-MSCs derived hepatocytes effectively treats liver disease in rat. FTIR microspectroscopy together with SR-FTIR microspectroscopy provides a practical tool to monitor stem cells differentiation and transplantation based on detecting the unique information about the biochemistry and molecular composition of cells and tissue.

BIOGRAPHY

Miss Danna Ye was born on March 19th, 1981 in Guangxi, P. R. China. In 2003, she graduated from Guangxi University, Nanning, Guangxi, P. R. China with Bachelor's Degree (B.Sc.) of Animal Science. In 2006, she received a Master degree (M.Sc.) in Agriculture from Animal Reproduction Institute, Guangxi University, Nanning, Guangxi, P. R. China. Her research topic was "Effect of Different Culture Medium Compositions and Culture Systems on Buffalo Embryo Development *in vitro*". She received a graduate student outstanding award from Guangxi University in 2006. In May 2007, she started study Ph.D at School of Biotechnology, Institute of Agricultural Technology, Suranaree University of Technology. Her Ph.D thesis title was "Rat Bone Marrow Derived Mesenchymal Stem Cells and Their Hepatogenic Differentiation".